On the ability of a global atmospheric inversion to constrain variations of CO_2 fluxes over Amazonia

Final response to the comments from Referee 1

Questions/comments from the Referee, answers to the comments and changes to the manuscript are presented according with the following notation:

Q) Questions, general, and technical comments
A) Answers to the comments
C) Changes to the manuscript

General Comments

Q.1) This paper evaluates CO2 fluxes over Amazonia that have been calculated using two atmospheric inversions, a control case and one that includes extra atmospheric CO2 measurements for the Amazonian region. The analysis focuses on the seasonal cycle of fluxes and on interannual variations, particularly years that were notably dry or wet. The overall impression of the results is that the fluxes vary quite substantially across the Tropical South American region and at times it is difficult to determine what extra information the Amazonian CO2 data adds. The authors acknowledge this, noting in their abstract that 'the results revealed critical limitations that prevent global inversion frameworks from capturing the data-driven seasonal patterns of fluxes across Amazonia' and recommending in their conclusions that denser observing networks and regional models might be required to overcome the limitations.

A) We thank the reviewer for her positive comments and sensible suggestions which made this review very helpful.

Q.2) While I agree that this is a valid conclusion from this study, there are two other suggestions that I would like to make, one which could be incorporated into a revision of this paper, while the other targets future inversion work. Firstly, much of the current analysis looked at, for example, the seasonal cycles averaged across the full time period of the inversion. Given the intermittent nature of the Amazonian atmospheric CO2 data, I wonder whether analysis targeted at periods when certain sites were active might yield clearer inversion impacts. Some suggestions are given in the specific comments below.

A) We agree with this general comment and we have followed the more specific suggestions provided below to includenew analyses and discussions on this topic in the revised manuscript (see our answers to the corresponding comments).

Q.3) Secondly, I think that as an inversion community we need to be smarter about how we include continuous CO2 measurements into our inversions. Each site has different characteristics and each transport model will represent those sites in different ways. We need to understand what parts of the CO2 record we can most reliably simulate and consequently include in the inversion. Afternoon measurements (as used here) may be appropriate for continental sites with large diurnal cycles, but I would suggest that coastal sites need a different selection strategy. Likewise the choice of sampling location from a transport model (nearest grid-point or an interpolation between points) might be dependent on the characteristics of the observing location.

A) We agree with these recommendations for better fitting the data with the model through site-specific studies. Actually, we feel that they are in line with our preliminary investigations regarding the representation of the diurnal cycle and day-to-day variations of CO_2 at the different sites that we have used. We finally based our data selection on rather traditional criteria (i.e., during the afternoon and when the wind speed is above a given threshold), supported by previous studies (e.g., Butler et al., Tellus (2010), 62B, 550–572; Gatti et al., Tellus (2010), 62B, 581–594), and we finally located the sites in the corresponding (in terms of space coordinates) model grid cells. However, we followedthe traditional approach only after a site-by-site investigation of the diurnal cycle and day-to-day time series at each of the nine model grid-cells at and around the site geographical locations. More details on this topic have been included in the revised manuscript, following some of the ideas brought by the reviewer's detailed comments on this topic below (see our answers to the corresponding comments).

Q.4) I recommend that the paper be published with minor revisions to address the technical corrections and to clarify and extend the analysis a little based on the suggestions in the specific comments.

A) We hope that our answers to the reviewer's comments, as well as the corrections applied to the original manuscript, are fully consistent with her suggestions.

Specific Comments

Q.5) Sometimes it is not clear which region an analysis has been performed for, with various terms used e.g. 'Tropical South America/TSA', 'whole region' (p 1926,line 15; p 1932, line 17), 'entire study area' (p 1926, line 16). Please ensure that each region is defined. Also in the text the inversion without extra sites is usually referred to as MACCv10.1 while the figures are labelled with CH2010. It would be preferable to use one or the other consistently in text and figures.

A) We have systematically clarified the region that is discussed by using a unique term for a given region and by clearly emphasizing the corresponding notations as soon as they will be used. Labelling the figures using CH2010 was a mistake which we have corrected. For consistency, the term MACCv10.1 now refers to the results or analysis of the control inversion. The term CH2010 is used to refer to results or conclusions from Chevallier et al. (2010) only.

Q.6) p 1924, line 5: Were the ocean fluxes not examined or just not presented in this paper? Just as the discussion of Fig 8 mentioned the possibility of dipoles in the flux across the South American region, a change in fluxes over the land can end up being compensated in the ocean. Given that some of the extra observing sites are coastal, I would expect that it would be worth at least checking the impact of the inversion on the ocean regions around South America.

A) Ocean fluxes were not presented in the original manuscript. Although the focus of our study is on NEE, now we illustrate the impact of the inversions on the ocean fluxes in an updated Fig. 6 (previous Fig. 8) below, over a larger area than that original shown.

Based on this figure, the article now explains that the increments from both inversions (MACCv10.1 and INVSAm) have large patterns which are nearly zonal (or along the prevailing winds) and which overlap continuously the ocean and the land. Therefore, the dipoles oppose different zonal bands rather than some ocean areas vs. some land areas. The zonal positions and strength (i.e. the amplitude of the dipole or of the zonal gradient) of these zonal increments are modified by the inclusion in the inversion of the data from the new stations in region Tropical South America. These effects are more visible when focusing on specific months, while the annual averages smoothens the patterns. In all cases, there is little evidence of direct compensation between land and ocean increments in the area.

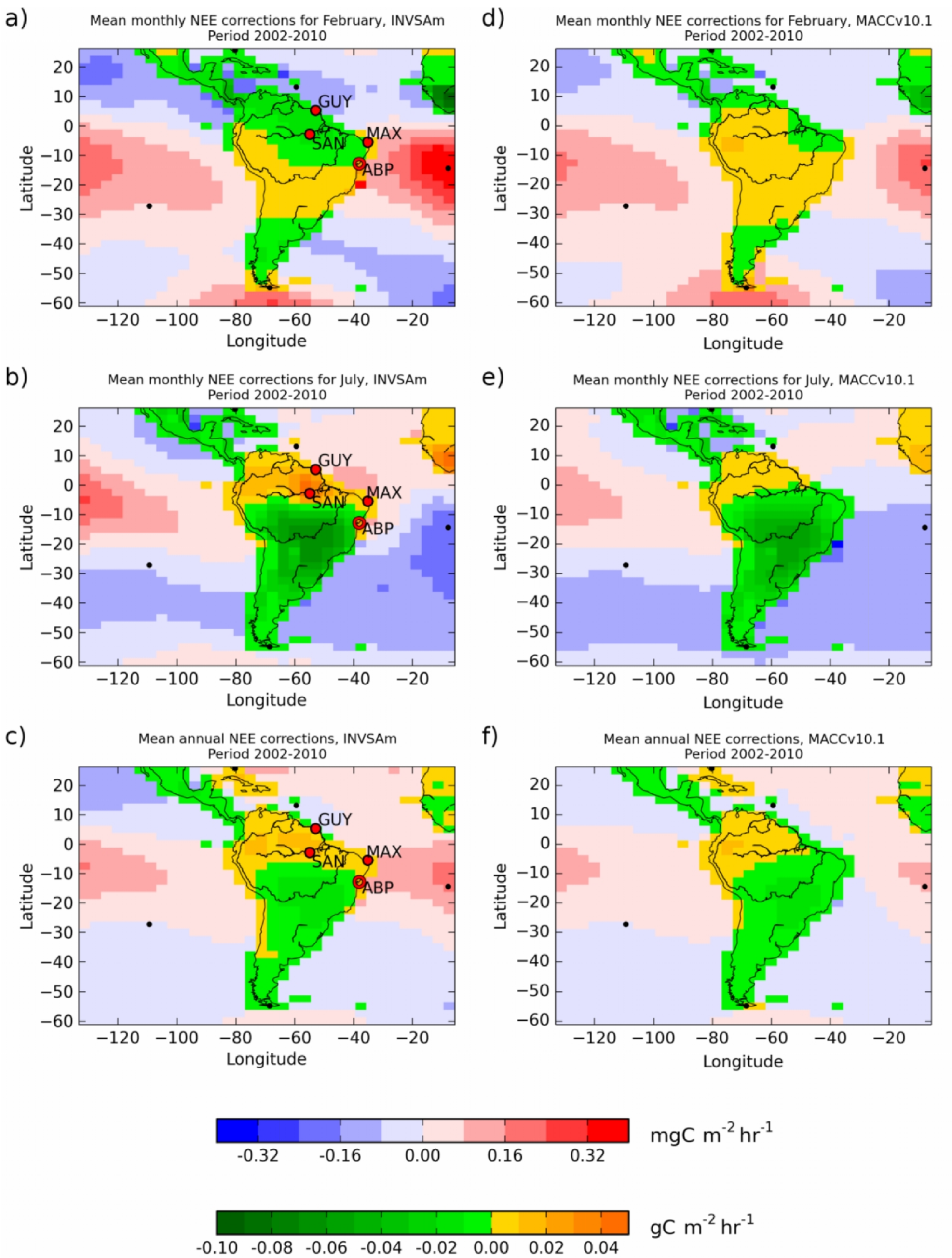

New Fig. 6: Spatial distribution of 2002–2010 mean flux corrections at the transport model resolution (3.75° × 2.50°) to ORCHIDEE from (left) INVSAm and (right) MACCv10.1 over the TSA region: mean for February, July, and mean over the full period 2002–2010. Flux increments over land and ocean are represented with two distinct colour scales and units: green–yellow for land, in gC m^{-2} hr^{-1}; blue–red for ocean, in mgC m^{-2} hr^{-1}. Filled circles indicate locations of sites with continuous measurements; and open circles indicate locations of sites with discrete air sampling.

C) The revised manuscript now includes a new section: "Sect. 3.2 Characterization of the monthly to annual mean inversion increments to the prior fluxes". In Sect. 3.2, we state:

"Figure 6 depicts the increments from both inversions, showing large patterns which are nearly zonal (or along the prevailing winds) and which overlap continuously over land and ocean. Since there is no correlation between the uncertainty in ocean and land fluxes in the B matrix, and given the typical length scale of the correlations in this matrix, this can be directly connected to the signature of atmospheric transport. The contiguous zonal patterns have alternate negative and positive flux increments. There is thus an opposition between corrections in the North and in the South of the TSA region. These corrections are rather negative in the North and positive in the South (positive in the North and negative in the South) during the austral summer (winter). As these corrections are stronger during the austral winter, it results in positive (negative) corrections in the North (South) at the annual scale. Such dipoles are a typical behaviour of inverse modelling systems in data-poor regions (Peylin et al., 2002). However, changes in the amplitude and latitudinal position of this zonal dipole appear to be the main impact from the assimilation of data in the TSA region. This dipole structure may thus yield sensible corrections to the NEE in the TSA area."

Q.7) p 1924, line 9: how does this length scale (500km) compare with the distance between the four sites added to the inversion?

A) Between SAN and GUY the geographical distance is roughly 1000km, but between the other sites it ranges between 2000 and 2600 km approximately. Considering the 500 km correlation length scale in the B matrix only (i.e. ignoring the effect of atmospheric transport), this could suggest that the area directly constrained by the South American sites is relatively small and that GUY and SAN would be the only couple of sites with overlapping areas of influence. However, the station footprint can be significant over land, as illustrated by Fig. 3. Furthermore, as demonstrated by the new Fig. 6, large increments are applied by both inversions, and the South American sites have a large impact on these increments over the entire South America. This is due to the long range extent of the footprints of the South American sites and other sites in the Southern Hemisphere. The South American sites are actually shown to constrain the large scale balance and between the positive and negative corrections north and south of South America and their spatial extent. We now include comments on this topic in the manuscript.

C) We have modified Fig. 3 (see answer to General comment Q.9) in the in the revised manuscript as a response to the comments of Referees on the stations' footprints. It now includes climatological wind speed and direction fields (cf. comment of Referee 3). To address the Referee's comment, Section 2.2 (Assimilated data) in the revised manuscript has been updated:

"Typical influence functions of fluxes for observations at GUY and SAN (the observation "footprints", in Fig. 3b and c, respectively) illustrate that the sensitivity of instantaneous mole fractions to the fluxes rapidly decreases with the distance, mainly due to the typically moderate horizontal wind speeds, so that they should bear a strong signature of local fluxes i.e., of the NEE in north-eastern Amazonia. This, and the fact that the geographical distance between the sites in the TSA region ranges from 1000 to 2600km, i.e. up to five times the correlation length scale in matrix B, could suggest that the area well constrained by the sites in the TSA region through inversion is limited. However, as illustrated in Fig. 3, the station footprints also have modest values over very extensive areas which may also result in significant large-scale constraint from the inversion on the land flux estimates."

C) In addition, based on the analysis of Fig. 6, in Sect. 3.2, we now state:

"(...) changes in the amplitude and latitudinal position of this zonal dipole appear to be the main impact from the assimilation of data in the TSA region. This dipole structure may thus yield sensible corrections to the NEE in the TSA area. The dipole has a high amplitude for MACCv10.1, and even higher for INVSAm. The increments from INVSAm to the annual fluxes often exceed 150% of the prior estimate in terms of absolute values. The highest increments are obtained during austral winter and when the SAN data are available (during the period 2002—2005, see Fig. S1), which is in line with the fact that this site is located more inland than the others. Such high control of the data in the TSA region (even when checking the SAN and MAX, or the MAX, ABP and GUY datasets only) over the zonal patterns of flux corrections also highlights the very large-extent impact of these data, and of the data in the southern hemisphere in general, despite the relatively small spatial correlation length scales in the B matrix, and the limited area in which the station footprints are very high."

Q.8) p 1925, first paragraph: it would be good to have some additional information about each site e.g. latitude, longitude, a brief site description e.g. the surrounding vegetation, distance from coast, sampling height. For ABP (line 10), are the weekly measurements selectively sampled under onshore flow, i.e. are they intended to minimise continental signals? How is the transport model sampled to represent these sites e.g. interpolation to the site location, nearest grid-cell? An offshore grid-cell can be more appropriate for a coastal site (e.g. Law et al, Tellus, 62B, 810-820, 2010).

A) We now include additional information about each site in the manuscript: geographic location in latitude and longitude, altitude of the station and/or sampling height, conditions of the site (i.e. coastal or inland, dominant vegetation type surrounding the site), and for ABP, the strategy for the weekly sampling.

As guessed by the reviewer, the weekly measurements at ABP are sampled under on-shore flow, and are also collected when wind speed > 2 m/s. This could support the idea of representing this coastal site using an off-shore model grid-cell.

However, we checked the wind directions from the ECMWF Interim Reanalysis (which drives the LMDZ transport model) during the time of the day when air samples are available at ABP. Figure A.1 shows the resulting frequency distribution of the ECMWF wind direction (i.e., direction from which the wind blows, in degrees, measured clockwise from the geographical North) at ABP when CO_2 is sampled. The figure confirms that according to ECMWF, ABP is mostly under marine influence, but this is not systematic and the instantaneous wind measurements that have been used to sample on-shore flow at ABP may hide the fact that these measurements were done under intermittent wind conditions so that the air masses could still bear the signature of land fluxes (e.g., from the North).

In any case, our final selection of the best transport model grid-cells to represent each site was based on an objective analysis of the day-to-day variations of the CO_2 selected during the analysis window (12:00 to 15:00 local time) and when the wind speed is > 2m/s. For a given station, the measured variations were compared to the ones modelled in the grid-cell corresponding to this station (in terms of space location), and in the 8 neighbouring cells (which encompassed inland and ocean grid cells when analysing CO_2 at a coastal site). The figure A.2 shows the resulting time series of observed and modelled CO_2 mole fractions at ABP (the layout of the plot corresponds to the geographic layout of the model grid-cells). For this site there is no critical difference between the mole fractions at the coastal and ocean model grid cells, certainly due to the threshold on the wind speed for the data selection. Based on the statistics of the misfits to the observations, we concluded that the grid-cells corresponding to the actual stations locations were systematically better adapted for the representation of these stations, even in the case of ABP.

A more flexible method where a given site could be modelled using different grid cells depending on the wind directions may yield better results. We highlight this in the revised manuscript.

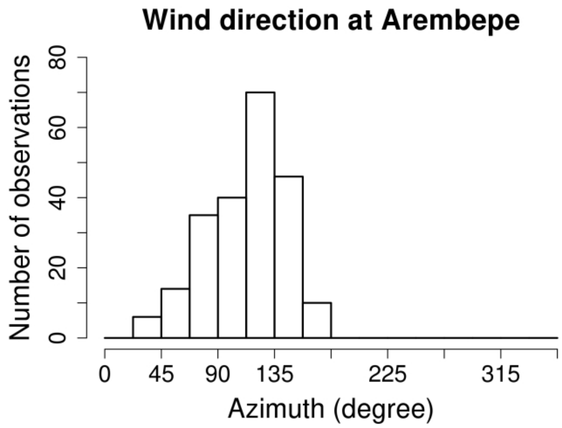

Fig. A.1: Frequency distribution of ECMWF wind direction at Arembepe, when CO_2 samples area available in the time window 12:00–15:00 local time.

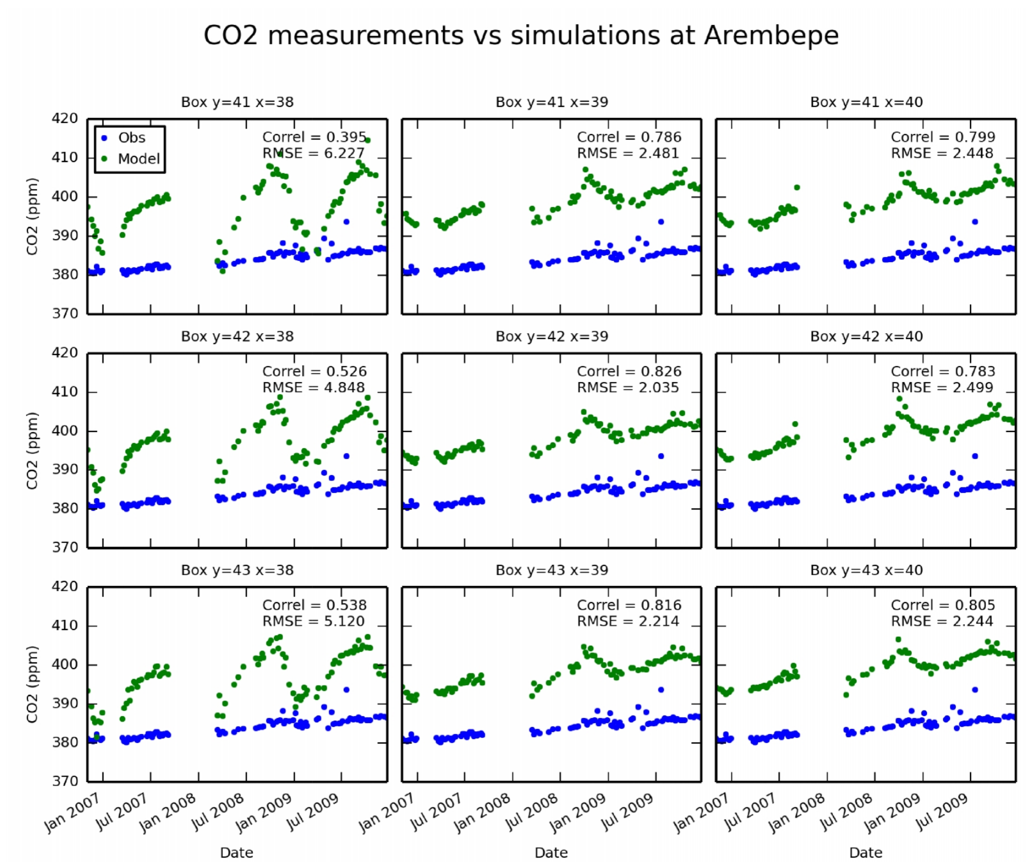

Fig. A.2: Evaluation of the grid-cell of the transport model that best represents the observations at Arembepe. Observations (blue) are selected within the time window 12:00 to 15:00 LT and have been already filtered for wind speed > 2 m/s. Simulated mole fractions (green) are calculated by transporting the prior surface fluxes described in the model setup (Section 2.1).

C) In the revised manuscript, Sect. 2.2 (Assimilated data) has been update as follows:

"MACCv10.1 assimilated measurements of atmospheric CO_2, expressed as dry air mole fractions in µmol mol^{-1} (abbreviated ppm), from 128 surface sites: 35 continuous measurement stations and 93 sites with measurements of CO_2 from discrete air samples collected approximately weekly. 29 sites are located in the tropics, but only two had continuous measurements over the analysis period and none of them were in TSA. In a similar inversion conducted specifically for this study, called INVSAm hereafter, we added new data from four surface sites located in the TSA region. Figure 1 shows the measurement sites used by MACCv10.1 and the four stations added in INVSAm. In the following of this section, we focus on the description of these four stations and on the selection and representation of their data. Details on the data selection and representation at the sites used by MACCv10.1 are provided in CH2010.

Arembepe (ABP) (12.77° S, 38.17° W, 1masl) and Maxaranguape (MAX) (5.51° S, 35.26° W, 15 masl) are coastal stations. The ABP site is located at the edge of the beach, where vegetation consists mostly of grass and beach plants. Data were collected at approximately 8 m above the ground, and consisted of weekly measurements of atmospheric CO_2 with discrete air samples, specifically under on-shore wind conditions, when wind speed > 2 m/s. Air samples were collected preferentially during the afternoon to avoid the influence of recycled air transported from land to the ocean by land breeze during the night and early morning, and transported back to land by sea-breeze during the morning. The MAX site is located on a cliff right next to the coast, and is surrounded by grass and beach plants. At MAX, CO_2 was measured with a continuous analyzer, at approximately 3 m above the ground, and data were reported as 30 min averages. This site is strongly under marine influence: winds are in general > 10 m s^{-1}, and wind direction varies preferentially between 100° and 140° (Kirchhoff et al., 2003) at its location, so that the measurements were taken mostly under on-shore wind conditions. Wind and CO_2 measurements at MAX indicate high CO_2 variations when the wind comes from land. These variations may be strongly influenced by the emissions from the nearby city of Maxaranguape (Kirchhoff et al., 2003). However, as in ABP, this does not occur during the afternoon, when the wind conditions are dominated by sea-breeze (Law et al. 2010).

The Guyaflux site (GUY) (5.28° N, 52.91° W, 40 masl) is located at approximately 11 km from the coast, and is surrounded by undisturbed tropical forest. At GUY, measurements were taken at approximately 55m above the ground (Bonal et al., 2008). They were made with a continuous analyzer, and data were reported as hourly averages. The Santarém site (SAN) (2.85° S, 54.95°W, 78 masl) is located in the tropical Tapajós National Forest, near km 67 of the Santarém-Cuiabá highway, at approximately 750 km from the coast. Measurements were made at 8 vertical levels ranging from ~1 to ~62 m above the ground with continuous analyzers, but only data from the highest level were used in INVSAm. Data were reported as hourly averages.

Figure 2 illustrates the temporal coverage of the observations available in TSA during the simulated period (2002—2010). There is little overlap among the site records, due to calibration problems, interruption of the measurements (e.g., at MAX) and the fact that

some stations have been installed only recently (e.g., at GUY). The longest records were from ABP (3 years: 2007-2009) and SAN (4 years: 2002—2005). Data from the four new sites in TSA have been calibrated on the WMO-X2007 CO_2 scale, managed by the ESRL/NOAA."

In addition, also in Sect. 2.2, we state:

"In a general way, we choose to represent the four measurements sites using the model horizontal grid-cell in which they are located since, for each site, it yields better statistical fit between the prior simulations and the selected measurements than when using neighbour grid-cells."

Q.9) p 1925, line 23 and p 1926, line 5: 'typical' circulation, 'typical' footprints. Is there much of a seasonal shift in circulation? A sentence to comment on this might be helpful.

A) The Fig. 3 has been updated and now depicts a climatology of wind fields from NCEP/NCAR reanalysis (1981-2010), averaged between the surface and a level of 600 hPa, over TSA region during (a) the austral summer (February), (b) austral winter (July), and (c) annual mean. The figure does not show critical seasonal changes in this average atmospheric circulation. The dominant, or typical, mode of horizontal circulation in the lower troposphere across Amazonia throughout the year is characterized by winds entering the Atlantic coast in north-eastern Brazil, through Amazonia and entering back into the Atlantic Ocean south of 20°S. Our selection of figures in Fig. 3 aims at illustrating this pattern. This is now better explained in the revised manuscript.

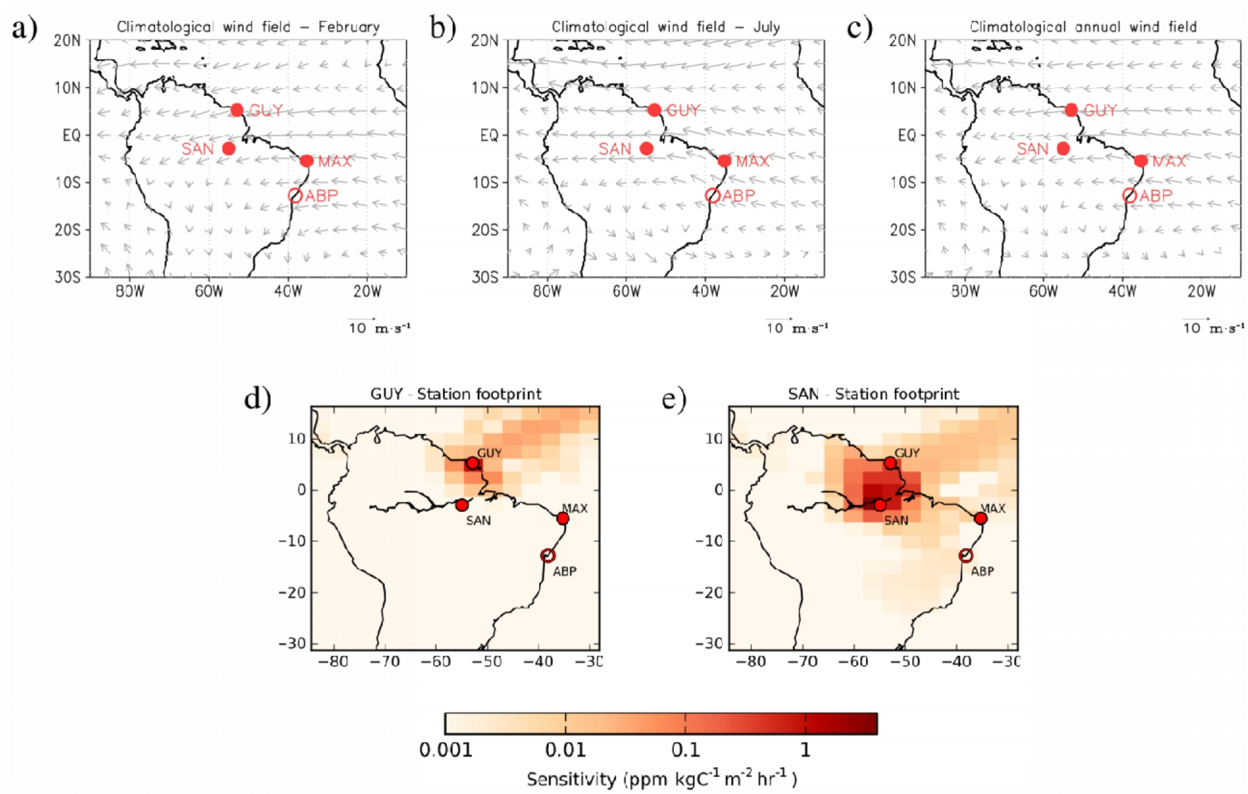

New Fig. 3: Top: Location of assimilated surface stations in South America and climatological wind speed/direction for February (a), July (b), and annual mean (c), averaged over 1981—2010 between the surface and a level of 600 hPa (Source: NCEP/NCAR Reanalysis). Sensitivity of surface atmospheric CO_2 mole fractions measured on 20 February 2009 at 10:00 UTC, at Guyaflux (UTC-3) (d) and Santarém (UTC-4) (e), to a constant increment of surface fluxes during the two days prior to the measurement. Sensitivity values are expressed in log-scale. Open circles: sites with discrete air samplings. Filled circles: measurements taken with continuous analyzers.

C) In the original manuscript, p1925, lines 22—25 have been updated:

“Prevailing winds in the lower troposphere across TSA convey air masses entering from the Atlantic Ocean near the Equator across the continent and back into the southern Atlantic Ocean generally south of 20°S. There are no critical seasonal variations of the mean winds in the area so that this typical behaviour applies throughout the year. The climatology of wind fields from the NCEP/NCAR reanalysis (over the period 1981-2010) for February, July and annual mean, shown in Fig. 3, illustrates this circulation pattern.”

Q.10) p 1925, line 25 to p 1926, line 1: Since MAX is a continuous site, are you able to distinguish in the CO2 observations between periods of onshore vs. offshore flow (e.g. periods of relatively constant ‘background’ CO2 versus highly variable CO2 events). If so, what proportion of the data is from onshore? Is your afternoon data selection favouring onshore flow e.g. due to a sea-breeze circulation? It seems plausible to me that your data selection may be removing those observations that are more likely to have been influenced by the land region.

A) The time series of hourly CO_2 and wind direction measured at the MAX station at any time or selected in the time window 12-15 LT are given figure A.3. The reviewer is right about assuming that we can see a clear signature of on-shore and off-shore flows. Indeed, there are two periods when larger variations in the CO_2 observations can be identified, associated to wind directions > 150º: between 2004-07-08 and 2004-09-21, and between 2005-03-20 and 2005-05-12. The rest of the time, CO_2 observations are rather stable.
The reviewer is also right about assuming that our selection of afternoon data makes us loose on-shore signal as demonstrated by the absence of occurrences of wind directions > 150° and of sub-periods of larger variations in CO_2 when selecting 12-15 data. However, assimilating data outside the chosen time window would have been a challenge, given the difficulties of the models to correctly represent the dynamics of the PBL.
We agree with the reviewer that this reveals that we could select and represent the data in a more flexible and sensible way than what we do here (see the answer to the previous comment on ABP) and this analysis at MAX will be discussed in the manuscript.

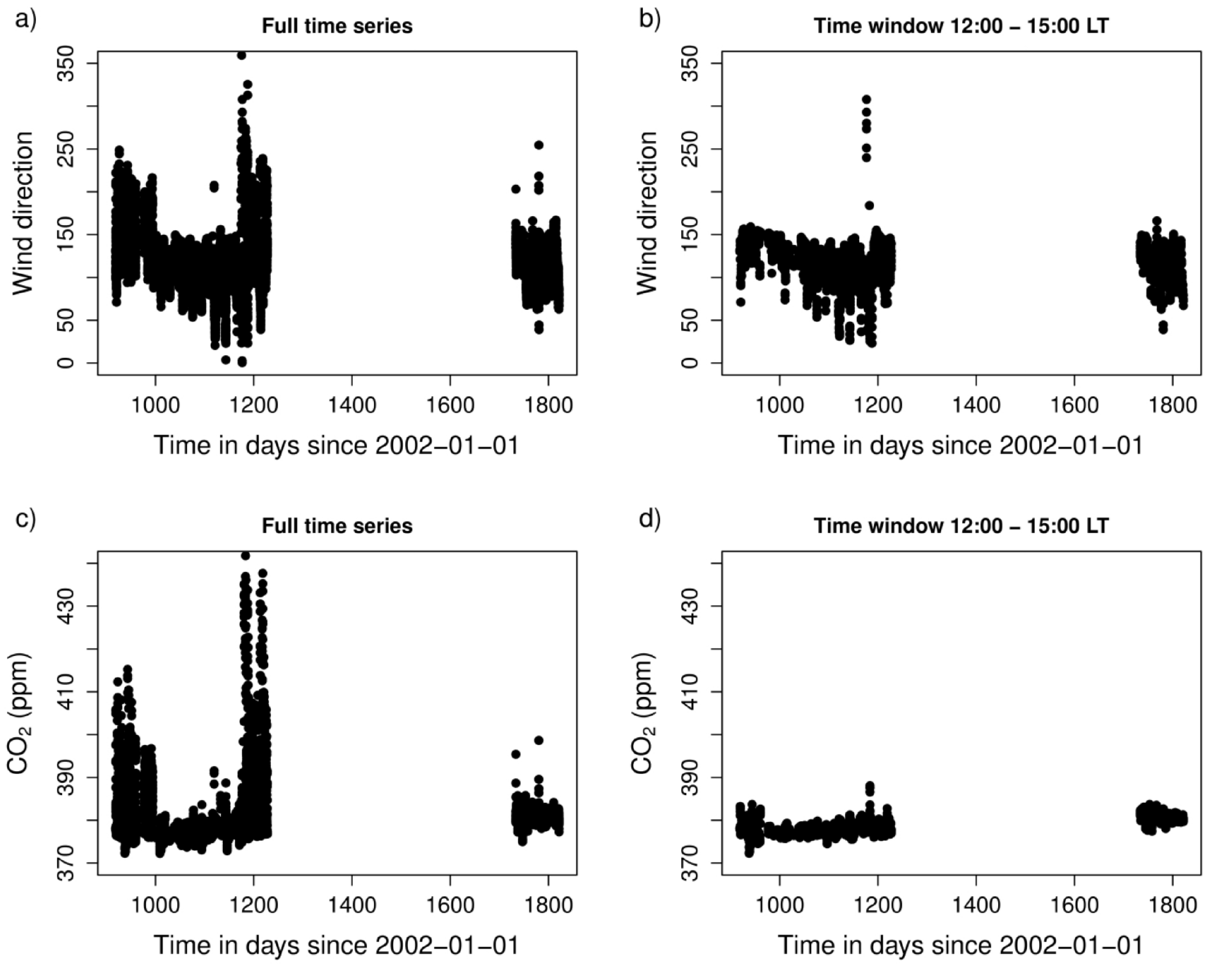

Fig. A.3 Time series of wind direction and CO_2 mole fraction measured at station Maxaranguape for: all the available observations (a,c) and observations within the time window 12:00 to 15:00 LT (b,d). Wind direction in degrees, measured clockwise from the geographic North.

C) In the revised manuscript, in the last paragraph in Sect. 2.2, regarding the site at MAX we state:

"This site is strongly under marine influence: winds are in general > 10 m s^{-1}, and wind direction varies preferentially between 100° and 140° (Kirchhoff et al., 2003) at its location, so that the measurements were taken mostly under on-shore wind conditions. Wind and CO_2 measurements at MAX indicate high CO_2 variations when the wind comes from land. These variations may be strongly influenced by the emissions from the nearby city of Maxaranguape (Kirchhoff et al., 2003)."

"(...) selection of the afternoon data results in ignoring the measurements of off-shore signal at MAX, as explained above, and as confirmed by the analysis of the MAX CO_2 and measured wind direction time series (not shown), and thus the potential for capturing a

clear signature of the regional NEE at this site such as at ABP. However, the off-shore signal is also strongly connected to the local anthropogenic emissions and the inversion cannot exploit reliably such a signature of the regional NEE when the dynamics of the PBL are poorly represented by the atmospheric transport model.”

Regarding the use of a more flexible, sensible strategy for data selection and representation, in the last paragraph in Sect. 4, we state:

“(...) adaptive strategies for the representation of the observations in the model simulations as a function of the sites and of the meteorological conditions (Law et al., 2010) could help loosen the selection of the data for the assimilation.”

Q.11) p 1926, line 18-22:‘root mean square of the annual biases’ It’s not clear to me what exactly has been calculated here- the difference between the CO_2 predicted at a site from the two sets of priors?? ‘given that the mean transport error at the yearly scale should be far smaller according to the hypothesis made when setting-up the inversion system.’ I don’t understand this sentence.

A) Actually, the reviewer correctly describes the comparison and assumptions made, and the text needed some clarification for explaining the aim of this comparison. At each site we calculate the quadratic mean of the annual mean differences between the CO_2 simulated using the two prior estimates of the fluxes (we do not check the data availability at a given site and just take all simulated afternoon values throughout the 2002—2010 period). These differences revealed that the differences in annual budgets between the two prior estimates of the fluxes should yield strong signals at the annual scale at all sites in South America. Given that the weight of the transport error at the annual scale is, in theory, very small (we assume that there is no temporal correlation in the transport), this strong signal should be easy to detect and correct by the inversion system. Therefore we can hope that the inversion system can control the IAV of the fluxes.

C) In the revised manuscript, we have suppressed the discussion on the experiment with the “flat prior” to capture the signal of interannual variability of NEE from the observations. We concluded that it was not clear for the reader and that the revised sections 3.1 and 3.2 discuss in a deeper, clearer manner our initial idea.

Q.12) p 1927-1928, section 3.1 and figure 4: These figures are quite hard to read as the observations are sometimes obscured but they are probably adequate to illustrate the main points covered by the text. (Figures that showed more detail might lead to more insights into the inversion behaviour?) As noted throughout the section the ABP results do not seem consistent with the other sites. The simplest explanation would be that somehow in the analysis/figure the CH2010 and INVSAm time series have been inadvertently switched. Assuming that this has been checked, it is really difficult to explain how an inversion without ABP (CH2010) can fit the ABP data better than the INVSAm case where ABP is included, especially when there is almost no temporal overlap of other Amazonian sites with ABP, so little possibility that the ABP fit is being compromised by fitting other nearby sites. As plotted it appears that the INVSAm case is weakly retaining the seasonality of the prior at ABP while CH2010 manages to almost completely remove it. Were there any inversion settings different between CH2010 and INVSAm which could explain this?

A) Thanks to this comment of the reviewer, we carefully checked the results for ABP. While there was no switch between the MACCv10.1 and INVSAm time series, we had made a mistake when extracting the time series from INVSAm. The new plot and statistics of the posterior model data misfits are much more consistent with what is expected from the assimilation of the ABP data. We apologize for this mistake and thank the reviewer for having helped us to detect it.
We have modified the markers used in Fig. 4 to make the comparisons between observations and modelled estimates easier. We have also updated Fig. 4 and Figure 5 (see below), which summarizes the statistics of the misfits between observations and model simulations. The analysis of those figures has been updated accordingly.

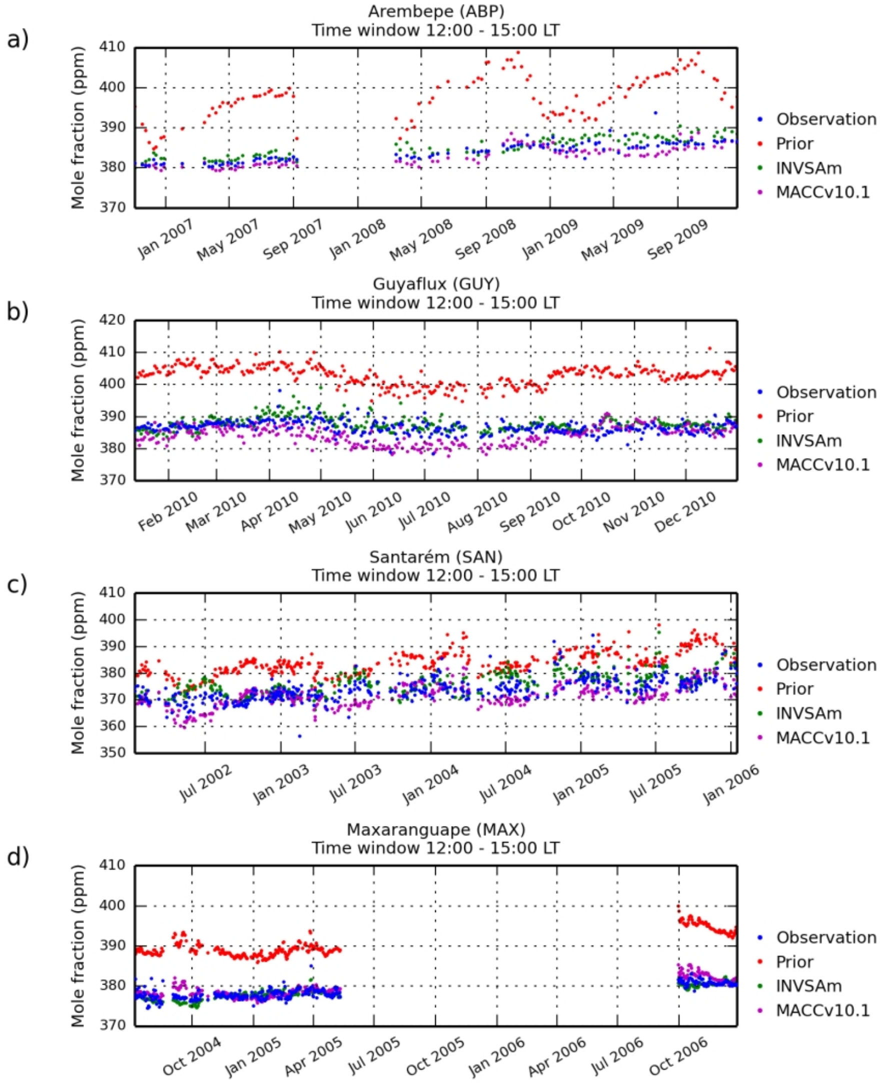

New Fig. 4. Comparison of assimilated CO_2 observations (blue) and corresponding simulated mole fractions using prior fluxes (red), INVSAm (green) and MACCv10.1 (purple), at the new surface sites in TSA. Data shown here correspond to daily average mole fractions between 12:00 and 15:00 local time (LT), when wind speed > 2 m s^{-1}.

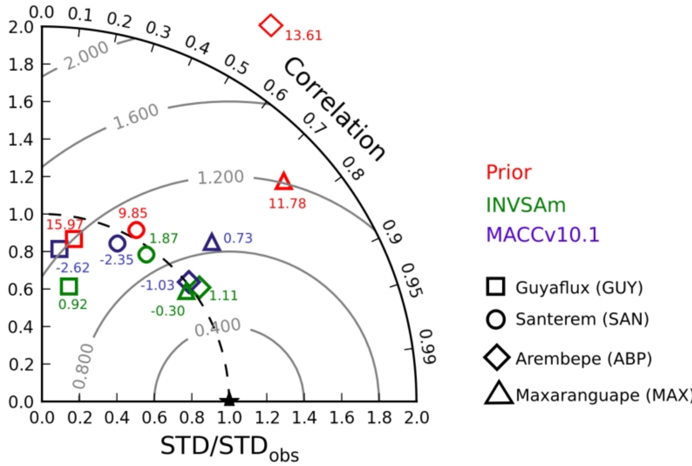

New Fig. 5. Taylor diagram of the statistics of misfits between observations and simulated CO_2 mole fractions between 12:00 and 15:00 LT at Guyaflux (square), Santarém (circle), Arembepe (diamond) and Maxaranguape (triangle), when wind speed > 2 m s^{-1}, using prior fluxes (red), INVSAm (green) and CH2010 (purple). Radial distance from the origin: ratio of SD of simulated mole fractions and SD of the observations. Angle measured from the y axis: coefficient of correlation. Numbers next to the symbols: bias (in ppm). Gray circles: SD of the misfits (in ppm).

Q.13) p 1928, line 12: I'm guessing the correlations are relatively low because you are using daily data but are estimating 8 day mean fluxes. It might be worth calculating the correlations on a monthly timescale as it would be interesting to see if they show a clear improvement between CH2010 and INVSAm because of an improved seasonal cycle.

A) We have now calculated the correlations for monthly mean data at each station and, indeed, in general correlations to the observations are increased for the prior, MACCv10.1 and INVSAm. The corresponding Taylor diagram is provided in figure A.4. We comment these results in the manuscript.

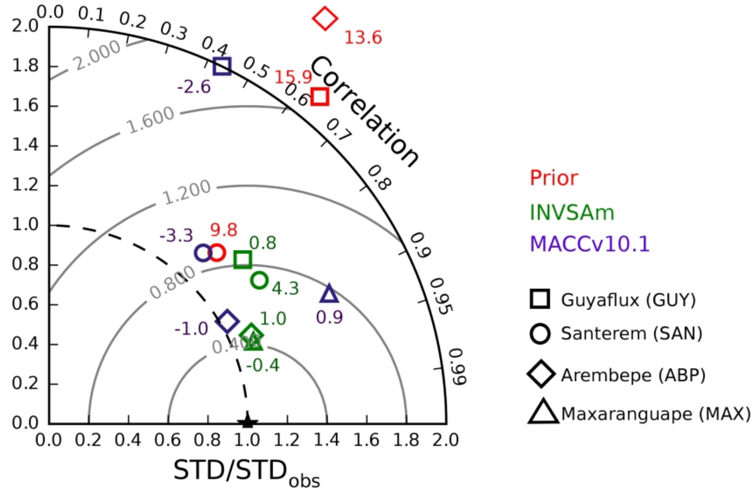

Fig A.4 Taylor diagram of the statistics of misfits between observed and simulated monthly mean CO_2 mole fractions at Guyaflux (square), Santarém (circle), Arembepe (diamond) and Maxaranguape (triangle). Observed monthly means are calculated with observations available between 12:00 and 15:00 LT, and when wind speed > 2 m s^{-1}. Simulated monthly means are calculated from simulated mole fractions between 12:00 and 15:00 LT. Radial distance from the origin: ratio of SD of simulated mole fractions and SD of the observations. Angle measured from the y axis: coefficient of correlation. Numbers next to the symbols: bias (in ppm). Gray circles: SD of the misfits (in ppm).

C) In the revised manuscript, in Sect. 3.1, we comment:

"The best correlations with the observations are obtained with INVSAm at all sites (Fig. 5). The values of these correlations remain generally low, ranging from 0.23 at GUY to 0.81 at ABP. These correlations are based on comparison of daily CO_2 mole fractions while the inversions control 8-day mean fluxes, which strongly limits the ability to impact the mole fractions at higher temporal resolution, and which can thus explain the low correlation values. Correlations between time series of observed and simulated monthly mean mole fractions are higher than those for daily values, ranging from 0.76 at GUY to 0.92 at ABP for INVSAm, with which, again, these correlations are the highest."

Q.14) p 1929, line 25-27: Perhaps it is also worth reinforcing the limited temporal coverage of the observations as another reason why there isn't a large impact on the seasonality.

A) We have added such a comment in the text. To avoid redundancies between the analysis in Sect. 3 and discussions in Sect. 4, we have updated the Sect. 4.

C) In the revised manuscript, Sect. 4, we state:

"The reliability in the seasonal patterns of the inverted fluxes is thus not high. This seems to confirm that the zonal dipoles of increments from the inversion are artificial patterns, which balance the overall correction in the Southern Hemisphere, and which are not necessarily consistent with the actual NEE in the TSA region. We thus conclude that the confidence in the corrections from MACCv10.1 and INVSAm in the TSA region is rather low. This is directly connected to the lack of CO_2 measurements in the TSA region, both in space and time."

Q.15) p 1930, line 3-12 and figure 6b: Am I correct in understanding that for the inversion this is just a regional selection of the data, the inversion itself doesn't do anything differently depending on the pft? If this is right, it might be worth mentioning. In Fig 6b the CH2010 line looks very similar to the CH2010 line in Fig 6a. Is this correct? The other cases all look noticeably different between Fig 6a and Fig 6b.

A) The reviewer is correct about the fact that the PFTs are not accounted for in the inversion configuration and that this analysis for TBE forests is, strictly speaking, just a space selection of the data. Still, we can hope that the spatial patterns of the increments from the inversion could be consistent with the spatial patterns potentially induced by the heterogeneity of the vegetation types in the actual world. This is briefly discussed in the revised manuscript.
There was an error in Fig. 6b concerning the fluxes from MACCv10.1 and we thank the reviewer for pointing out this. The referred figure is now Fig. 7. This figure has been updated (cf. figures below) and shows differences for MACC between Fig. 7a and 7b, as well as for the other flux estimates.

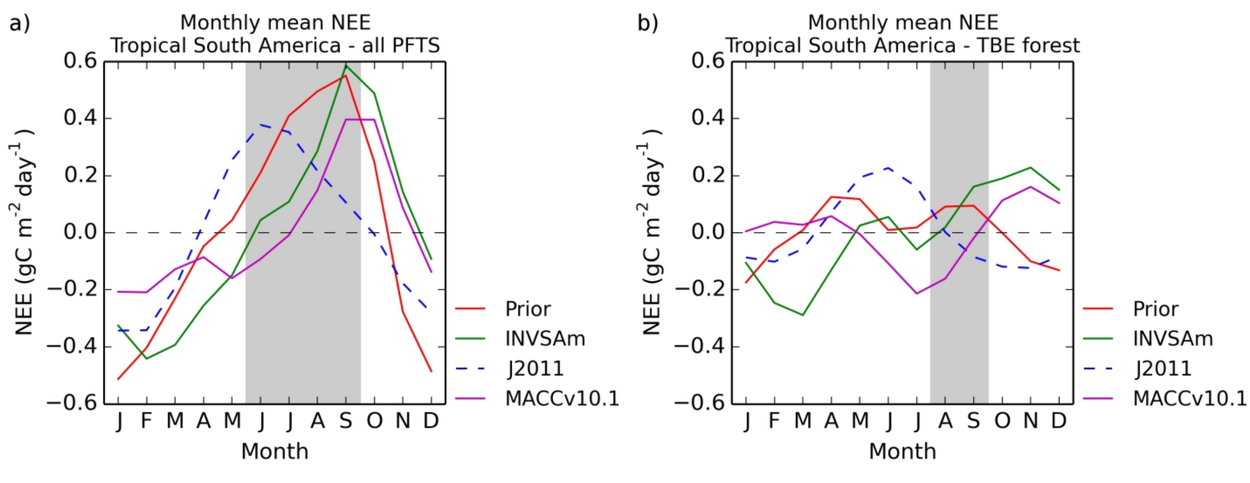

New Fig. 7, panels a,b. Monthly mean NEE integrated over (a) the whole TSA region and (b) over pixels dominated by TBE forests in ORCHIDEE for 2002—2010 . The shaded areas denote dry seasons, defined as months with precipitation < 100 mm, based on monthly totals from TRMM data over 2002–2010. Estimates from prior fluxes (red), INVSAm (green), MACCv10.1 (purple) and J2011 (dashed blue).

C) In Sect. 3.3.1 in the revised manuscript, we comment:

"The inland data are prone to bear a stronger signature from fluxes in tropical broadleaf evergreen and raingreen (TBE) forests (Fig. 8), while the mean seasonal behaviour over the whole TSA region could be mainly related to other PFTs. Therefore, we isolate the results for the area of TBE forests, this area being defined by the selection the model grid-cells dominated by this vegetation type. The configuration of the prior uncertainties in the inversion does not account for PFTs, so that the spread of the flux corrections in the inversions is not forced a priori to depend on vegetation type. We still expect that the variations in the measurements, when their footprint covers different distributions of PFTs, reflect differences in NEE of the PFTs."

Q.16) p 1930, line 13-26: The flux tower precipitation and NEE plots (Fig 6c-f) are not really described in the text and need to be more strongly linked with the results presented in the rest of Figure 6.

A) Previous Fig. 6 is now updated (see previous comment) and renumbered as Fig. 7. The flux tower and precipitation data in previous Fig. 6c-f were not fully exploited in the manuscript, as the reviewer observes. The plots depict the seasonal behaviour of both NEE and precipitation at those sites, and the message we meant to convey from these figures, i.e. the spatial variability of the seasonal cycle of NEE across Amazonia, was already well illustrated by the number of studies referred to in the introduction. We have removed that information from the new Fig. 7. The description of the sites is now provided along those data in Fig. S2 (see below) in the supplementary material.

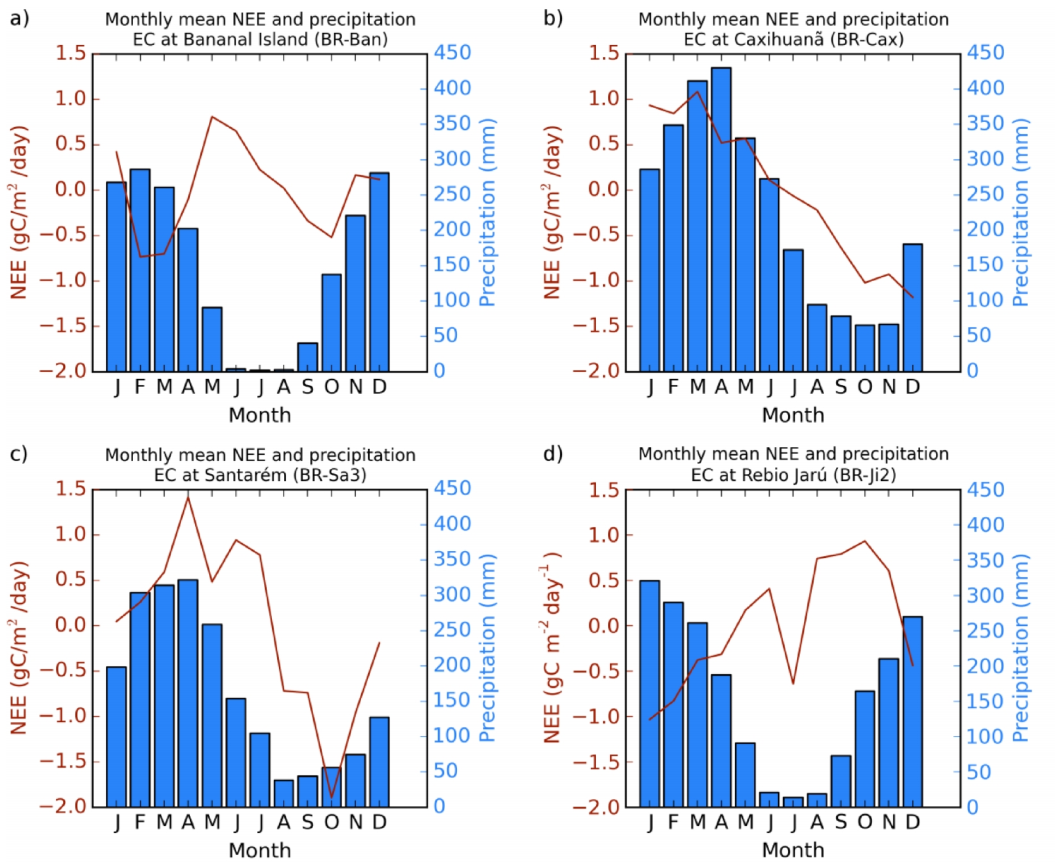

Figure S2. Red: Monthly mean NEE measurements from EC stations at (a) Bananal Island (BR-Ban), (b) Caxihuanã (BR-Cax), (c) Santarém (BR-Sa3) and (d) Rebio Jarú (BR-Ji2). Blue: mean monthly precipitation at the respective station, calculated with data from Tropical Rainfall Measuring Mission (TRMM 3B43 (v6) product) for the same periods for which EC data are available. Location of the EC stations is shown in Fig. S3. For the site at BR-Ban data were available for the period 2000-2002. It is located in a floodplain, in an area of transition between forest and savannah vegetation. A full description is found in Borma et al. (2009). At BR-Cax data were available for 2001-2002. The station is located in an area covered by terra firme humid forest, described by Carswell et al. (2002). At BR-Ji2 data were available for 2000-2002, and is also located in a terra firme humid forest von Randow et al. (2004). At BR-Sa3 data shown were collected at the Tapajós km 83 tower site, an area covered by tropical humid forest, over 2001-2002. A description of the site can be found in Goulden et al. (2004) and Miller et al. (2004).

C) In the revised manuscript we have removed the information regarding the EC and precipitation data. The text has been updated as follows:

"The strong spatial heterogeneity of the time variations of the NEE in TBE forests has been discussed in the introduction. Figure S2 illustrates it with results of local NEE mean seasonal cycle estimated from EC measurements across TSA. This figure also shows the

mean seasonal cycle of the precipitation at these sites to illustrate the spatial heterogeneity of the drivers of NEE within TSA.”

Q.17) p 1931, line 14-18: The change in seasonality in Zone 1 for the INVSAm case might be even clearer if the seasonal cycle was calculated separately for 2002-2005 (when SAN was active) and 2006-2010. A stronger signal in the earlier period would be good confirmation of the influence of SAN data.

A) Following this suggestion, we calculated the seasonal cycle of the four NEE estimates for zone 1 over the two proposed periods: 2002–2005 and 2006–2010 and shown in Figure A.5. The dry season extends September–November on both periods. As anticipated, the strongest changes between MACC and INVSAm take place during the first period, when data from SAN are available, which confirms the critical influence of this site in zone 1. However, there are still significant changes between MACCv10.1 and INVSAm occurring in zone 1 between 2006 and 2010. And, as noticed in answer to major comment 5 of Referee 2, corrections in a zone can be driven by remote measurements and by their difference to South American data as revealed by the large scale structure of the increments shown in the new Fig. 6. So there is no need for having a South American site located in the vicinity of a zone for getting a significant change between MACC and INVSAm in this zone. We comment this in the revised manuscript.

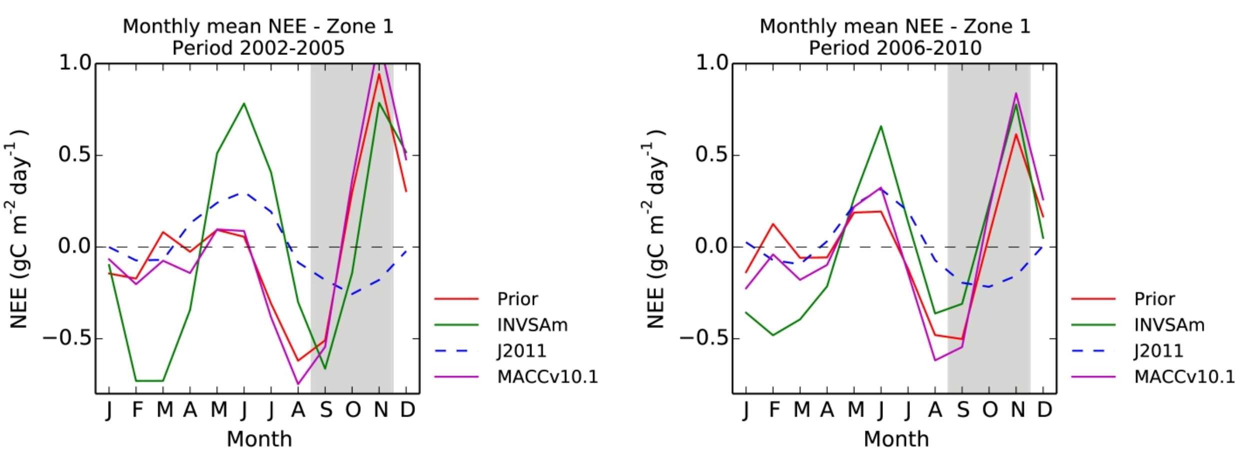

Fig. A.5 Monthly mean NEE at the Zone 1 predicted by (red) prior fluxes, (dashed blue) J2011, (green) INVSAm and (magenta) MACCv10.1 for two periods: (left) 2002–2005, when SAN is active, and (right) 2006–2010.

C) In the revised manuscript, in Sect. 3.3.1, we comment:

“The influence of SAN over this zone is clearer when splitting the analysis period of the mean seasonal cycles between 2002-2005 and 2006-2010 (not shown). The differences between INVSAm and MACCv10.1 are more accentuated during the period 2002-2005,

when SAN is active. However, there are still significant changes between these two estimates during 2006-2010. The changes between MACCv10.1 and INVSAm in Zone 2 (Fig. 7d) are also significant, even though Zone 2 seems hardly observed by the TSA observation network. As analysed in Sect. 3.2, the control of the long-range dipole (of its amplitude and latitudinal position) by the measurements in region TSA explains such an impact of these measurements on the results in Zone 2, as well as that of measurements outside South America, which explains the departure of MACCv10.1 from the prior NEE in zone 2."

Q.18) p 1932, line 1-13 (Figure 8): This is an interesting figure but how do the INVSAm flux corrections compare to the CH2010 flux corrections? Are the CH2010 ones more uniform across the region? This is another figure where averaging over 2002-2005 and 2006-2010 separately would be interesting to try and maximise the signal from SAN.

A) As mentioned above, previous Fig. 8 has been updated and is now new Fig. 6, introduced above, and now shows the results for MACCv10.1, as well. The average increments over land from INVSAm and MACCv10.1 and for the periods 2002-2005 and 2006-2010 are also shown in the Fig. S1. This complements the discussions given above in answer to the comment on ocean fluxes and on the corrections applied in zone 1 by the reviewer.

The assimilation of data in South America generally shifts the zonal dipole in the increment (with a negative / positive gradient from the South to the North in February / July) to the south and amplifies it. Such a behaviour applies to winter and summer, and for the 2002-2005 and 2006-2010 periods. But it is particularly strong in July and for the period 2002-2005, emphasizing the higher weight of data at the most inland site i.e. SAN. The results of new Fig. 6 and Fig. S1 (provided as supplementary material) have lead us to insert a discussion in a new section 3.2.

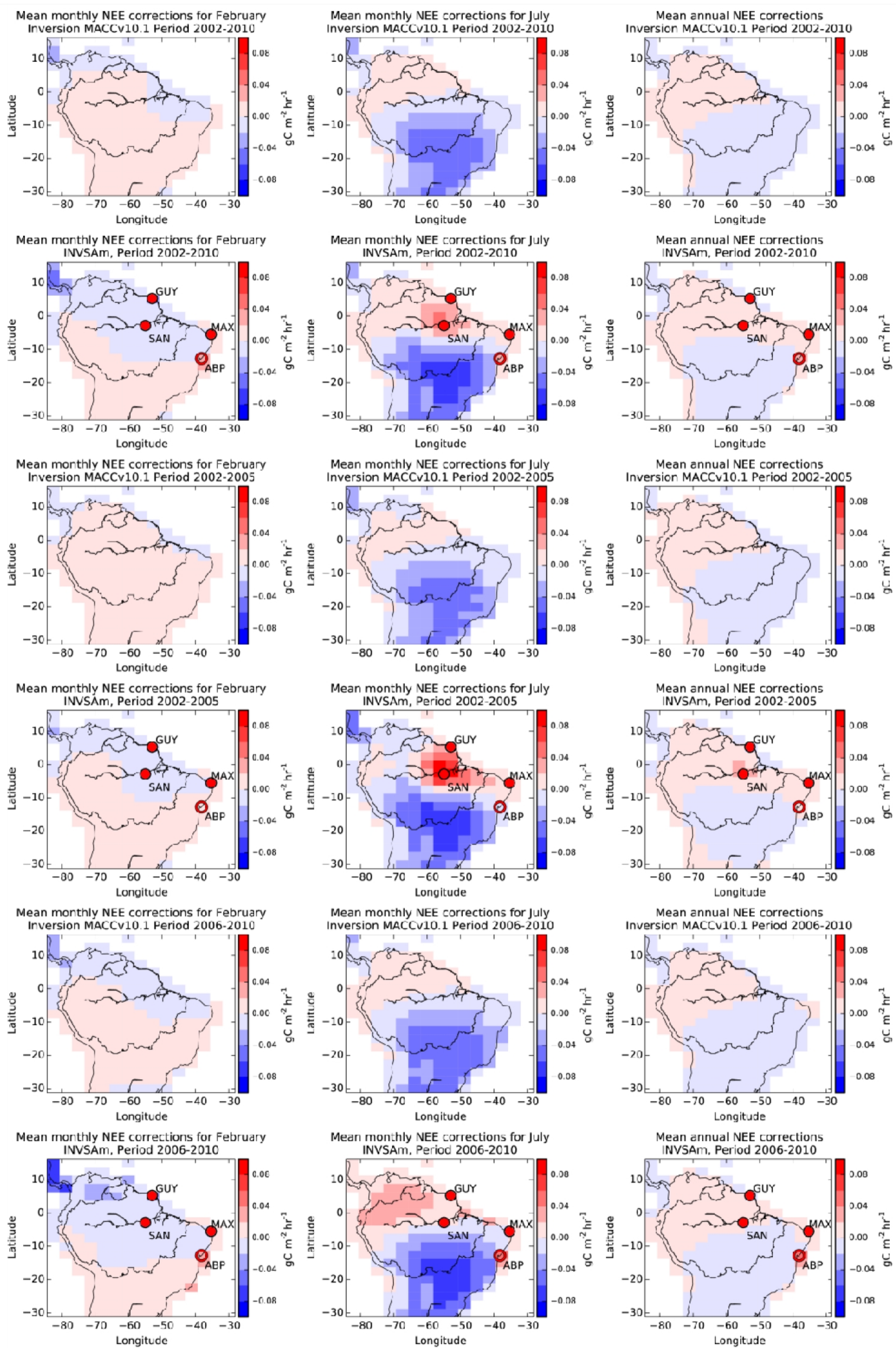

Fig S1. Spatial distribution of mean flux corrections at the transport model resolution (3.75° × 2.50°) to ORCHIDEE from INVSAm and MACCv10.1 over the TSA region: mean for (left column) February, (middle column) July, and (right column) annual mean over the full period 2002–2010(rows 1,2), for 2002–2005 (rows 3,4), for 2006–2010 (rows 5,6). Filled circles indicate locations of sites with continuous measurements; and open circles indicate locations of sites with discrete air sampling.

C) In the revised manuscript, we have inserted the new Sect. 3.2:

"3.2 Characterization of the monthly to annual mean inversion increments to the prior fluxes

Figure 6 shows the spatial distribution of the mean corrections applied during the period 2002—2010 by INVSAm and MACCv10.1 over land and ocean, across an area that covers the TSA area and neighbour regions. In complement, Figure S1 shows the spatial distribution of the corrections over land in the TSA region for the full 2002—2010 period, and for the 2002—2005 and 2006—2010 sub-periods. Both give results for the full years and for the months of February and July. As such, these figures are indicative of the amplitude and spatial extent of the corrections from the inversions, and of the impact of the assimilation of the measurements in South America. Figure S1 even dissociates the impact of assimilating data at SAN and MAX and that of assimilating data at MAX, ABP and GUY by splitting the results between the time periods when these two different sets of data are available. The analysis of the annual mean corrections and of mean corrections for February and July should also give first insights on the significance of the corrections applied to the seasonal cycle and IAV of the NEE in the TSA region.

Figure 6 depicts the increments from both inversions, showing large patterns which are nearly zonal (or along the prevailing winds) and which overlap continuously over land and ocean. Since there is no correlation between the uncertainty in ocean and land fluxes in the B matrix, and given the typical length scale of the correlations in this matrix, this can be directly connected to the signature of atmospheric transport. The contiguous zonal patterns have alternate negative and positive flux increments. There is thus an opposition between corrections in the North and in the South of the TSA region. These corrections are rather negative in the North and positive in the South (positive in the North and negative in the South) during the austral summer (winter). As these corrections are stronger during the austral winter, it results in positive (negative) corrections in the North (South) at the annual scale. Such dipoles are a typical behaviour of inverse modelling systems in data-poor regions (Peylin et al., 2002). However, changes in the amplitude and latitudinal position of this zonal dipole appear to be the main impact from the assimilation of data in the TSA region. This dipole structure may thus yield sensible corrections to the NEE in the TSA area. The dipole has a high amplitude for MACCv10.1, and even higher for INVSAm. The increments from INVSAm to the annual fluxes often exceed 150% of the prior estimate in terms of absolute values. The highest increments are obtained during austral winter and when the SAN data are available (during the period 2002-2005, see Fig. S1), which is in line with the fact that this site is located more inland than the others.

Such high control of the data in the TSA region (even when checking the SAN and MAX, or the MAX, ABP and GUY datasets only) over the zonal patterns of flux corrections also highlights the very large-extent impact of these data, and of the data in the southern hemisphere in general, despite the relatively small spatial correlation length scales in the B matrix, and the limited area in which the station footprints are very high. The inversion also generates patterns of corrections of smaller spatial scale close to the measurement sites in the TSA region when these sites are used by the inversion. This raises hope that

the NEE over the whole TSA region is strongly constrained by the observations, but can also raise questions regarding the spatial variations of the corrections applied by the inversion to the NEE within the TSA region, at least when considering areas at more than 500 km from the measurement sites. However, various pieces of evidence (Fig. 5 and 6, the analysis of the decrease in misfits to the observations from the inversion in section 3.1, and the previous analysis of the high increments to the monthly mean and annual mean NEE over the entire TSA region) indicate that the corrections from the inversion are significant."

Q.19) p 1932-1933, section 3.2.2: I assume the FLAT inversion included the 4 Amazonian sites. This should be noted in the text. Fig 10a shows a large difference in flux anomaly between CH2010 and INVSAm for 2008. Any ideas why, since during this year only ABP data is available and it is relatively remote from zone 1? I'm not sure that I am convinced that 'some patterns of the IAV in the NEE from the inversion seem robust and strongly driven by atmospheric measurements' (p1934, line 24) - even for the significant drought/wet years the results seem quite mixed depending on which region is considered and what prior was used.

A) We have clarified in the revised text that FLAT includes the four new surface sites in TSA region.

Regarding the interannual anomaly for a specific year such as 2008, anomalies can be modified by increments during other years given that the posterior annual anomalies are calculated against the posterior average of the NEE during 2002-2010 (this will be better explained in the manuscript). This explains why large differences in such anomalies can occur between MACC and INVSAm even during years there are few data in South America.

The general behaviour of the inversions illustrated by the new Fig. 6 and Fig. S1 indicates that zones 1 and 2, such as the area of TBE forest, are often located at the edge of the zonal dipole controlled by the assimilation of data in south America, leading to varying (depending on which data are assimilated) interannual anomalies in these zones/areas, as discussed for zone 2 and year 2003 in answer to the comment 5 by Referee 2. However, results should be more stable when considering the entire TSA region.

When referring to the robustness of some IAV patterns (based on the similarity of the results from the different inversions), we referred more specifically to the anomaly observed in 2009 over TSA region, when considering all PFTs (Fig. 9a). This discussion about the fact that the edge of the dipole, crossing the TBE forest area and zones 1 and 2, may give further insights into why the consistency between the IAV from the different inversions does not apply when restricting the analysis to these areas/zones will be conducted in the new manuscript. We have also modified the text to be more cautious when speaking about the 'robustness' of the results.

C) In the revised manuscript, in Sect. 3.3.2, we state:

"FLAT assimilates the data from the four surface sites in TSA in addition to that used by MACCv10.1 such as INVSAm. Of note is that even if increments on the NEE annual budget of a given year from an inversion are weak, the changes in the corresponding annual anomaly from the inversion can be high because the inversion modifies the 2002—2010 average against which the anomaly is computed."

C) In the revised manuscript, the statement referred by Referee 1 has been reformulated:

"(...) some patterns of the IAV in the NEE seem consistent between the different inversion estimates when the atmospheric measurements have a strong control on it: across the TSA region, the estimates from the prior fluxes, MACCv10.1, INVSAm and FLAT indicate small positive flux annual anomalies (CO_2 release) during the drought in 2005 and a strong negative (CO_2 sink) anomaly in 2009, presumably related to lower temperatures and more humid conditions in 2009. However, in 2010 there is a divergence of the results between the FLAT estimate and the others."

Technical corrections

Q) p 1917, line 13-15: Suggest rewrite start of sentence as 'We focused on the NEE impact of the strong droughts ...'

C) The sentence has been reformulated as:

"We attempt at assessing the impact on NEE of the strong droughts in 2005 and 2010 (due to severe and longer-than-usual dry seasons), and of the extreme rainfall conditions registered in 2009."

Q) p 1919, line 14: 'reversal' instead of 'reversion'?

A) We have incorporated this change.

Q) p 1919, line 16: delete ')' at end of sentence

A) Wehave corrected the error.

Q) p 1920, line 20: ‘the inverted pattern...’ Do you mean the opposite pattern is seen in S and W Amazonia compared to E Amazonia? I would rewrite this sentence and avoid the word ’inverted’ because of the potential confusion with using an inversion method to estimate fluxes.

C) We have reformulated the sentence:

“...that also suggests an opposite pattern...”

Q) p 1921, line 5: Figure 1 could be referenced here

A) We have inserted the reference to Fig 1.

Q) p 1921, line 15-22: I would consider moving this description of the J2011 data until later (maybe have a short section 2.3 for ‘comparison data’) in which case you need to change ‘J2011’ on p1921, line 27 to ‘independent flux estimates’.

A) We have moved that description to the section: Sect. 2.3 Analysis of an alternative estimate of the NEE for the evaluation of the inversions.

Q) p 1921, line 22: replace ‘were’ with ‘where’

A) We have incorporated this change.

Q) p 1925, line 17-21: I think the sampling periods are adequately covered in the figure and it is probably sufficient to reduce these three sentences to ‘The longest records were from ABP and SAN.’

C) We have reformulated the sentence:

“The longest records were from ABP (3 years: 2007-2009) and SAN (4 years: 2002-2005).”

Q) p 1926,line 9: Suggest paragraph break before ‘To further ...’. Suggest add ‘designed to remove interannual variations’ following ‘ "flat prior"’.

A) The text in lines 9-24 in the original manuscript has been removed. As mentioned in an answer to Referee 1, this part of the text was not clear for the reader and we decided to convey the message through the discussion in sections 3.1 and 3.2.

Q) p 1926, line 17: insert ‘variability and’ between ‘spatial’ and ‘the temporal’

A) This part of the text has been removed. See previous comment.

Q) p 1928, line 7: ‘amplitude of variations’, on what time scale? Seasonal?

A) We refer to seasonal variations. We have clarified this in sentence.

Q) p 1930, line 26: suggest paragraph break before ‘To examine’

A) We have incorporated the change.

Q) p 1931, line 19: suggest add ‘other’ before ‘sub-regions’

A) We have incorporated the change.

Q) p 1931, line 21: suggest add ‘where the dry season is potentially earlier and more extreme (Fig 6c,f)’ after ‘Amazonia.’ and delete following sentence ‘Both ... (2011)’.

A) We have added the suggested phrase but decided to keep the following sentence because it was actually the study of Lewis et al. (2011) that motivated us to inspect areas most affected in terms of water deficit during the extreme climatic events of 2005 and 2010, first to look at impacts on the seasonality and then for interannual variations of NEE predicted by the different inversion estimates.

Q) p 1931,line 23: suggest delete ‘here’ and add ‘any’ between ‘provide’ and ‘further’

C) We have reformulated the sentence as follows:

"The results, however, do not provide any further information than Fig. 7c,d and are not shown."

Q) p 1931, line 28: might want to note that the slight modifications to NEE are to be expected since there is not much data in the southern part of the TSA region.

C) At the end of the sentence, we add: "maybe because of insufficient data in the southern part of the TSA region. "

Q) p 1933, line 2: suggest adding to the end of the sentence 'opposite to the response for the whole TSA region.'

A) We have incorporated the suggested change.

Q) Figure 1: It would be helpful to label the red sites, perhaps with their initial letter.

A) We have updated the figure.

Q) Figure 2: The vertical line between 2008 and 2009 appears to be missing

A) We have corrected the figure.

Q) Figure 3 caption: perhaps give local time as well as UT for the sensitivity plots

A) We have incorporated the suggested change.

Q) Figure 6 caption: The caption doesn't actually say that it is a NEE anomaly that is shown.

A) We have clarified this in the caption. Figure 6 in the original manuscript corresponds to Fig. 7 in the revised manuscript.

Q) Figure 7 caption: Replace 'Dominating PFTs' with 'Dominant PFT'

A) We have incorporated the suggested change. Figure 7 in the original manuscript corresponds to Fig. 8 in the revised manuscript.

On the ability of a global atmospheric inversion to constrain variations of CO_2 fluxes over Amazonia

Final response to the comments from Referee 2

Questions/comments from the Referee, answers to the comments and changes to the manuscript are presented according with the following notation:

Q) Questions, general, and technical comments
A) Answers to the comments
C) Changes to the manuscript

Q) This study attempts to examine the seasonal and interannual variations of NEE over Amazonia via a top-down approach. Using the MACC project as a baseline, the study added four more surface stations to the observational network and compared the resultant flux estimates. The authors also compared their estimates to those obtained from a bottom-up study in order to isolate the value of: (a) global inversions to constrain fluxes over Amazonia, and (b) additional information from the four surface sites that were not used in the MACC project. Results are disappointing, however, in the sense that these four surface sites added modest positive information, and in certain instances seemingly degraded the quality of the flux estimates (see General Comment #5).

A) We thank the reviewer for his acute comments and sensible suggestions, which strongly helped improving the analyses and discussions of our results.We hope that our answers to his comments demonstrate that we have strengthened these analyses and discussions.

Q) It is unclear whether this is due to an inherent limitation of global inversion frameworks, due to artefacts with the specific inversion framework used in this study or combination of both.

A) It is definitely difficult to distinguish between the limitations that are inherent to the specific global inversion system we use and those that are universal. However, the new analyses in the revised manuscript help characterizing the limitations that are inherent to the existing in situ ground-based network. The lack of information to improve the regional configuration of the inversion parameters such as the prior error covariance matrix and the observation error covariance matrix in Amazonia is now better discussed in relation to the General/Technical Comments of the reviewer.

Q) Neither the methodological framework nor the overall conclusions (i.e., challenge associated with teasing out subtle regional signals from a global coarse-resolution inversion) are new.

A) Still, our attempt at analyzing results from global inversions at high resolution over Amazonia in such detail, and the analyses of the impact of the assimilation of regional measurements that have been barely (never, for some of them) used previously, is new. Some conclusions are directly connected to these specific aspects of the study.

Q) While the paper may be acceptable for publication in ACP (as part of the special issue), I would strongly recommend that the authors incorporate a discussion on the uncertainties associated with their flux estimates (see #1 below). This would make the study, and the overall findings, more robust and valuable to the community.

A) We have included a discussion on the uncertainties in Sect. 2.1 (see response to General Comment Q.2) and on the significance of our results in Sect. 3.1 (response to General Comment Q.1.3) and Sect. 3.2 (response to General Comment Q.3) that follows the answers given below to the comments of the reviewer on those specific topics.

General Comments:

Q.1.1) My biggest disappointment is that no attempt has been made to provide posterior uncertainty estimates, which makes the study incomplete. The authors sidestep the calculation of uncertainties due to the computational expense (Page 1922, Lines 25-27); presumably because for the variational approach a Monte-Carlo algorithm has to be implemented (e.g., Chevallier et al. [2007], JGR-A, doi:10.1029/2006JD007375).

A) Yes, this is the case and it is clarified in the manuscript (see also our answer to General Comment Q.2 from Referee #2). Of note is also that, in general, such Monte Carlo experiments are conducted for a typical year only, due to their huge computational cost. However, here, in order to assess the impact of the South American sites, which have a weak overlapping in time, such experiments would have had to be conducted for at least 4 different years and for the two MACCv10.1 and INVSAm configurations. Actually, since this study focuses on mean seasonal cycles and inter-annual variations, the Monte Carlo computations wouldhave had to be conducted for an even larger number of years.
We should also mention that this request for computationally intensive Monte Carlo simulations is the drawback of solving for the fluxes at the weekly and transport grid scale. A coarser-resolution inversion system may have provided posterior error estimates much more easily. However, it would have been more difficult to investigate the spatial variability of the fluxes within Amazonia and to avoid aggregation errors (which likely already hamper the results in this study) with such a coarser system.

Q.1.2) But any attempt to reconcile the top-down and bottom-up estimates cannot be assessed when we do not know whether the differences between the two sets of estimates are significant or not.

A) The analysis of the increments from INVSAm vs. those from MACCv10.1 (see response to General Comment Q.3 of Referee #2, and figures 7 and 9 in the revised

manuscript) demonstrates that the impact of the South American sites is high (at the transport grid scale, the increments from INVSAm to the annual fluxes generally exceed 150% of the prior estimate in terms of absolute values). Large increments from the inversion indicate that the theoretical uncertainty reduction is high provided that the error statistics assigned in the inversion system are consistent with the actual errors. In that sense, the impact of the South American sites should be significant. The computation of theoretical uncertainty would not bring much more information about the significance of the impact of the South American stations given the modest confidence that we have in the error statistics for the Amazonian area, as explained in the answer to the second major comment of the reviewer. This is now discussed in a new section in the revised manuscript.

Q.1.3) At a minimum, do the simulated observations from INVSAm capture the assimilated observations within 95% of their confidence intervals?

A) Table A1 below (provided as supplementary material) compares the standard deviations of the prior and posterior misfits between the simulations and the observation, and the ~95% confidence interval (two standard deviations) of the configuration of the observation errors (for hourly observations) in the inversion system (following section 2.1). The prior misfits are much larger than our observation errors at ABP, MAX, and GUY which makes the prior simulation lie outside the 95% confidence interval of the observation error except at SAN (where prior misfits are still slightly larger than the observation error). Misfits between MACCv10.1 and the observations are similar to the prior misfits at SAN and GUY and much smaller than the prior misfits at the coastal sites ABP and MAX, which could be related to a very large scale improvement of the fluxes in the Southern Hemisphere. The corrections from MACCv10.1 thus make the posterior simulation fall within the 95% confidence interval of the observation error at all the sites but GUY. When assimilating the data from the South American sites, misfits are decreased compared to both the prior and MACCv10.1 at all sites. The INVSAm posterior simulation still lies in the 95% level interval of the observation error at ABP, MAX, and SAN and nearly reaches the threshold at GUY. It is close to the 68%confidence interval at MAX and within this interval at SAN, while it was not the case for MACCv10.1. This and the high increments (in terms of relative difference to the prior fluxes) applied to the fluxes in South America both in MACCv10.1 and when adding South American stations lead us to consider that the corrections from the inversion are significant, even though we do not have the means for deriving the actual statistical significance. We discuss this in Sect. 3.1 of the revised manuscript.

Table A1

	Standard deviation of the misfits Model – Observation			
Station	**Prior**	**INVSAm**	**MACCv10.1**	**2 * (Standard deviation of the model error)**
ABP	**4.4**	**1.5**	**1.6**	**2.2**
MAX	**2.1**	**1.1**	**1.5**	**2.0**
SAN	**4.6**	**4.0**	**4.6**	**9.6**
GUY	**4.0**	**3.5**	**4.1**	**3.3**

C) In the revised manuscript, Sect. 3.1, we include the following discussion:

"The significance of the reduction of the misfits between the mole fractions observed and simulated from the inversion is seen from the comparison between the standard deviations of these misfits and the estimate of the standard deviation of the observation errors (i.e. of the transport model errors) for hourly values in the configuration of the R matrix (Table A1, in supplementary material).According to this comparison, the prior misfits are much larger than the observation errors at ABP, MAX, and GUY, but are slightly smaller than these at SAN. Misfits between MACCv10.1 and the observations are similar to the prior misfits at SAN and GUY and are much smaller than the prior misfits (and smaller than the 95% confidence interval of the observations) at the coastal ABP and MAX sites. Misfits are further decreased when assimilating the data from the South American sites: they are about the standard deviation of the observation errors at all sites but GUY (where they are twice as large)."

Q.1.4) Error bounds will also allow better judging the performance in Figures 6 and 9. Hence, I would strongly encourage the authors to reconsider their decision to skip the calculation of these posterior uncertainties.

A) As explained above, deriving theoretical uncertainties for the mean seasonal cycle and the inter-annual anomalies is not affordable in the framework of this study (see our answer to General Comment Q.1.1 from Referee #2). Furthermore, as detailed in the answer to the reviewer's General Comment Q.1.2, such theoretical numbers are not critical for judging the performance of the system. Even though we prefer not to launch such computations of the theoretical uncertainties, we discuss better this topic in the revised manuscript, based on our answers to the reviewer.

Q.2) The lack of discussion on uncertainties is also related to choices that have been made about the prior covariance. Why did the authors persist with using correlations in B that are based on data from towers in the Northern Hemisphere? Are there alternatives to the Chevallier et al. [2006] approach that the authors could have used to determine a more suitable B for the study region? Even though this study solves for global fluxes, the use of correlations that are appropriate for the Amazon basin seems necessary. Can the authors comment on their choice?

A) The reviewer is right about the fact that some lack of confidence in the configuration of the prior and observation error covariance for the limited and specific area, on which this study focuses, is an important explanation why we think that the computation of theoretical uncertainties would not be useful while highly expensive. A reliable estimate of the posterior uncertainty and uncertainty reduction strongly depends on the reliability of the description of prior and observation errors in the configuration of the inversion system.
The statistics of B are based not only on results from Chevallier et al. (2006) but also on that from Chevallier et al. (2012) which made use of available eddy covariance sites in south America (see the figure 1 in Chevallier et al. (2012), GBC, doi:10.1029/2010GB003974). We believe that the use of eddy covariance measurements is presently the best way to assess the statistics of the prior uncertainties at the time and space scales for which the B matrices need to be setup. Some computations of the standard deviation of misfits between ORCHIDEE and eddy covariance measurements in South America indicated that the configuration of the standard deviation of the prior uncertainty at the weekly scale was robust for this continent as well as for others.
However, the small number of eddy covariance measurement sites in South America prevented us from deriving spatial correlations specifically for this continent. This explains why we used in South America the scales derived using the global eddy covariance dataset, which is strongly biased by the higher number of sites in the Northern hemisphere.
Furthermore, the method used to model the observation error in CH2010 and in our study has been developed and evaluated based on analysis of model data comparisons using mainly atmospheric data from the mid latitudes in the Northern Hemisphere (due to the limited coverage of other areas). Specific sources of transport modelling errors in Amazonia (Parazoo et al., Atmos. Chem. Phys., 8, 7239–7254, 2008), such as the deep convection, may not be well reflected by the computation proposed by CH2010.
Finally, the configuration of the prior and observation error covariances in MACCv10.1, as is often the case in global inversion systems, have been evaluated at very large spatial scales, which are the primary target of such global inversion systems. Focusing on Amazonia and even on some specific sub-areas of this region questions the reliability of this configuration when analyzing finer scales, and in particular the use of an isotropic and homogeneous correlation modelling.
The analysis and discussion of our results with real data suggested little confidence on these statistics for Amazonia. This leads us to think that the theoretical computations of the uncertainty reduction would not bring more insights about the reliability of the increments from MACCv10.1 and INVSAm. We now discuss this topic in the revised manuscript.

C) In the revised manuscript, Sect. 2.1, we comment:

“There is a moderate confidence in the adequacy of these error statistics assigned in the global inversion system for the specific TSA area studied here, both because B was designed mostly with statistics gathered in the Northern Hemisphere, and because R may not well account for the uncertainty in the atmospheric convection model, while this could be high in Amazonia (Parazoo et al., 2008). We also investigate here variations of the fluxes within TSA at spatial scales that are not much larger than the e-folding correlation length in B, and these variations in the inversion results may be affected by our simple hypothesis of isotropic correlations in the prior uncertainty. This lack of confidence in the input error statistics weakens our confidence in the posterior error statistics that can be derived based on the inversion system, even though they may be realistic at zonal scale for the Tropics (Chevallier and O’Dell, 2013). In this context, and given the relatively high computational burden of the posterior uncertainty computations for grid-point inversion systems (using Monte Carlo approaches with ensembles of inversions, Chevallier et al. 2007), we do not derive these posterior uncertainties for our domain and its sub-domains.”

Q.3) How likely is it that the dipole issue (Figure 8, also Page 1932, Lines 5-12) is related to the spatial correlations that have been pre-specified in B? In fact in Lines 10-12, the authors seem to question their own choice of B. In order to completely investigate this dipole issue, the authors may need to look at the ocean fluxes. As the focus of this study is on the land component, I agree with the decision of the authors to skip any discussion on the ocean fluxes (Page 1924, Line 4). But in light of the dipole issue as well as the negative results, it may be worthwhile to add as supplementary material a discussion on the ocean fluxes; for example, even a spatially-aggregated evaluation with respect to the MACCv10.1 (or CH2010) product may provide some insights on the performance of the inversion system.

A) The answer to General Comment Q.2 from the reviewer gives more details about the lack of confidence in B over Amazonia.However, regarding the dipole, it seems to be mainly driven by a large-scale behaviour of the inversion connected to the atmospheric transport rather than by the B matrix, as demonstrated by the increments to the ocean fluxes. We comment this in the revised manuscript. Our original discussion on the dipole could have been misleading regarding the role of B in the dipole and has been reformulated in the new section 3.2.
Previous Fig. 8 has been updated (new Fig. 6 in the revised manuscript, see below)andnow depicts corrections for both the ocean and land fluxes (with different colour scales and units due to the different order of magnitude between increments over land and ocean) and over an area larger than that shown originally. Based on this figure, the manuscript now explains that the increments from both inversions have large patterns which are nearly zonal (or along the prevailing winds) and which overlap continuously the ocean and the land. This continuity, and the fact that in the B matrix there is no correlation between the land and the ocean, demonstrate that the dipole is not mainly driven by the structure of B. Actually, the dipole opposes different zonal bands rather than some ocean areas vs. some land areas. The zonal positions and strength (i.e. the amplitude of the dipole or of the zonal gradient) of these zonal increments are

modified by the inclusion in the inversion of the data from the new stations in the Tropical South America region. These effects are more visible when focusing on specific months, while the annual averages smoothens the patterns. This is commented in the new Sect. 3.2.

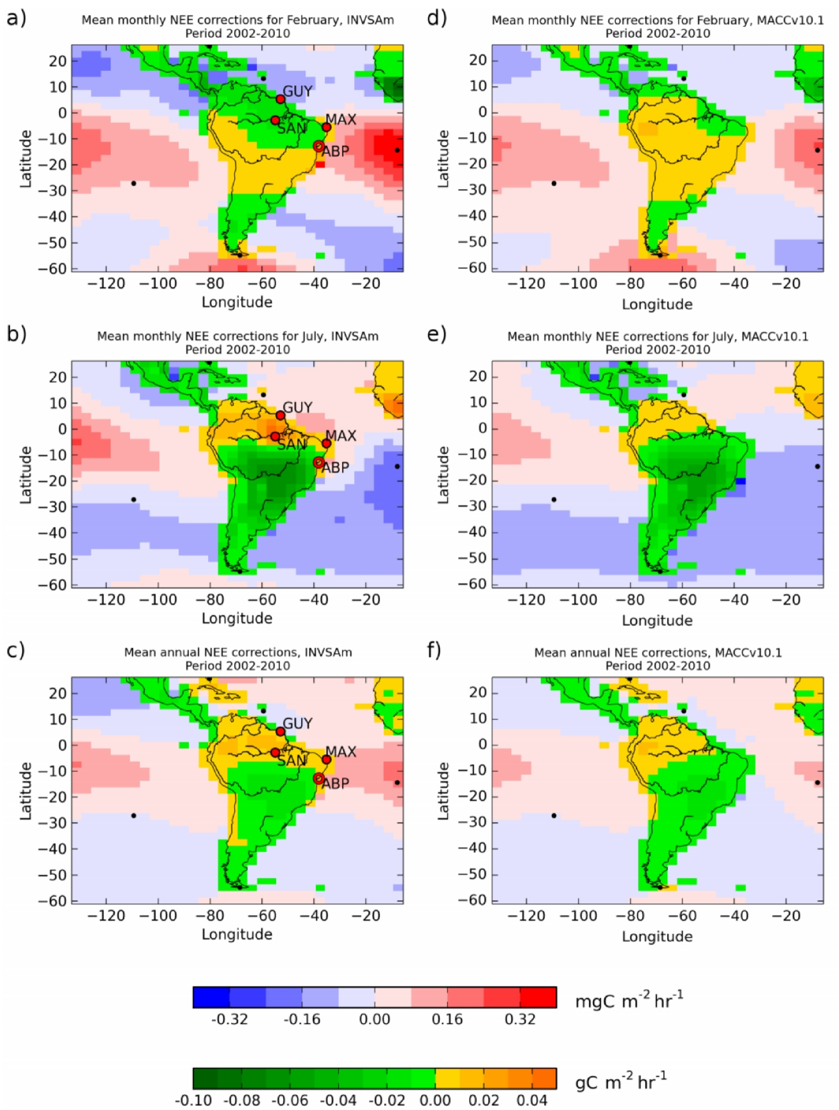

New Fig. 6: Spatial distribution of 2002-2010 mean flux corrections at the transport model resolution (3.75° × 2.50°) to ORCHIDEE from (left) INVSAm and (right) MACCv10.1 over a larger area than TSA region: mean for February, July, and mean over the full period 2002-2010. Flux increments over land and ocean are represented with two distinct colour scales and units: green-yellow for land, in gC m^{-2} hr^{-1}; blue-red for ocean, in mgC m^{-2} hr^{-1}. Filled circles indicate locations of sites with continuous measurements; and open circles indicate locations of sites with discrete air sampling.

C) A new section, "3.2 Characterization of the monthly to annual mean inversion increments to the prior fluxes" has been included in the manuscript. In this section we state:

"Figure 6 depicts the increments from both inversions, showing large patterns which are nearly zonal (or along the prevailing winds) and which overlap continuously over land and ocean. Since there is no correlation between the uncertainty in ocean and land fluxes in the B matrix, and given the typical length scale of the correlations in this matrix, this can be directly connected to the signature of atmospheric transport. The contiguous zonal patterns have alternate negative and positive flux increments. There is thus an opposition between corrections in the North and in the South of the TSA region. These corrections are rather negative in the North and positive in the South (positive in the North and negative in the South) during the austral summer (winter). As these corrections are stronger during the austral winter, it results in positive (negative) corrections in the North (South) at the annual scale. Such dipoles are a typical behaviour of inverse modelling systems in data-poor regions (Peylin et al., 2002). However, changes in the amplitude and latitudinal position of this zonal dipole appear to be the main impact from the assimilation of data in the TSA region. This dipole structure may thus yield sensible corrections to the NEE in the TSA area. The dipole has a high amplitude for MACCv10.1, and even higher for INVSAm. The increments from INVSAm to the annual fluxes often exceed 150% of the prior estimate in terms of absolute values. The highest increments are obtained during austral winter and when the SAN data are available (during the period 2002-2005, see Fig. S1), which is in line with the fact that this site is located more inland than the others.

Such high control of the data in the TSA region (even when checking the SAN and MAX, or the MAX, ABP and GUY datasets only) over the zonal patterns of flux corrections also highlights the very large-extent impact of these data, and of the data in the southern hemisphere in general, despite the relatively small spatial correlation length scales in the B matrix, and the limited area in which the station footprints are very high. The inversion also generates patterns of corrections of smaller spatial scale close to the measurement sites in the TSA region when these sites are used by the inversion. This raises hope that the NEE over the whole TSA region is strongly constrained by the observations, but can also raise questions regarding the spatial variations of the corrections applied by the inversion to the NEE within the TSA region, at least when considering areas at more than 500 km from the measurement sites. However, various pieces of evidence (Fig. 5 and 6, the analysis of the decrease in misfits to the observations from the inversion in section 3.1, and the previous analysis of the high increments to the monthly mean and annual mean NEE over the entire TSA region) indicate that the corrections from the inversion are significant."

Q.4) Page 1934, Lines 18-20: The authors state – "...the inversion system may have applied corrections in response to events registered by only a single station at a time". I am not sure what the authors mean here. Do the authors imply that even though observations from a particular site were available for a few years, it negatively impacted the analyses over other time periods? Based on my understanding, in the variational system the analysis window spanned the full period from 2002-2010. If so, did the authors consider breaking up the analysis window into smaller time-chunks, for example, 2 or 3 year periods with overlapping 2-3 months in between?

A) Our statement was a bit confusing and has been reformulated. Corrections applied in response to a specific event at a given site should not spread in time to such an extent that it would impact the results during years when there is no data available at this site, and we do not think that we should verify it by conducting inversions on 2-3 year periods (however, see the analysis of the results for 4-5 year periods in answer to the Referee#1, in figure S1, which helps isolate the impact of the different sites; see also the results for the year 2003 when SAN data only were available in answer to the General Comment Q.5 of Referee #2). Still, these specific corrections would have less weight in the average increments in the area if the data availability was higher. We confusingly made a shortcut between giving more weight to a short term event in the mean corrections and applying mean corrections in answer to such short term events.
In the revised manuscript we discuss this topic based on the answers to the Referee#1 and to the General Comment Q.5.

C) Lines 11-20, p1934, of the original manuscript have been rewritten. The original statement above has been reformulated as follows:

"The limited overlap among the TSA observations is a critical issue since measurements are often only available at a single site at once, and consequently, temporary model errors at this site can get far more weight in the inversion than if it had been balanced by information from other sites."

Q.5) Figure 10, Panel b: For 2003, the annual NEE anomalies in Zone 2 are extremely counter-intuitive. What causes the difference in sign of the anomalies, i.e., negative anomalies from INVSAm but positive anomalies from MACCv10.1 (or CH2010)? If we use the J2011 as a baseline (ignoring the magnitude and only looking at the sign of the NEE anomaly), then the INVSAm anomaly is likely inaccurate. For Zone 2, a plausible cause of the difference between INVSAm and MACCv10.1 is due to the assimilation of data from the SAN site. But again based on the limited footprint information (Figure 3), the observations at SAN may not be sensitive to Zone 2 fluxes. Hence if there are no useful information in the SAN observations to constrain Zone 2, shouldn't the INVSAm fluxes and thereby the anomalies be of similar sign and magnitude to the MACCv10.1 and/or close to the prior flux estimates?

A) The anomaly for a given year can actually be modified by increments during other years given that the posterior annual anomalies are calculated against the posterior average of the NEE during 2002-2010. This is now clarified in the revised manuscript.
Furthermore, figure A.6 (showing the inversion increments in 2003) below demonstrates that while MACCv10.1 applies positive increments in zone 2 in 2003, INVSAm applies

negative increments due to the assimilation of SAN data. Since, on average over 2002-2010, both inversions apply positive increments in this zone (cf. new Fig. 6) this leads to a clear negative anomaly in zone 2 for INVSAm. The discussion on the dipole (cf. answer to General Comment Q.3) and on its zonal structure indicates that the footprint of the sites needs to be considered entirely, i.e. that the inversion strongly uses the parts of these footprints where the values of sensitivity are relatively low to apply long-range corrections. Corrections in zone 2 in INVSAm could be driven by remote measurement sites and by their difference to SAN data. This corresponds to the amplification and displacement of the zonal dipole discussed in answer to the General Comment Q.3 and which we also observe in 2003 as indicated by Fig. A.6. The anomaly in 2003 for INVSAm can thus be considered as an artefact from the limited data availability in South America. This is discussed in the revised manuscript.

The comparison to J2011 is delicate since J2011 exhibits too little interannual variability for region TSAand bears substantial uncertainties (see answer to the Technical Comment Q.T13).

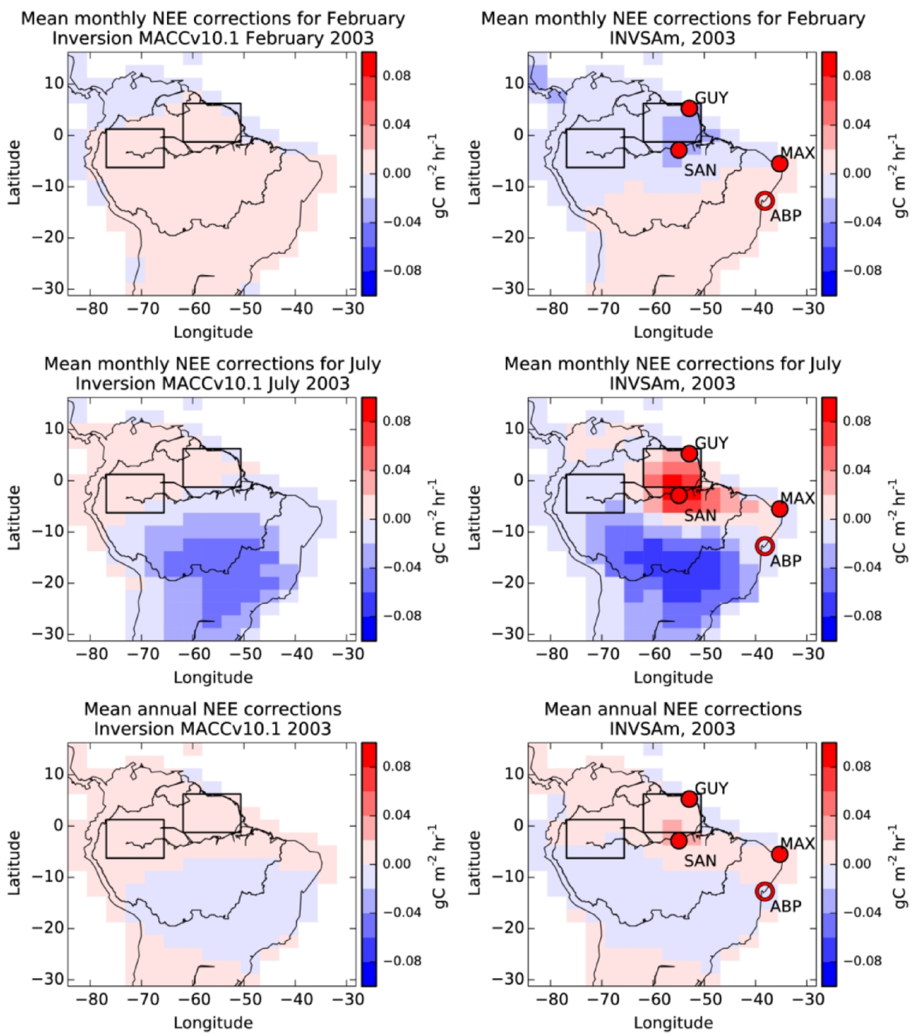

Fig. A.6 Spatial distribution of mean flux corrections in 2003 at the transport model resolution (3.75° × 2.50°) to ORCHIDEE from (left column) MACCv10.1 and (right column) INVSAm over the TSA region. Mean for February (top), July (middle), and mean over the whole year (bottom). Filled circles indicate locations of sites with continuous measurements; and open circles indicate locations of sites with discrete air sampling.

C) In Sect. 3.3.2 of the revised manuscript we state:

"Of note is that even if increments on the NEE annual budget of a given year from an inversion are weak, the changes in the corresponding annual anomaly from the inversion can be high because the inversion modifies the 2002-2010 average against which the anomaly is computed."

C) Also in Sect. 3.3.2, we state:

"The example of the divergences of the results between MACCv10.1 and INVSAm in 2003 in Zone 2 illustrates, again, some weak ability to precisely constrain the fluxes in such a small area, which is quite distant from the measurement sites in TSA. Indeed, the analysis of the maps of increments from MACCv10.1 and INVSAm, for the annual mean NEE in 2003 (not shown), demonstrates that the assimilation of data at SAN during this year shifts the northern border of the pattern of negative corrections in MACCv10.1 from North of Zone 2 to the south of Zone 2.Since, on average, over 2002-2010, both inversions apply positive increments in this Zone (see Fig.6) this leads to a clear negative annual anomaly in Zone 2 and for the year 2003 for INVSAm."

Specific/Technical Comments:

Q.T1) Page 1917, Lines 9-13: Consider rephrasing this sentence. The only comparison presented in this paper is to Jung et al. [2011]; but this statement gives the impression that the authors have looked at a suite of bottom-up modelling reports, and compared their top-down estimates to these bottom-up estimates.

C) The text has been reformulated as follows:

"The estimates of net ecosystem exchange (NEE) optimized by the inversion were compared to an independent estimate of NEE upscaled from eddy-covariance flux measurements in Amazonia. They were also qualitatively evaluated against reports on the seasonal and interannual variations of the land sink in South America from the scientific literature."

Q.T2) Abstract: The authors should mention at the outset the time period/duration over which fluxes are being estimated, i.e., 2002-2010. The reader does not get this information till the end of the Introduction.

A) We now specify the analysis period in the abstract.

Q.T3) Page 1918, Line 4: Change from "...is the topic of active research" to "...a topic of active research".

A) We have incorporated the suggested change.

Q.T4) Page 1919, Line 16: There is an extra ')' after the word emissions. Delete.

A) We have corrected the error.

Q.T5) Page 1921, Line 13-14: It is unclear what the authors mean by –"...the reliability of these modelled fluxes should be analyzed".

A) The text has been reformulated based on our answers to the reviewer and the referred sentence has been suppressed.

Q.T6) Page 1921, Line 22: Replace the word 'were' with 'where'.

A) The correction has been made. In addition, as suggested by Referee 1, the paragraph in lines 15-23, p1921 in the original manuscript, regarding the description of the product J2011, has been moved from this section to a new section: "Sect. 2.3 Analysis of an alternative estimate of the NEE for the evaluation of the inversions."

Q.T7) Page 1922, Line 9: Replace the word 'henceforward' with 'hereafter'

A) The word has been replaced.

Q.T8) Page 1926, Line 17: Do the authors mean "spatial and temporal variability", or only "temporal variability"? Kindly clarify.

A) This phrase has suppressed since the text in lines 9-24 in the original manuscript has been removed. We concluded that this part of the text was not clear for the reader and we decided to convey the message through the discussion in sections 3.1 and 3.2

Q.T9) Page 1926, Line 18: It is unclear what the authors mean by "root mean square of the annual biases". How is this quantity calculated? In fact the entire discussion about the "flat prior" or the poor man's prior is difficult to follow. The authors may want to revise this piece, and make it a separate paragraph (for e.g., paragraph break at Line 9).

A) The phrase has been suppressed. See previous Technical Comment (Q.T8).

Q.T10) Section 3: Throughout the text the authors mention MACCv10.1 but in the figures, the results are presented as CH2010. This is highly confusing. It is better to stick with MACCv10.1 in both the text and the figures, and use CH2010 to specifically refer to a conclusion/finding from that study.

A) We have systematically changed the references in the figures and in the text as suggested.

Q.T11) Page 1931, Lines 23-24: Consider rephrasing part of this sentence as – ". . .not shown here since these did not provide further information than presented in Figures 6g, 6h".

C) The sentence has been reformulated as follows:

"The results, however, do not provide any further information than Fig. 7c,d and are not shown."

Q.T12) Page 1931, Lines 27-28: It should be clarified here that this is an expected outcome, given that there are no observations to constrain the fluxes in this region.

C) In the revised manuscript, we have added:

"This is an expected result due to insufficient data in the southern part of the TSA to constrain fluxes in that region."

Q.T13) Page 1933, Lines 11-12: It is not clear why there is a difference in magnitude between the NEE anomaly estimates from this study, and those from J2011. The authors need to comment on this discrepancy.

A) Based on the comparison of the gross primary productivity (GPP) simulated by 10 process-based models and the GPP estimated by Jung et al. (2011), Piao et al. (2013), Glob. Chang. Biol., doi:10.1111/gcb.12187, comment on the likely underestimation of the interannual variability of GPP by Jung et al. (2011): Jung et al. (2011) use spatial gradients among the available flux towers to train their algorithm. The derived relationships are then extrapolated to temporal gradients. However, this supposes that spatial and temporal response of GPP to climate is the same, which might not be the case.

C) In the revised manuscript we comment:

"However, the product of J2011 must be used cautiously, especially when evaluating IAV of NEE. J2011 relied on a limited number of EC stations across the Amazon basin, with short time series, to estimate MTE based on spatial gradients among the sites, and then extrapolated to temporal gradients. This is valid assuming that spatial and temporal NEE patterns have the same sensitivity to climate, which may be incorrect (Piao et al., 2013)."

Q.T14) Figure 3: Is there a specific reason for showing the footprints only for February? Are these footprints typical of the entire year?

A) The seasonal changes in the atmospheric circulation in TSA are not critical in general. We have updated Fig. 3 (below), which now depicts a climatology of wind fields from NCEP/NCAR reanalysis (1981-2010), averaged between the surface and a level of 600 hPa, in TSA during (a) the austral summer (February), (b) austral winter (July), and (c) annual mean. Across the Amazon Basin, the dominant, or typical, circulation pattern in the lower troposphere is that of winds entering the Atlantic coast in north-eastern Brazil, then continue across the basin, and as they approach the Andes, turn back into the Atlantic Ocean south of 20°S. Our selection of figures aimed at illustrating this pattern. This is now better commented in the revised manuscript.

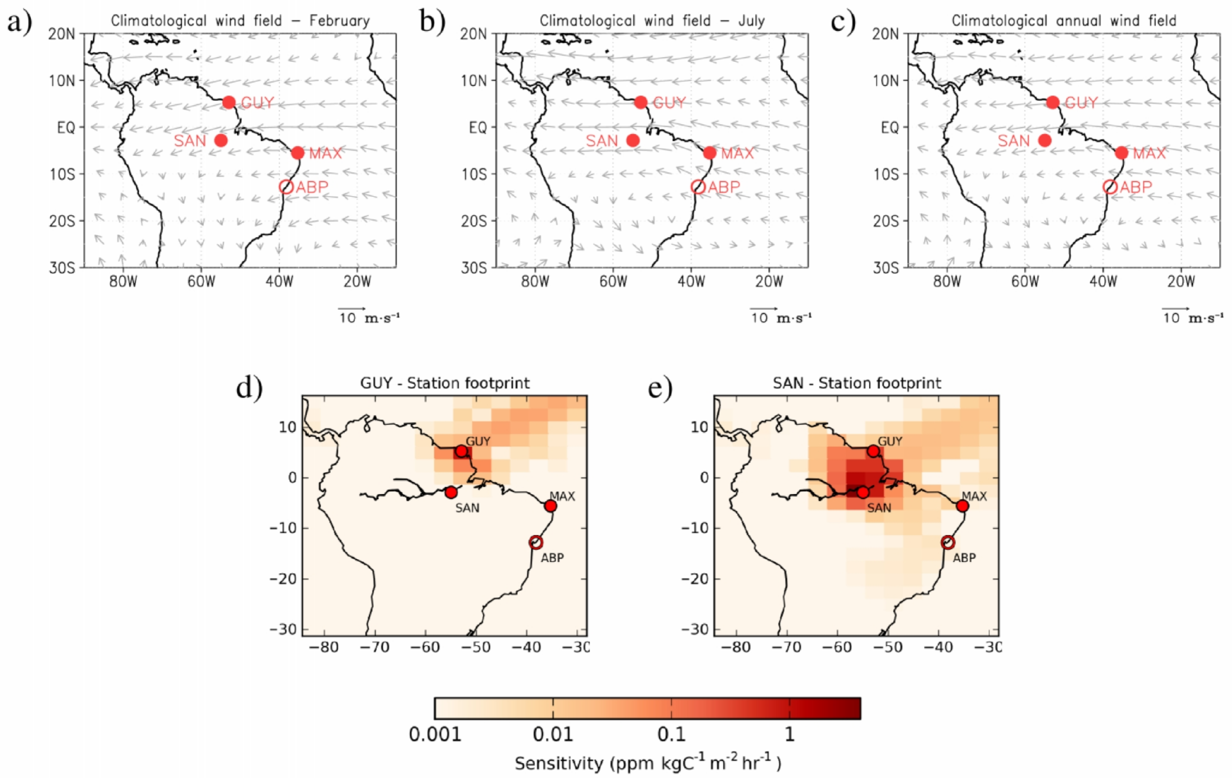

New Fig. 3: Top: Location of assimilated surface stations in South America and climatological wind speed/direction for February (a), July (b), and annual mean (c), averaged over 1981—2010 between the surface and a level of 600 hPa (Source: NCEP/NCAR Reanalysis). Sensitivity of surface atmospheric CO_2 mole fractions measured on 20 February 2009 at 10:00 UTC, at Guyaflux (7:00 LT) (d) and Santarém (6:00 LT) (e), to a constant increment of surface fluxes during the two days prior to the measurement. Sensitivity values are expressed in log-scale. Open circles: sites with discrete air samplings. Filled circles: measurements taken with continuous analyzers.

C) Lines 22-25, p1925 of the original manuscript have been rewritten as follows:

“Prevailing winds in the lower troposphere across TSA convey air masses entering from the Atlantic Ocean near the Equator across the continent and back into the southern

Atlantic Ocean generally south of 20° S. There are no critical seasonal variations of the mean winds in the area so that this typical behaviour applies throughout the year. The climatology of wind fields from NCEP/NCAR Reanalysis (over the period 1981-2010) for February, July and annual mean, shown in Fig. 3, illustrates this circulation pattern."

Q.T15) Figure 4, Panel a: In 2009, the simulated mole fractions from MACCv10.1 (or CH2010) seem to fit the observations better than INVSAm. This is also true for early-2007 period. Differences are as large as 10-15 ppm. Can the authors comment on the reason(s) for the poor performance of INVSAm?

A) We made a mistake when sampling the fields of optimized CO_2 mole fractions. The results are now more consistent with the expected results from the assimilation of data at ABP. The figure below replaces Fig. 4 panel a. The corresponding statistics of the misfits between measurements and simulated mole fractions have also be updated in Fig. 5 (below).

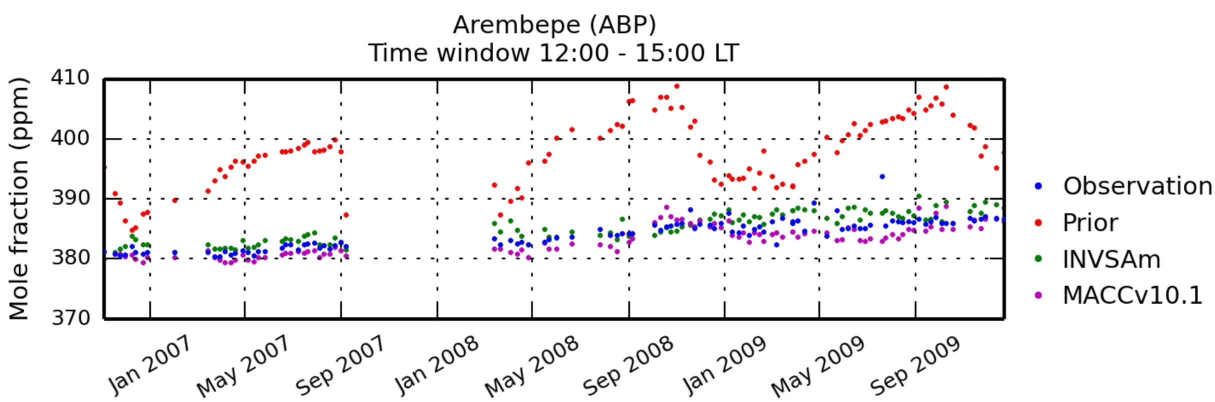

New Fig. 4a. Comparison of assimilated CO_2 observations (blue) and corresponding simulated mole fractions using prior fluxes (red), INVSAm (green) and MACCv10.1 (purple), at Arembepe (ABP). Data shown here correspond to daily average mole fractions between 12:00 and 15:00 local time (LT), when wind speed > 2 m s-1.

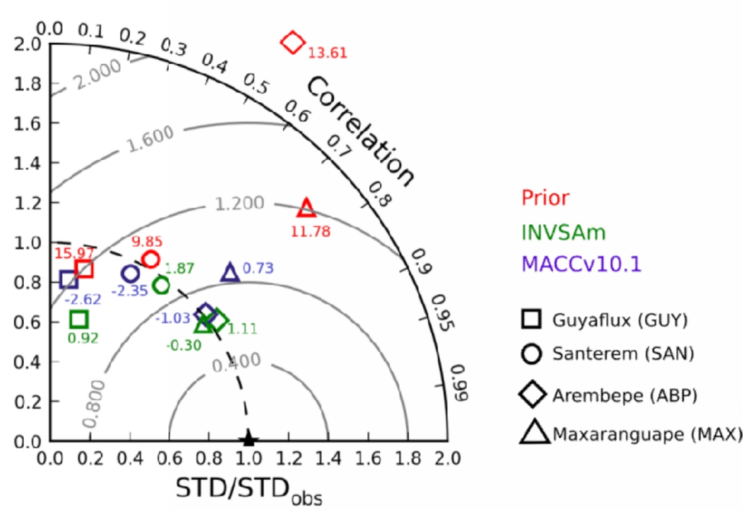

New Fig. 5.Taylor diagram of the statistics of misfits between observations and simulated CO_2 mole fractions between 12:00 and 15:00 LT at Guyaflux (square), Santarém (circle), Arembepe (diamond) and Maxaranguape (triangle), when wind speed > 2 m s-1 , using prior fluxes (red), INVSAm (green) and CH2010 (purple). Radial distance from the origin: ratio of SD of simulated mole fractions and SD of the observations. Angle measured from the y axis: coefficient of correlation. Numbers next to the symbols: bias (in ppm). Gray circles: SD of the misfits (in ppm).

Q.T16) Figure 4, Panel c: Again over periods in 2002-2003, the INVSAm estimates are closer to the prior (and farther from the observations) than MACCv10.1 (or CH2010). It is very discouraging that using the observations from the site degrades the result. The authors need to discuss/clarify this in the text.

A) Figure 4c below has been updated, since it erroneously included observations and simulated mole fractions outside the assimilation time window (12:00-15:00 LT). The corresponding Fig. 5 has also been updated (see previous Technical Comment).

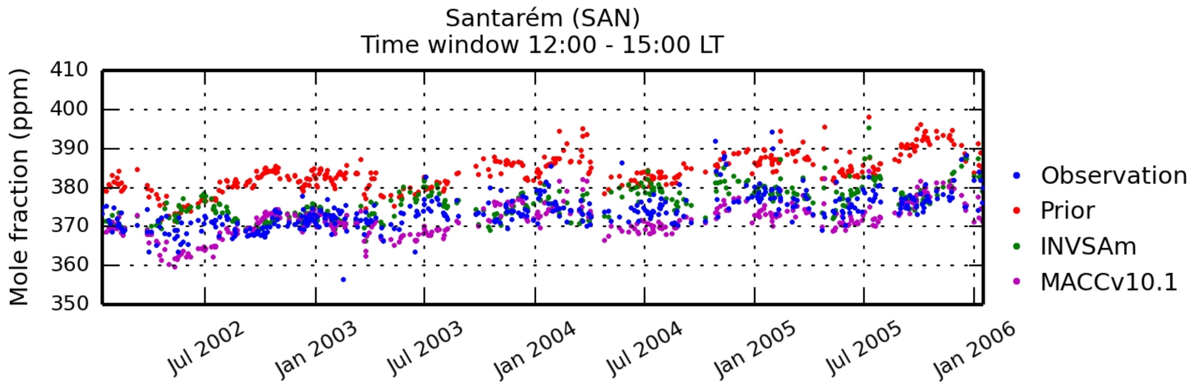

New Fig. 4c. Comparison of assimilated CO_2 observations (blue) and corresponding simulated mole fractions using prior fluxes (red), INVSAm (green) and MACCv10.1 (purple), at Santarém (SAN). Data shown here correspond to daily average mole fractions between 12:00 and 15:00 local time (LT), when wind speed > 2 m s-1.

Q.T17) Figure 8: Have the authors looked at the corresponding figures from MACCv10.1 (or CH2010)? If so, it would be worthwhile to add a second column to this figure showing those results.

A) See our answer to the General Comment Q.3 from the reviewer.Figure 8 in the original manuscript corresponds to Fig. 6 in the revised manuscript.

Q.T18) Figure 9, panel b: Change the scale on the y-axis (for e.g., -0.15 to 0.15). Currently this figure cannot be evaluated.

A) We have set a new scale for the y-axis: -0.3 to 0.25.

On the ability of a global atmospheric inversion to constrain variations of CO_2 fluxes over Amazonia

Final response to the comments from Referee 3

Questions/comments from the Referee, answers to the comments and changes to the manuscript are presented according with the following notation:

Q) Questions, general, and technical comments
A) Answers to the comments
C) Changes to the manuscript

Q.1) Tropical South America is a geographical region where we know very little about the carbon balance on a large scale, with implications for quantifying the carbon balance over other regions. This paper examines the ability of using CO2 mole fraction measurements from four additional sites on the eastern coast of South America, relative to a control calculation that has used all other available mole fraction data. I have a few comments but none of them are sufficiently negative to prevent this work being published – they can be addressed quickly.

A) We thank the reviewer for his analysis of our paper and for his very useful comments, which have certainly improved the revised manuscript through new analysis and discussions that have been incorporated.

Q.2) To some extent this is (yet) another paper that highlights the many difficulties using measurements that represent constraints on spatial scales and temporal scales that are not described well by current models. In this experiment, the model resolution is very coarse that could easily compromise its ability to capture reliably observed variations on certain time scales. It would be good to learn a bit more about the model error that takes this into account because it plays an important role in determining the results.

A) Values of the configuration of the model uncertainty assinged in the inversion system are provided in the revised manuscript (see Table A1 in response to Comment Q.9) but they cannot fully reflect the actual values of the model errors given the modest confidence in this configuration, further to the limited experience acquired for the representation of ground-based in situ measurements in this area using global transport models.

Q.3) The new sites look great but there is precious little information to judge whether they are actual useful.

A) Based on figures 6 (previous Fig. 8, now updated), 7 and 9 in the revised manuscript, we discuss (see also our answer to Comment Q.6 of Referee #3 and General Comment Q.1.2 of Referee #2) the fact that the impact of these new sites on the increments from the inversion is large and spread over a large area (at the transport grid scale, the increments from INVSAM to the annual fluxes generally exceed 150% of the prior estimate in terms of absolute values). Still, the analysis of the increments demonstrates that the reliability of this impact is quite low.

Q.4) I assume they have been calibrated on a scale that is common to the data assimilated as part of the MACC project, but this point needs to be confirmed. More details would be helpful for this reader.

A) This information is now provided in the revised manuscript.

C) In Sect. 2.2 Assimilated data, at the end of the fourth paragraph, we state:

"Data from the four new sites in TSA have been calibrated on the WMO-X2007 CO_2 scale, managed by the ESRL/NOAA."

Q.5) I appreciate that these measurements are difficult to sustain over long periods but I am left concerned about the role of sampling frequency on the results. A simple simulation could be used to determine the ability of each site to constrain estimates of NEE and ocean fluxes. This would strengthen the ultimate message of the paper.

A) We are not sure about the kind of simulation that the reviewer had in mind. However, given the relatively short correlation length scales in B, and despite the long-range (in time) corrections associated with the data in global inversions, we assume that corrections applied in response to data assimilation at a given site and over given years does not spread to the other years when there is no data available at this site. Therefore we do not think that we should verify it by conducting separate inversions on each 2/3-year periods when one South American site only is available. Still, we now provide analysis of the results for 4/5-year periods in response to General Comment Q.18 of Referee #1 (see the Fig. S1 in the corresponding document) which shows the influence of SAN and MAX on the one hand, and of GUY and ABP on the other hand.

Q.6) Incidentally, what about the ocean fluxes?

A) Thanks to the comments from the three referees, we now provide an analysis of the increments to the ocean fluxes, which brings new insights on the general patterns of the inversion over land, and in particular on the so-called dipole. However, we still keep our focus on the land fluxes to avoid a digression with a deeper analysis of corrections to the ocean fluxes.

The new Fig. 6below depicts corrections for both the ocean and land fluxes (with different colour scales and units due to the different order of magnitude between increments over land and ocean) and over an area larger than that shown originally. Based on this figure, the revised manuscript explains that the increments from both the inversions have large patterns which are nearly zonal (or along the prevailing winds) and which overlap continuously the ocean and the land. The zonal positions and strength (i.e. the amplitude of the zonal gradient) of these zonal increments are modified by the inclusion in the inversion of the data from the new stations in the Tropical South America region. These effects are more visible when focusing on specific months, while the annual averages smoothens the patterns.

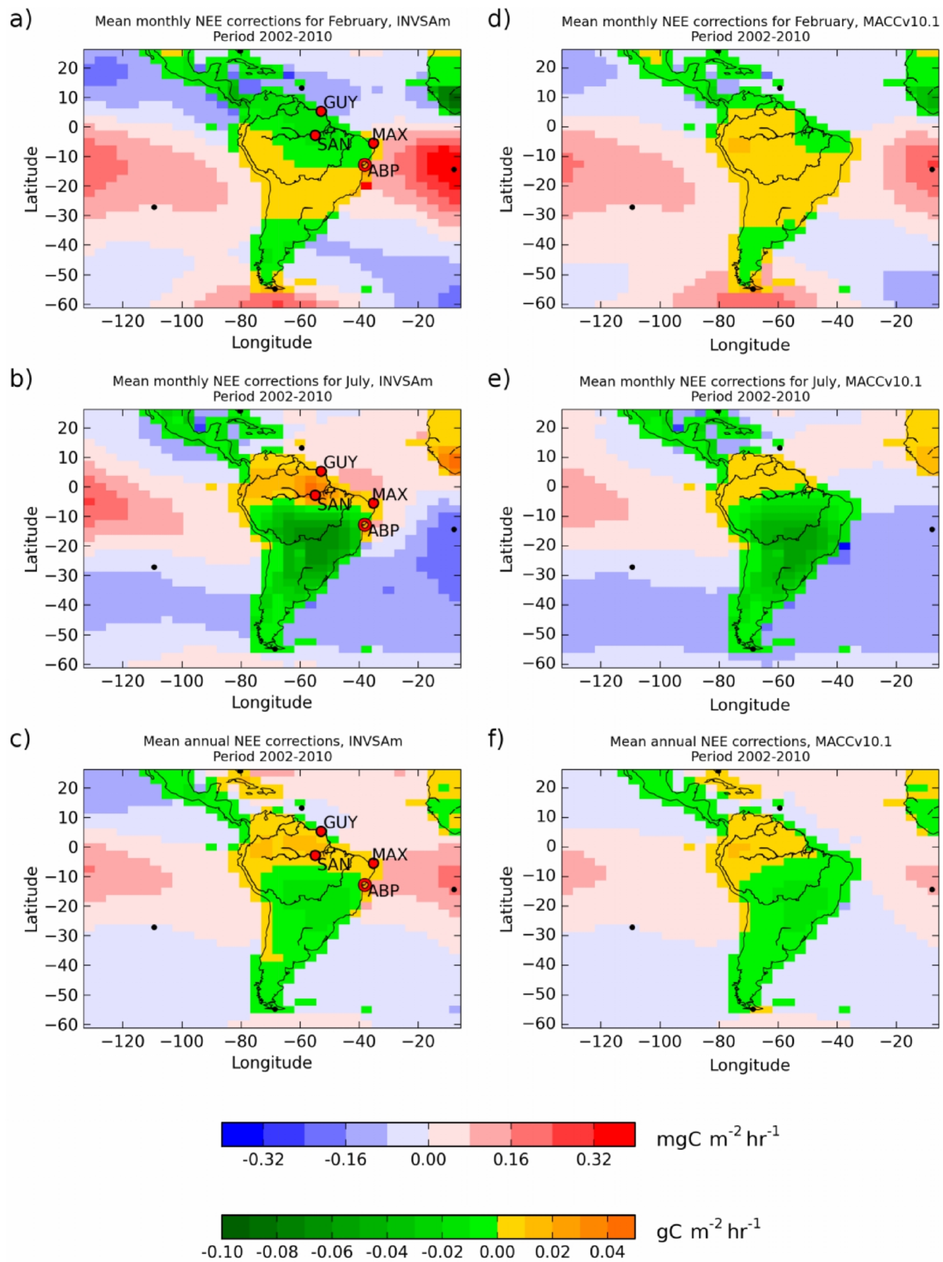

New Fig. 6. Spatial distribution of 2002–2010 mean flux corrections at the transport model resolution (3.75º × 2.50º) to ORCHIDEE from (left) INVSAm and (right) MACCv10.1 over a larger area encompassing TSA: mean for February, July, and mean over the full period 2002–2010. Flux increments over land and ocean are represented with two distinct colour scales and units: green–yellow for land, in gC m^{-2} hr^{-1}; blue–red for ocean, in mgC m^{-2} hr^{-1}. Filled circles indicate locations of sites with continuous measurements; and open circles indicate locations of sites with discrete air sampling.

C) We have inserted a discussion on the flux increments applied by the inversion in a new section: "Sect. 3.2 Characterization of the monthly to annual mean inversion increments to the prior fluxes". In this new section we state:

"Figure 6 depicts the increments from both inversions, showing large patterns which are nearly zonal (or along the prevailing winds) and which overlap continuously over land and ocean. Since there is no correlation between the uncertainty in ocean and land fluxes in the B matrix, and given the typical length scale of the correlations in this matrix, this can be directly connected to the signature of atmospheric transport. The contiguous zonal patterns have alternate negative and positive flux increments. There is thus an opposition between corrections in the North and in the South of the TSA region. These corrections are rather negative in the North and positive in the South (positive in the North and negative in the South) during the austral summer (winter). As these corrections are stronger during the austral winter, it results in positive (negative) corrections in the North (South) at the annual scale. Such dipoles are a typical behaviour of inverse modelling systems in data-poor regions (Peylin et al., 2002). However, changes in the amplitude and latitudinal position of this zonal dipole appear to be the main impact from the assimilation of data in the TSA region. This dipole structure may thus yield sensible corrections to the NEE in the TSA area."

Q.7) Regarding the footprints that are shown for a day in February 2009. Are these representative of the season, year? Either a more comprehensive discussion of the site footprints or a climatology of wind fields would help to explain to the reader why these sites were chosen and potentially why that can add to what we know about NEE over the geographical region.

A) In the revised manuscript, we have updated Fig. 3 (below), which now depicts a climatology of wind fields from NCEP/NCAR reanalysis (1981-2010), averaged between the surface and a level of 600 hPa, in tropical South America (TSA), during (a) the austral summer (February), (b) austral winter (July), and (c) annual mean. According the Fig. 3, the seasonal changes in the atmospheric circulation across region TSA are, in general, not critical. The dominant circulation patterns in the lower troposphere over TSA is that of winds entering Amazonia from the north-east, and as they reach the Andes they turn south back into the Atlantic ocean south of 20°S. With the network configuration in TSA, coastal stations ABP and MAX receive information from background CO_2 incoming from the Atlantic Ocean. GUY and SAN, subject to the influence of vegetation, on the other hand, help establish a gradient between the coast and north-eastern Amazonia; this information is used by the inversion system to constrain surface fluxes for the area between those stations. The analysis of the new Fig. 6 (see response to Comment Q.6) also reveals that the inversion relies on the long-range extent of the station footprints to apply corrections at very large scale over South America. The inversion uses data from the South American sites and their long-range gradients to other sites in the Southern

Hemisphere to control the fluxes with large zonal patterns of corrections (in the direction of the long-range prevailing winds). We comment this in the revised manuscript.

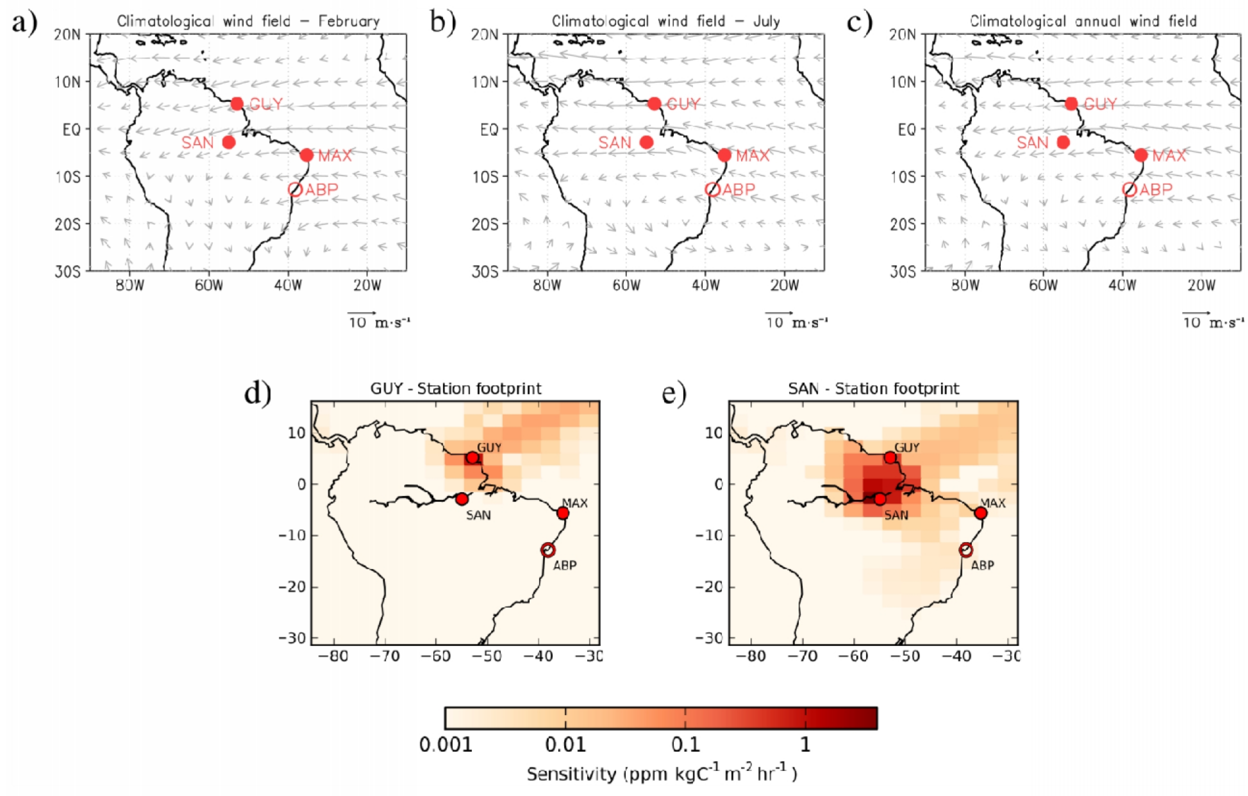

New Fig. 3: Top: Location of assimilated surface stations in South America and climatological wind speed/direction for February (a), July (b), and annual mean (c), averaged over 1981—2010 between the surface and a level of 600 hPa (Source: NCEP/NCAR Reanalysis). Sensitivity of surface atmospheric CO_2 mole fractions measured on 20 February 2009 at 10:00 UTC, at Guyaflux (UTC-3) (d) and Santarém (UTC-4) (e), to a constant increment of surface fluxes during the two days prior to the measurement. Sensitivity values are expressed in log-scale. Open circles: sites with discrete air samplings. Filled circles: measurements taken with continuous analyzers.

C) In Section 2.2, the text from line 22, p1925, to line 9, p1926, in the original manuscript has been reformulated:

"Prevailing winds in the lower troposphere across TSA convey air masses entering from the Atlantic Ocean near the Equator across the continent and back into the southern Atlantic Ocean generally south of 20° S. There are no critical seasonal variations of the mean winds in the area so that this typical behaviour applies throughout the year. The climatology of wind fields from the NCEP/NCAR reanalysis (over the period 1981—2010)

for February, July and annual mean, shown in Fig. 3, illustrates this circulation pattern. This confirms that the variations of CO_2 at coastal stations (ABP, MAX) are mainly influenced by air–ocean exchanges and fluxes in distant lands. These stations should thus provide more information on the atmospheric CO_2 content upwind of TSA, than on the fluxes within Amazonia. Fig. 3 also shows that GUY and SAN receive a signal from the ecosystems of the north-eastern Amazon Basin. Despite GUY being not far from the coast considering the Amazon-wide scale, this site is still located inland, in an area covered by undisturbed, tropical wet forest. SAN is located considerably further inland than GUY. Typical influence functions of fluxes for observations at GUY and SAN (the observation "footprints", in Fig. 3b and c, respectively) illustrate that the sensitivity of instantaneous mole fractions to the fluxes rapidly decreases with the distance, mainly due to the typically moderate horizontal wind speeds, so that they should bear a strong signature of local fluxes i.e., of the NEE in north-eastern Amazonia. This, and the fact that the geographical distance between the sites in the TSA region ranges from 1000 to 2600km, i.e. up to five times the correlation length scale in matrix B, could suggest that the area well constrained by the sites in the TSA region through inversion is limited. However, as illustrated in Fig. 3, the station footprints also have modest values over very extensive areas which may also result in significant large-scale constraint from the inversion on the land flux estimates."

Q.8) The authors mention a comment on page 1928 line 20: "...results at ABP may reveal some local issues." What are they?

A) The phrase made reference to the analysis of a version of figures 4a and 5, where the results shown for ABP were wrong. We made a mistake when extracting the time series from INVSAm at this site. Figures 4 and 5 have been updated. The true results are much more in line with what is expected from the inversion after assimilating the new sites in TSA.

Q.9) Perhaps my most serious concern is the absence of a discussion about uncertainties. How well did the model fit these new data? Can you give the reader a sense of the ratio of posterior and prior uncertainties associated with the NEE and ocean fluxes? What about the spatial correlated associated with the posterior NEE fluxes shown in Figure 8? For some of the estimates how does this reader know whether these new data have improved our knowledge of NEE? I expect the authors will respond by saying that the assimilation approach does not easily provide posterior uncertainties but I would argue that these results are difficult to interpret without this information.

A) With the high spatial and temporal resolution of our inversion framework, the computation of the theoretical posterior uncertainties is highly expensive (it should be based on a Monte Carlo estimate with ensemble experiments that are not affordable in

the framework of this study). Furthermore, due to their huge computational cost, such computations are generally made for typical years, while here, since the reviewers ask for checking the impact of 4 specific sites and for the critical quantities analyzed in this study i.e., the mean seasonal cycle and the inter-annual variability, this would have required the computation of uncertainty reduction for a large number of years (see our response to General Comments Q.1 and Q.2 from Referee #2).

Furthermore:

- We believe that Fig. 6, Fig. 7 and Fig. 9 demonstrate the high impact on the inversion increments from the data in South America. If the error statistics assigned in the inversion configuration are consistent with actual errors, large increments when using real data should demonstrate that the theoretical uncertainty reduction is high (for the inversion, statistically, corrections to the prior decrease the uncertainty). In response to reviewer #2 (General Comment Q.1.3), we have also compared the prior and posterior misfits between simulated and measured mole fractions, to the setup of the observation errors in the inversion configuration. Such comparisons indicate a decrease of the misfits due to the inversion, and in particular when assimilating the data in South America, which is significant compared to the theoretical observation errors (Table A1, below). These different results indicate that significant improvements of the fluxes in Amazonia could be, in principle, expected from the large increments from INVSAm, which are strongly driven by the sites in South America. The theoretical computation of uncertainty reduction would thus quantify this qualitative indication.

Table A1

	Standard deviation of the misfits Model – Observation			
Station	Prior	INVSAm	MACCv10.1	2 * (Standard deviation of the model error)
ABP	4.4	1.5	1.6	2.2
MAX	2.1	1.1	1.5	2.0
SAN	4.6	4.0	4.6	9.6
GUY	4.0	3.5	4.1	3.3

- The theoretical computation of uncertainty reduction and posterior uncertainties strongly relies on the configuration of the prior uncertainties and observation errors in the inversion system. However, as detailed in the answer to the reviewer #2 (General Comment Q.2), this configuration has been derived and evaluated at very large scale

using global datasets (eddy covariance flux measurements in Chevallier et al. [2012] and atmospheric mole fraction measurements in CH2010) that mainly sample the Northern hemisphere. There are reasons to think that it is not so robust at higher resolution and for a particular region, especially in the Amazon area, which is poorly sampled by these datasets. Actually, the results and discussion from this study question the inversion configuration for the Amazon region. This does not give confidence in the theoretical computation of posterior uncertainties and uncertainty reduction. Therefore, we do not really agree that such theoretical computation can give useful insights on the results in this study.

We comment the points above in the revised manuscript. We hope this clarifies our choice of not performing the uncertainty analysis.

C) In Sect. 2.1 in the revised manuscript we comment:

"There is a moderate confidence in the adequacy of these error statistics assigned in the global inversion system for the specific TSA area studied here, both because B was designed mostly with statistics gathered in the Northern Hemisphere, and because R may not well account for the uncertainty in the atmospheric convection model, while this could be high in Amazonia (Parazoo et al., 2008). We also investigate here variations of the fluxes within TSA at spatial scales that are not much larger than the e-folding correlation length in B, and these variations in the inversion results may be affected by our simple hypothesis of isotropic correlations in the prior uncertainty. This lack of confidence in the input error statistics weakens our confidence in the posterior error statistics that can be derived based on the inversion system, even though they may be realistic at zonal scale for the Tropics (Chevallier and O'Dell, 2013). In this context, and given the relatively high computational burden of the posterior uncertainty computations for grid-point inversion systems (using Monte Carlo approaches with ensembles of inversions, Chevallier et al. 2007), we do not derive these posterior uncertainties for our domain and its sub-domains."

C) In the revised manuscript, Sect. 3.1, we comment:

"The significance of the reduction of the misfits between the mole fractions observed and simulated from the inversion is seen from the comparison between the standard deviations of these misfits and the estimate of the standard deviation of the observation errors (i.e. of the transport model errors) for hourly values in the configuration of the R matrix (Table A1, in supplementary material).According to this comparison, the prior misfits are much larger than the observation errors at ABP, MAX, and GUY, but are slightly smaller than these at SAN. Misfits between MACCv10.1 and the observations are similar to the prior misfits at SAN and GUY and are much smaller than the prior misfits

(and smaller than the 95% confidence interval of the observations) at the coastal ABP and MAX sites. Misfits are further decreased when assimilating the data from the South American sites: they are about the standard deviation of the observation errors at all sites but GUY (where they are twice as large).”

Abstract. The exchanges of carbon, water, and energy between the atmosphere and the Amazon Basin have global implications for current and future climate. Here, the global atmospheric inversion system of the Monitoring of Atmospheric Composition and Climate service (MACC) ~~was used to further~~ is used to study the seasonal and interannual variations of biogenic CO_2 fluxes in Amazonia during the period 2002–2010. The system assimilated surface measurements of atmospheric CO_2 mole fractions made ~~over~~ at more than 100 sites over the globe into an atmospheric transport model. ~~This study added~~ The present study adds measurements from four surface stations located in tropical South America, a region poorly covered by CO_2 observations. The estimates of net ecosystem exchange (NEE) optimized by the inversion ~~were compared to independent estimates~~ are compared to an independent estimate of NEE upscaled from eddy-covariance flux measurements in Amazonia~~, and~~. They are also qualitatively evaluated against reports on the seasonal and interannual variations of the land sink in South America from the scientific literature. We ~~focused on the impact of the interannual variation~~ attempt at assessing the impact on NEE of the strong droughts in 2005 and 2010 (due to severe and longer-than-usual dry seasons), and of the extreme rainfall conditions registered in 2009. The spatial variations of the seasonal and interannual variability of optimized NEE ~~were~~ are also investigated. While the inversion ~~supported~~ supports the assumption of strong spatial heterogeneity of these variations, the results ~~revealed critical limitations that prevent global inversion frameworks from capturing the data-driven seasonal patterns of fluxes across Amazonia. In particular, it highlighted issues due to the configuration of the~~ reveal critical limitations of coarse resolution transport model, of the surface observation network in South America ~~and the lack of continuity of the measurements~~during the recent years, and of the present knowledge of modelling uncertainties in South America that prevent our inversion from capturing the seasonal patterns of fluxes across Amazonia. However, some ~~robust~~ patterns from the inversion ~~seemed~~ seem consistent with the ~~abnormal~~ anomaly of moisture conditions in 2009.

1 Introduction

The forests of Amazonia cover 6.77 million km^2 (INPE, 2011). It is the world's largest continuous area of tropical forest and reservoir of aboveground organic carbon (Malhi et al., 2008). Changes in the carbon dynamics of this ecosystem thus have global significance (Wang et al., 2013). However, the natural variability of CO_2 exchange in Amazonia, as well as its short and long term response to natural and anthropogenic disturbance across scales, is still poorly understood and ~~is the~~ a topic of active research.

There is intense debate about the timing and magnitude of the seasonal cycle of CO_2 fluxes across Amazonia. Studies employing remote sensing data as a proxy for canopy photosynthetic activity have suggested a widespread enhancement of gross primary productivity (GPP) of the Amazonian rainforest during the dry season (Huete et al., 2006). Yet, direct and continuous measurements of net ecosystem exchange (NEE) between the atmosphere and forest canopy at a local scale (from 1 ha to 1 km^2 scale) based on eddy-covariance (EC) systems do not support such large-scale behaviour. Several EC observations in central eastern Amazonia (Saleska et al., 2003) and northeastern Amazonia (Bonal et al., 2008) also indicate that tropical forest areas take up CO_2 during the dry season, but similar EC studies in central Amazonia have suggested an opposite seasonality (Grace et al., 1996; Araújo et al., 2002). Finally, remote sensing measurements of the vertically integrated columns of CO_2 (XCO_2) retrieved from the GOSAT satellite, suggest stronger CO_2 uptake during the wet season in southern Amazonian forest than during the dry season (Parazoo et al., 2013). These measurements thus reveal a large heterogeneity in space of the phase of the seasonal cycle of NEE within Amazonia. However, most dynamic global vegetation model (DGVM) simulations predict stronger uptake during the wet season throughout Amazonia (Verbeeck et al., 2011; Saleska et al., 2003; Baker et al., 2008; Poulter et al., 2009)~~;~~, although limitations related to mortality or land use ~~, do~~ restrict the ability of these generic global models to simulate CO_2 fluxes and carbon stocks of Amazonian forest (Gloor et al., 2012).

Uncertainty associated with potential spatial heterogeneity is also apparent in the estimates of the interannual variability (IAV) of CO_2 fluxes in Amazonia, in particular during years with extreme climatic conditions. Remote sensing observations during the severe Amazonian drought of 2005 suggested a widespread enhancement of photosynthetic activity, or greening, across Amazonia (Saleska et al., 2007). The resilience of forests to water stress suggested by the "drier-yet-greener" papers was originally attributed to a combination of deep rooting, hydraulic redistribution, and more available solar radiation (Saleska et al., 2007). However, the validity of enhanced vegetation index (EVI) satellite data has been recently challenged by Morton et al. (2014) and by losses in canopy functioning detected in radar-based measurements (Saatchi et al., 2012). The observations from optical satellite sensors remain controversial because other studies did not find such an impact of droughts on Amazonian forest (Xu et al., 2011; Samanta et al., 2010, 2012). Moreover, observations of microwave backscatter from QuickSCAT have suggested large-scale, persistent negative effects of the drought of 2005 on forest canopy structure (Saatchi et al., 2012). Biometry measurements, consisting of periodic measurements of the allocation of photosynthetic products to wood growth, provide another perspective on the effects of drought on Amazonian forest trees. In a large-scale, long-term biometric study, Phillips et al. (2009) found a ~~reversion~~ reversal of the carbon sink due to the effect of the drought of 2005 on tree mortality. This is consistent with a synthesis of yearly estimates of natural fluxes (NEE plus biomass-burning emissions) from an ensemble of DGVMs compiled at http://www.globalcarbonatlas.org~~)~~.

The scientific community has used atmospheric inversions for more than two decades in an effort to improve the knowledge of CO_2 fluxes at large scale. Whereas EC or biometric studies give flux estimates that are valid at local scale (Ometto et al., 2005), atmospheric inversion offers the possibility to derive measurement-based estimates for the whole of Amazonia, with spatial resolutions larger than 500 km, provided that atmospheric observations can adequately sample the Amazonian flux signal. Inversions use available measurements of atmospheric CO_2 to provide corrections to prior surface flux estimates using an atmospheric transport model and statistical inversion methods. The method estimates statistically optimal fluxes within the boundaries of uncertainties in the measurements, the transport model, and prior flux estimates (Enting et al., 1995; Ciais et al., 2010). The flux corrections ~~are applied by the inversion system to prior fluxes to which measurements are sensitive in space and time (as a function of the atmospheric transport), and are extrapolated~~ spread beyond the vicinity of the measurement footprint~~by the system~~ , as defined by the transport model, through hypotheses on the spatial and temporal correlation of the uncertainties in the prior fluxes. We define, hereafter, the tropical South America (TSA) region as the continental land encompassed between 16.25° N–31.25° S and 84.38° W–28.18° W, which covers the whole Amazonian forest. Peylin et al. (2013) show that the different inverted seasonal cycles and IAVs of natural CO_2 fluxes from several state-of-the-art global atmospheric inversions are characterized by a large scatter over ~~tropical South America (TSA)~~a very similar tropical area of South America. This is explained by the variety of prior estimates used by the different global inversion systems, and by the large-scale corrections that are applied in regions poorly covered by observation networks, such as TSA, in order to balance the global CO_2 budget, rather than to match local measurements. For these reasons, atmospheric inversions have not been included in the review of the carbon cycle in South America made by Gloor et al. (2012). Lloyd et al. (2007) and Gatti et al. (2010) applied the principle of atmospheric inversion to exploit vertical CO_2 ~~profile~~ profiles data from airborne measurements in Amazonia. Their studies, based on measurements near Manaus, in central Amazonia (Lloyd et al., 2007), and Santarém in eastern Amazonia (Gatti et al., 2010), constitute important efforts to constrain surface CO_2 fluxes at regional scale, measuring and exploiting some of the few atmospheric data sets available for South America. Their results suggested CO_2 efflux from the ecosystem during the wet season in eastern Amazonia. ~~The recent study of Gatti et al. (2014) , using vertical profiling of air columns,~~ By analysing vertical CO_2 profiles collected approximately every two weeks ~~, over the two-year~~ over the period 2010–2011, ~~provides~~ the recent study of Gatti et al. (2014) provided a basin-scale picture that confirms this regional signal, but ~~suggests the inverted~~ that also suggests an opposite pattern in southern and western Amazonia. Their study reported on the first data-driven estimate of CO_2

fluxes for the whole Amazon basin ~~, in an unprecedented effort that overcame limitations of both local and model-based estimates of fluxes in Amazonia (?) ; it provides an~~ and it provides insight into the sensitivity of this important ecosystem to moisture stress~~, and~~. It suggests the importance of ~~including~~ conducting such estimates over longer time periods.

Our goal here is to study the seasonal cycle and IAV of NEE over Amazonia during 2002–2010. This period offers the opportunity to investigate significant anomalies in the interannual variability of carbon fluxes, particularly those associated with the severe droughts of 2005 and 2010, and with the extreme rainfall registered across the Amazon basin in 2009 (Marengo et al., 2010). The study is based on the global MACC inversion system initially described by Chevallier et al. (2010) (hereafter CH2010). We used ~~v10.1~~ version 10.1 of the MACC CO_2 inversion product released in August 2011. We ~~added~~ also use a similar inversion in which we add four ground-based atmospheric measurement sites surrounding the northeast of Amazonia to the assimilated data (Fig. 1). Despite the limitations of ~~this~~ the state-of-the-art global inversion approach in South America, highlighted above and by Gloor et al. (2012), ~~this new attempt at characterizing~~ our analysis of these MACC inversions can help characterizing the temporal variations in the NEE over Amazonia ~~based on atmospheric inversions, can be justified by the use of these stations located in the region. In particular, we are the first to use continuous measurements from French Guyana: the impact of this inclusion can be assessed through comparisons with inversions ignoring these sites. The use of these stations was expected to increase significantly the~~ for several reasons. First, it relies on a detailed evaluation of the inversion results over and within this region, hoping that some reliable inversion patterns can be isolated. Such a detailed evaluation has not been conducted in the above-mentioned inter-comparisons of the global atmospheric inversions in TSA. It makes sense to conduct it here on the MACC inversions since the MACC system uses a variational inversion which solves for the fluxes at $\sim$3°and 8-day spatial and temporal resolution. Second, the use of the stations located in the region can strengthen the robustness of the inversion results through a significantly increased sampling of the atmospheric signature of the fluxes in Amazonia. ~~Moreover, when global inversions do not assimilate data from this region, they produce large increments of NEE in Amazonia – the reliability of these modelled fluxes should be analyzed.~~

~~Our analysis of the inversion results was compared to the independently derived NEE estimated by Jung et al. (2011) (hereafter J2011). J2011 used model tree ensembles, a machine-learning technique, to upscale FLUXNET eddy-covariance observations, based on remote sensing, climate, and land-use data as drivers, thereby producing gridded estimates of NEE and other surface fluxes at the global scale at 0.5resolution. As discussed in J2011, large uncertainties affect their annual mean NEE estimates and associated seasonal and interannual variations. This is likely particularly true in TSA, were few FLUXNET measurements are available. Yet, its comparison to the NEE from the inversion could give useful insights for the analysis of the latter~~In particular, we are the first to use continuous measurements from French Guyana. The assessment of the impact of these stations on the inverted NEE (based on the comparison between our different MACC inversions with and without these stations) can help identify the reliable patterns of the inversion.

The rest of this paper is structured as follows. We present each component of the ~~inversion setup~~ standard MACCv10.1 inversion setup and the use of the additional sites around Amazonia in Sect. ~~2, the~~ 2. The results of the ~~inversion~~ inversions, with a focus on the impact of these additional sites, and their comparison to ~~the standard MACCv10.1 inversion (not constrained by the four stations positioned around Amazonia) as well as to J2011~~ an independent flux estimate are presented in Sect. 3. In Sect. 4, we discuss the results and conclude the study.

2 The inversion method

This study builds on MACC the global atmospheric inversion framework ~~of~~ (whose first version is described in detail in CH2010) to correct a prior estimate of NEE from the model ORCHIDEE (Organizing Carbon and Hydrology in Dynamic Ecosystems, Krinner et al., 2005) and of ocean fluxes, based on the assimilation of in situ measurements of atmospheric CO_2 mole fractions into a global atmospheric transport model. The approach relies on a Bayesian framework to estimate the conditional probability of the "true" NEE and ocean fluxes given the statistical information from the prior fluxes and the set of in situ measurements of atmospheric CO_2 (~~henceforward observations~~hereafter *observations*). Assumption of unbiased Gaussian distribution of the uncertainties in the prior fluxes and of those underlying the simulation of the observations using the transport model, allows us to derive an updated estimate of NEE and ocean fluxes (hereafter the posterior fluxes) that also has an unbiased Gaussian distribution. The statistically optimal fluxes (i.e., the mean of the posterior distribution of the fluxes) are found by calculating the minimum of the cost function (Tarantola, 2005)

$$J(\boldsymbol{x}) = (\boldsymbol{x} - \boldsymbol{x}^{\mathrm{b}})^{\mathrm{T}} \mathbf{B}^{-1} (\boldsymbol{x} - \boldsymbol{x}^{\mathrm{b}}) + (\boldsymbol{y}^{\mathrm{o}} - H(\boldsymbol{x}))^{\mathrm{T}} \mathbf{R}^{-1} (\boldsymbol{y}^{\mathrm{o}} - H(\boldsymbol{x})) \quad (1)$$

where $\boldsymbol{x}$ is the control vector and mainly denotes the NEE (defined as the difference between the gross CO_2 uptake through photosynthesis and output through total ecosystem respiration), and air–ocean exchanges that are optimized at a chosen spatial and temporal resolution. $\boldsymbol{x}^{\mathrm{b}}$ represents the prior NEE and ocean fluxes, and $\boldsymbol{y}^{\mathrm{o}}$ is the vector of observations. H is the operator projecting $\boldsymbol{x}$ into the observation space, and is based on an atmospheric transport model and fossil fuel and biomass-burning CO_2 emission estimates.

$\mathbf{B}$ and $\mathbf{R}$ are the covariance matrices of the normal distribution of the uncertainty ~~on~~ in $\boldsymbol{x}^{\mathrm{b}}$ (the "prior uncertainty") and of the sum in the observation space of the other uncertainties when comparing $\cancel{H\boldsymbol{x}^{\mathrm{b}}}$ $H(\boldsymbol{x}^{\mathrm{b}})$ to $\boldsymbol{y}^{\mathrm{o}}$, respectively (the "observation errors"). The latter includes the measurement, model transport and model representation errors. A complete solution to the inversion problem requires the estimation of the uncertainty in the optimized fluxes ~~. This~~ (the "posterior uncertainty"), which is a function of the prior and of the observation errors. As explained below in Sect. 2.1, this estimation was not performed in this study~~since it would have been highly demanding in terms of computation. CH2010 provides details on this estimation and typical results of uncertainty reduction that should be nearly valid here for regions outside TSA~~. The following sections present a brief description of each component of the inversion configuration used in this study with a focus on parameters that are specific to this study, while CH2010 provides more details on the parameters which apply to all the MACC inversion configurations.

2.1 Inversion modelling setup

~~Following CH2010, the~~ The link between CO_2 fluxes and observations ~~was~~ in the MACC inversion is simulated by the global circulation model of the Laboratoire de Météorologie Dynamique (LMDZ) (version 4, Hourdin et al., 2006), which is the atmospheric component of the coupled climate model of the Institut Pierre Simon Laplace IPSL-CM4. Tracer transport ~~was~~ is simulated by LMDZ at a horizontal resolution of $3.75° \times 2.75°$ (longitude $\times$ latitude) and with a vertical resolution of 19 levels between the surface and the top of the atmosphere. LMDZ ~~was~~ is nudged to winds modelled by the European Centre for Medium-Range Weather Forecasts (ECMWF).

Prior NEE in MACCv10.1 was estimated at $3.75° \times 2.75°$ and 3 h resolution from a global simulation of the ORCHIDEE model at 0.7° resolution by Maignan et al. (2011). ORCHIDEE was forced with the atmospheric conditions of ECMWF reanalysis ERA-Interim (Berrisford et al., 2009). ~~Here ORCHIDEE NEE does~~ The ORCHIDEE NEE did not take into account disturbance from land use or wildfires. Prior ocean–atmosphere CO_2 exchanges were obtained from the climatology of air–ocean CO_2 partial pressure difference by Takahashi et al. (2009).

To complement these fluxes that were controlled by the inversion, the H operator also included fixed estimates of the fossil fuel and biomass-burning CO_2 emissions. Fossil fuel emissions were obtained from the EDGAR-3.2 Fast Track 2000 database (Olivier and Berdowski, 2001), scaled annually with the global totals of the Carbon Dioxide Information Analysis Center (CDIAC). CO_2 emissions from biomass burning were taken from the Global Fires Emission Database version 2 (GFEDv2, Randerson et al., 2007). Assuming that the vegetation recovers rapidly from fire events, the CO_2 emissions from fires that affected the vegetation in a given year were offset by an equivalent ~~,~~ compensatory regrowth CO_2 uptake evenly distributed throughout the year.

The inversion controlled 8-day mean daytime and nighttime NEE and 8-day mean ocean fluxes at the spatial resolution of the transport model. The analysis in this study ~~focused~~ focuses on NEE, thus the impact of the inversion on ocean fluxes ~~was not examined~~is not detailed here, but Sect. 3.2 still uses an illustration of this impact to raise insights into the corrections from the inversion over land. At the grid scale, uncertainties in the prior NEE are estimated ~~as~~ to be proportional to the heterotrophic respiration fluxes from ORCHIDEE. Spatial correlations of the uncertainties in $\mathbf{B}$ decay exponentially as a function of the distance between corresponding pixel-based estimates of the fluxes with a length scale of 500 km for NEE (1000 km for ocean fluxes). Temporal correlations of the uncertainties decay exponentially as a function of the lag-time between the corresponding 8-day mean daytime or nighttime estimate of the fluxes with a timescale of one month, but without correlation between daytime and nighttime uncertainties. The resulting correlations in $\mathbf{B}$ are estimated as the product between the temporal and the spatial correlations. This setup of the correlations for $\mathbf{B}$ is based on the estimates by Chevallier et al. (2006) and Chevallier et al. (2012) of differences between the NEE simulated by ORCHIDEE and EC flux measurements ~~. However, their study used EC data from flux towers~~ (mostly located in the Northern Hemisphere~~, and thus the resulting estimation of correlation might not apply well to ecosystems in tropical Amazonia~~).

In the inversion framework, the misfits between simulated CO_2 mole fractions and the measurements that are not due to uncertainty in the prior NEE or ocean fluxes must be accounted for in the covariance matrix $\mathbf{R}$. Uncertainties in fire and anthropogenic CO_2 emissions are assumed to have negligible impact at the measurement locations used here. Therefore, they are ignored in the setup of $\mathbf{R}$. Following CH2010, the measurement errors are assumed to be negligible in comparison to the uncertainties in the transport model. Model transport and representation errors are modelled as half the variance of the high frequency variability of the deseasonalized and detrended CO_2 time series of the ~~measurement~~ measurements that are assimilated at a given station. The resulting values of these model errors for the stations in South America will be discussed in Sect. 3.1.

There is a moderate confidence in the adequacy of these error statistics assigned in the global inversion system for the specific TSA area studied here, both because $\mathbf{B}$ was designed mostly with statistics gathered in the Northern Hemisphere, and because $\mathbf{R}$ may not well account for the uncertainty in the atmospheric convection model, while this could be high in Amazonia (Parazoo et al., 2008) . We also investigate here variations of the fluxes within TSA at spatial scales that are not much larger than the e-folding correlation length in $\mathbf{B}$, and these variations in the inversion results may be affected by our simple hypothesis of isotropic correlations in the prior uncertainty. This lack of confidence in the input error statistics weakens our confidence in the posterior error statistics that can be derived based on the inversion system, even though they may be realistic at zonal scale for the Tropics (Chevallier and O'Dell, 2013) . In this context, and given the relatively high computational burden of the posterior uncertainty computations for grid-point inversion systems (using Monte Carlo approaches with ensembles of inversions, Chevallier et al. , 2007), we do not derive these posterior uncertainties for our domain and its sub-domains.

However, we will see at the beginning of Sect. 3 that the inverted fluxes are more consistent with the CO_2 atmospheric observations in TSA than the prior fluxes, and that their difference to the prior fluxes over TSA (i.e. the flux increments generated by the inversion in order to better fit with the observations) are significant. This indicates that the inverted fluxes are strongly driven by the atmospheric data and as such, are worth analysing. This also suggests that the inversions yield a large uncertainty reduction for TSA.

2.2 Assimilated data

MACCv10.1 assimilated measurements of atmospheric CO_2, expressed as dry air mole fractions in $\mu mol\, mol^{-1}$ (abbreviated ppm), from 128 surface sites: 35 continuous measurement stations and 93 sites with measurements of CO_2 from discrete air samples collected approximately weekly~~at 93~~

~~sites. Out of all the stations,~~ . 29 ~~were~~ sites are located in the tropics~~(~~, but only two ~~of these stations~~ had continuous measurements ~~) but none of these tropical stations were located~~ over the analysis period and none of them were in TSA. In ~~this study~~ a similar inversion conducted specifically for this study, called INVSAm hereafter, we added new data from four surface sites located in ~~this~~ the TSA region. Figure 1 ~~maps the measurement stations~~ shows the measurement sites used by MACCv10.1 and the four stations added in ~~this study. At~~ INVSAm. In the following of this section, we focus on the description of these four stations and on the selection and representation of their data. Details on the data selection and representation at the sites used by MACCv10.1 are provided in CH2010.

Arembepe (ABP) ~~, data consist~~ (12.77° S, 38.17° W, 1 masl) and Maxaranguape (MAX) (5.51° S, 35.26° W, 15 masl) are coastal stations. The ABP site is located at the edge of the beach, where vegetation consists mostly of grass and beach plants. Data were collected at approximately 8 m above the ground, and consisted of weekly measurements of atmospheric CO_2 with discrete air samples~~.~~ ~~At the other three stations~~, specifically under on-shore wind conditions, when wind speed $> 2\,\mathrm{m\,s^{-1}}$. Air samples were collected preferentially during the afternoon to avoid the influence of recycled air transported from land to the ocean by land breeze during the night and early morning, and transported back to land by sea-breeze during the morning. The MAX site is located on a cliff right next to the coast, and is surrounded by grass and beach plants. At MAX, CO_2 was measured with ~~continuous analyzers~~ a continuous analyzer, at approximately 3 m above the ground, and data were reported as ~~hourly averagesof these measurements at Santarém (SAN) and Guyaflux~~ 30 min averages. This site is strongly under marine influence: winds are in general $> 10\,\mathrm{m\,s^{-1}}$, and wind direction varies preferentially between 100°and 140°(Kirchhoff et al., 2003) at its location, so that the measurements were taken mostly under on-shore wind conditions. Wind and CO_2 measurements at MAX indicate high CO_2 variations when the wind comes from land. These variations may be strongly influenced by the emissions from the nearby city of Maxaranguape (Kirchhoff et al., 2003) . However, as in ABP, this does not occur during the afternoon, when the wind conditions are dominated by sea-breeze (Law et al., 2010) .

The Guyaflux site (GUY) ~~, and 30~~(5.28° ~~min averagesat Maxaranguape (MAX) .~~ N, 52.91° W, 40 masl) is located at approximately 11 km from the coast, and is surrounded by undisturbed tropical forest. At GUY, measurements were taken at approximately 55 m above the ground (Bonal et al., 2008) . They were made with a continuous analyser, and data were reported as hourly averages. The Santarém site (SAN) (2.85° S, 54.95° W, 78 masl) is located in the tropical Tapajós National Forest, near km 67 of the Santarém–Cuiabá highway, at approximately 750 km from the coast. Measurements were made at 8 vertical levels ranging from ∼1 to ∼62 m above the ground with continuous analyzers, but only data from the highest level were used in INVSAm. Data were reported as hourly averages.

Figure 2 illustrates the temporal coverage of the observations available in TSA during the simulated period (2002–2010). There is little overlap among the site records, due to calibration problems, interruption of the measurements (e.g., at MAX) and the fact that some stations have been ~~setup~~ installed only recently (e.g., at GUY). The longest records were from ABP ~~, with data spanning November 2006 to December 2010, and SAN , covering January 2002 to December 2005. At MAX the information covered the periods July 2004 to May 2005 and mid-September 2006 to December 2006. GUY is the most recent station, with data covering October 2009 to December 2010.~~

~~Figure~~ (3 ~~depicts average wind fields in February over 2002–2010, which illustrates the typical circulation pattern. Winds~~ years: 2007–2009) and SAN (4 years: 2002–2005). Data from the four new sites in TSA have been calibrated on the WMO-X2007 CO_2 scale, managed by the ESRL/NOAA.

Prevailing winds in the lower troposphere across TSA convey air masses entering from the Atlantic Ocean near the Equator across the continent and back into the southern Atlantic Ocean generally south of 20° S. ~~This pattern of advective transport suggests~~ There are no critical seasonal variations of the mean winds in the area so that this typical behaviour applies throughout the year. The climatology of wind fields from the NCEP/NCAR reanalysis (over the period 1981–2010) for

February, July and annual mean, shown in Fig. 3, illustrates this typical circulation pattern. This confirms that the variations of CO_2 at coastal stations (ABP, MAX) are mainly influenced by air–ocean exchanges and fluxes in distant lands. These stations should thus provide more information on the ~~relatively homogeneous background~~ atmospheric CO_2 content upwind of TSA, than on the fluxes within Amazonia. ~~On the other hand, stations like~~ Fig. 3 also shows that GUY and SAN receive a signal from ~~ecosystems in~~ the ecosystems of the northeastern Amazon Basin. Despite GUY being not far from the coast considering the Amazon-wide scale, this site is ~~actually located~~ still located inland, in an area covered by undisturbed, tropical wet forest~~(Bonal et al., 2008)~~. SAN is located considerably further inland than GUY. Typical influence functions of fluxes for observations at GUY and SAN (the observation "footprints", in Fig. 3b and c, respectively) illustrate that the sensitivity of instantaneous mole fractions to ~~fluxes decreases rapidly with~~ the fluxes rapidly decreases with the distance mainly due to the typically moderate horizontal wind speeds, so that they should bear a strong signature of local fluxes i.e., of the NEE in northeastern Amazonia. ~~To further evaluate the sensitivity of these four stations to the pattern of interest in the regional NEE, we estimated the difference between mole fractions modelled using the standard prior NEE of the system and an NEE estimate called "flat prior". The flat prior was built by applying an annual offset to the prior NEE of MACCv10.1 so that the interannual variations of annual budgets become null. This annual offset was calculated as the difference between the mean flux for a given year over the whole region and the mean flux over the simulation period and the entire study area. Thus, the flat prior interannual anomalies were null but the spatial the temporal variability at scales smaller than a year were preserved. The root mean square of the annual biases ranges from 0.39(GUY and MAX) to 0.60~~This, and the fact that the geographical distance between the sites in the TSA region ranges from 1000 to 2600 ~~(SAN).This shows that the signature of the interannual variability of the NEE in Amazonia should be easy to filter out from the measurement time series given that the mean transport error at the yearly scale should be far smaller according to the hypothesis made when setting-up the inversion system. Therefore, this supported the attempt at controlling the interannual variability of the NEE in Amazonia through the inversion using the observations from the four sites in TSA~~km, i.e. up to five times the correlation length scale in the matrix $\mathbf{B}$, could suggest that the area well constrained by the sites in the TSA region through inversion is limited. However, as illustrated in Fig. 3, the station footprints also have modest values over very extensive areas which may also result in significant large-scale constraint from the inversion on the land flux estimates. This will be analyzed below in Sect. 3.2.

We assimilated observations from the South American sites between 12:00 and 15:00 local time (LT), when the boundary layer (BL) is well developed and likely to be ~~better~~ well represented by the transport model (Butler et al., 2010; Gatti et al., 2010). ~~This should avoid the difficulties the transport model has in simulating nighttime stratification, and morning and evening transitions in the BL diurnal cycle~~Such a selection of the afternoon data results in ignoring the measurements under off-shore flow at MAX, and thus the potential for capturing a clear signature of the regional NEE at this site such as at ABP. However, this potential is rather low since under off-shore flow conditions the signal at MAX is also connected to the local anthropogenic emissions, and the inversion cannot reliably exploit such a signature of the regional NEE when the dynamics of the PBL are poorly represented by the atmospheric transport model. Observations were also screened for low wind speed ($> 2\,\mathrm{m\,s^{-1}}$), thus removing the effect of local emissions (and sinks) that may not be well captured by the transport model at resolution $3.75° \times 2.5°$~~resolution and to monitor the signal of fluxes at larger scales~~. Under such on-shore flow conditions, the model correctly simulates CO_2 in the grid-cells corresponding to the horizontal location of the coastal sites, even though these grid-cells bear a significant NEE due to the overlapping of both land and ocean. This reduces the need for ad hoc changes of the model grid-cells to better represent CO_2 at the coastal sites (e.g., Law et al. , 2010). In a general way, we choose to represent the four measurements sites using the model horizontal grid-cell in which they are located since, for each site, it yields better statistical fit between the prior simulations and the selected measurements than when using neighbour grid-cells.

2.3 Analysis of an alternative estimate of the NEE for the evaluation of the inversions

Our analysis of the inversion results is compared to the independently derived NEE estimated by Jung et al. (2011) (hereafter J2011). J2011 used model tree ensembles (MTE), a machine-learning technique, to upscale FLUXNET eddy-covariance observations, based on remote sensing, climate, and land-use data as drivers, thereby producing gridded estimates of NEE and other surface fluxes at the global scale at 0.5°resolution. As discussed in J2011, large uncertainties affect their annual mean NEE estimates and associated seasonal and interannual variations. This is likely particularly true in TSA region, where few FLUXNET measurements are available. Yet, its comparison to the NEE from the inversion could give useful insights for the analysis of the latter.

3 Results

In this section we first analyze the statistical misfits between observations and simulated mole fractions from prior and posterior fluxes at the sites in the TSA area, as a measure of the efficiency of the inversion in reducing the misfits to the measurements. This is a first indicator of the significance of the corrections applied to the fluxes. We then examine the ~~impact of inversion~~ amplitude and spatial distribution of the increments from both inversions to give a further indicator of this significance, and to characterize the impact of assimilating the measurements from the sites in South America. Finally we focus on the impact of the inversions on the seasonal patterns and IAV of NEE which are the aim of this study. This analysis ~~was~~ is supported by the comparison to the product of J2011.

3.1 Comparison to observed CO_2 mole fractions

The time series of assimilated observations and the corresponding simulated CO_2 mole fractions using the prior fluxes, the inverted fluxes from MACCv10.1 and ~~our inverted fluxes (henceforth INVSAm)~~ that from INVSAm at the four sites in the TSA region are plotted in Fig. 4. The statistics ~~for bias and mean error between~~ of the misfits between these measured and simulated CO_2 mole fractions ~~for the four stations in South America~~ are summarized in Fig. 5. ~~Although the information from these four stations seems to~~ At each site in the TSA region, the smallest quadratic mean and standard deviation of the misfits between the simulations and the observations were obtained with INVSAm, which is a logical consequence of the assimilation of these observations. However, the misfits are also strongly decreased at all sites when comparing MACCv10.1 to the prior simulation. While, compared to the prior simulation, MACCv10.1 strongly decreases the standard deviation of the misfits at MAX and APB, it does not significantly reduce it at GUY and SAN. The decrease of the misfits at all sites in MACCv10.1 is thus explained by the strong decrease of the bias in these misfits. Indeed, both inversions critically reduce a large-scale bias over TSA, since the presence of a few marine stations on the globe is enough to introduce this effect by correcting the global growth rate of CO_2 (CH2010). However, the information from the local network significantly impacted the seasonality of the simulated CO_2 ~~.~~ in the TSA region.

The resulting optimized mole fractions from INVSAm generally shifted from ~~minima to maxima~~ a minimum to a maximum around June every year at SAN or from ~~maxima to minima around October and April~~ a maximum to a minimum around October (both in 2004 and 2006) at MAX with respect to the prior ~~fluxes~~ simulation and MACCv10.1 (Fig. 4c) and in agreement with the observations. While yielding a phase of seasonality at GUY comparable to that of the prior ~~fluxes~~ simulation and MACCv10.1, ~~INVSAm exhibited~~ and comparable to that of the data, INVSAm exhibits a significant rescaling of the seasonal variations in the period from May to September at ~~GUY~~ this site (Fig. 4b) compared to these two other simulations~~; this was~~ , in agreement with the observations. At ~~ABP, INVSAm surprisingly yielded an amplitude of the decrease of concentrations between January and May in 2007 and 2009 at ABP that was higher than that of the observations and of~~ SAN, during the austral fall-winter, while the misfits are negative with MACCv10.1, ~~even though smaller than that of the prior flux simulations (Fig. 4a)~~ they become positive with INVSAm. The positive increments from the assimilation of data at SAN (no other data are assimilated in TSA in 2002 and 2003) are thus too high.

Subsequently, when compared to MACCv10.1, INVSAm ~~improved~~ improves the amplitude of the seasonal variations of the simulated mole fractions with respect to the prior ~~flux~~ simulation at GUY and MAX and ~~did~~ does not impact it at SAN~~, but degraded it at ABP, even though, as well as~~. At ABP, the seasonality is less visible in both the measurements and the inversion posterior simulations and it is difficult to assess whether INVSAm improves it compared to MACCv10.1, ~~it still provided a better~~ but both inversions dramatically decrease the large amplitude of the ~~variations than that of the prior flux simulations at all sites~~prior seasonal variations, consistent with the data. The best correlations with the observations ~~were~~ are obtained with INVSAm ~~except at ABP, but the values remained low in all cases~~at all sites (Fig. 5). The values of these correlations remained generally low, ranging from 0.23 at GUY to ~~0.79 at MAX~~0.81 at ABP. These correlations are based on comparison of daily CO_2 mole fractions while the inversions control 8-day mean fluxes, which strongly limits the ability to impact the mole fractions at higher temporal resolution, and which can thus explain the low correlation values. Correlations between time series of observed and simulated monthly mean mole fractions are higher than those for daily values, ranging from 0.76 at GUY to 0.92 at ABP for INVSAm, with which, again, these correlations are the highest.

The significance of the reduction of the misfits between the mole fractions observed and simulated from the inversion is seen from the comparison between the standard deviations of these misfits and the estimate of the standard deviation of the observation errors (i.e. of the transport model errors) for hourly values in the configuration of the $\mathbf{R}$ matrix (Table A1, in supplementary material). According to this comparison, the prior misfits are much larger than the observation errors at ABP, MAX, and GUY, but are slightly smaller than these at SAN. Misfits between MACCv10.1 and the observations are similar to the prior misfits at SAN and GUY and are much smaller than the prior misfits (and smaller than the 95% confidence interval of the observations) at the coastal ABP and MAX sites. Misfits are further decreased when assimilating the data from the South American sites: they are about the standard deviation of the observation errors at all sites but GUY (where they are twice as large).

These results suggest that the ~~inversion~~ assimilation of data in ~~South America~~ the TSA region helped improve the phasing of the seasonal variations~~compared to the data~~, whereas MACCv10.1 did not impact it~~, except at ABP~~. MACCv10.1 mainly improved the amplitude of the seasonal variations at the coastal sites and decreased the biases~~and~~. INVSAm improved the amplitude of the seasonal variations ~~only. There is thus some hope of having improved the seasonal variations of the NEE in INVSAm. However, the rather low values of correlations to the data and the large remaining discrepancies in~~ at GUY. More generally, unlike MACCv10.1, INVSAm led to an improvement of the ~~data, even when using INVSAm, may reveal that this improvement is not significant enough. Furthermore, results at ABP may reveal some local issues. Finally, given the very large bias from the prior flux simulation being mainly related to an erroneous global growth rate, and~~ variability of the simulated CO_2 at the inland sites, which are more sensitive to the NEE in Amazonia.

3.2 Characterization of the monthly to annual mean inversion increments to the prior fluxes

Figure 6 shows the spatial distribution of the mean corrections applied during the period 2002–2010 by INVSAm and MACCv10.1 over land and ocean, across an area that covers the TSA area and neighbour regions. In complement, Fig. S1 shows the spatial distribution of the ~~inversion having varying efficiency to decrease it depending on the sites or on the year, it seems hard to interpret part of this decrease as a result of improvement of the interannual variability in~~ corrections over land in the TSA region for the full 2002–2010 period, and for the 2002–2005 and 2006–2010 sub-periods. Both give results for the full years and for the months of February and July. As such, these figures are indicative of the amplitude and spatial extent of the corrections from the inversions, and of the impact of the assimilation of the measurements in South America. Figure S1 even dissociates the impact of assimilating data at SAN and MAX and that of assimilating data at MAX, ABP and GUY by splitting the results between the time periods when these two different sets of data are available. The analysis of the annual mean corrections and of mean corrections for February and July should also give first insights on the significance of the corrections applied to the seasonal cycle and IAV of the NEE in the TSA region.

Figure 6 depicts the increments from both inversions, showing large patterns which are nearly zonal (or along the prevailing winds) and which overlap continuously over land and ocean. Since there is no correlation between the uncertainty in ocean and land fluxes in the $\mathbf{B}$ matrix, and given the typical length scale of the correlations in this matrix, this can be directly connected to the signature of atmospheric transport. The contiguous zonal patterns have alternate negative and positive flux increments. There is thus an opposition between corrections in the North and in the South of the TSA region. These corrections are rather negative in the North and positive in the South (positive in the North and negative in the South) during the austral summer (winter). As these corrections are stronger during the austral winter, it results in positive (negative) corrections in the North (South) at the annual scale. Such dipoles are a typical behaviour of inverse modelling systems in data-poor regions (Peylin et al., 2002) . However, changes in the amplitude and latitudinal position of this zonal dipole appear to be the main impact from the assimilation of data in the TSA region. This dipole structure may thus yield sensible corrections to the NEE in the TSA area. The dipole has a high amplitude for MACCv10.1, and even higher for INVSAm. The increments from INVSAm to the annual fluxes often exceed 150% of the prior estimate in terms of absolute values. The highest increments are obtained during austral winter and when the SAN data are available (during the period 2002–2005, see Fig. S1), which is in line with the fact that this site is located more inland than the others. Such high control of the data in the TSA region (even when checking the SAN and MAX, or the MAX, ABP and GUY datasets only) over the zonal patterns of flux corrections also highlights the very large-extent impact of these data, and of the data in the southern hemisphere in general, despite the relatively small spatial correlation length scales in the $\mathbf{B}$ matrix, and the limited area in which the station footprints are very high. The inversion also generates patterns of corrections of smaller spatial scale close to the ~~NEE~~measurement sites in the TSA region when these sites are used by the inversion. This raises hope that the NEE over the whole TSA region is strongly constrained by the observations, but can also raise questions regarding the spatial variations of the corrections applied by the inversion to the NEE within the TSA region, at least when considering areas at more than 500 km from the measurement sites. However, various pieces of evidence (Fig. 5 and 6, the analysis of the decrease in misfits to the observations from the inversion in Sect. 3.1, and the previous analysis of the high increments to the monthly mean and annual mean NEE over the entire TSA region) indicate that the corrections from the inversion are significant.

3.3 Diagnostics of the biogenic CO_2 fluxes

3.3.1 Seasonality

Figure ~~6a~~ 7a illustrates the mean seasonal cycle of NEE from the prior fluxes, J2011, MACCv10.1 and INVSAm over TSA. The mean for the full period 2002–2010 was removed because uncertainties in the long-term mean can be large for the inversions as well as for the J2011 product, and because this long-term mean can differ significantly between the different estimates. Removing the ~~means~~ mean allows us to focus on the seasonal variations. Hereafter, positive values of NEE indicate anomalous CO_2 release to the atmosphere; negative values indicate anomalous uptake by the ecosystems. The shaded area indicates the dry season, defined as months with precipitation $< 100\,\mathrm{mm}$ according to data from the Tropical Rainfall Measuring Mission (TRMM 3B43 (v6) product), averaged over January 2002 to June 2010. The results of Fig. ~~6a were~~ 7a are calculated considering all the plant functional types (PFTs) represented in ORCHIDEE over the ~~study~~ TSA region. The vegetation map of ORCHIDEE, originally at a spatial resolution of 0.72°, was aggregated according to the transport model grid, and Fig. ~~7~~ 8 illustrates the dominant PFTs in terms of area for each transport model ~~grid cell~~grid-cell.

Both the prior ~~flux~~ simulation and the inversions ~~predicted~~ predict a maximum of NEE (i.e., likely a maximum of CO_2 release) in the dry season and a minimum of NEE (i.e., likely a maximum of CO_2 uptake) in the wet season (Fig. ~~6a~~7a). This behaviour ~~was also observed~~ is also seen in J2011. However, J2011 ~~indicated~~ places the maximum of NEE during the transition between the wet and dry season while the prior ~~flux~~ simulation and the inversions ~~indicated that it occurs~~ place it at the end of the dry season. Even though the inversions ~~seemed~~ seem to delay or lengthen this maximum, such a modification ~~was~~ is not significant and their seasonal phasing ~~was~~ is likely strongly constrained by the patterns of the prior fluxes. In particular, according to the comparison between INVSAm and MACCv10.1, the assimilation of data from the four stations in ~~South America did~~ the TSA region does not seem to impact this phasing. ~~However, such~~

The inland data are prone to ~~bring a constraint on fluxes mainly~~ bear a stronger signature from fluxes in tropical broadleaf evergreen and raingreen (TBE) forests (Fig. ~~7~~8), while the mean seasonal behaviour over the whole ~~analyzed domain~~ TSA region could be mainly related to other PFTs.

Therefore, we ~~isolated~~ isolate the results for ~~TBE forests and calculated the mean seasonal cycle of NEE over model grid cells~~ the area of TBE forests, this area being defined by the selection the model grid-cells dominated by this vegetation type~~(~~. The configuration of the prior uncertainties in the inversion does not account for PFTs, so that the spread of the flux corrections in the inversions is not forced a priori to depend on vegetation type. We still expect that the variations in the measurements, when their footprint covers different distributions of PFTs, reflect differences in NEE of the PFTs. Consequently, the spatial patterns of the increments from the inversion may be consistent with the spatial patterns of NEE induced by the distribution of the different vegetation types. The mean seasonal cycle of NEE for the area of TBE forests within the TSA region is given in Fig. ~~6b). This did not yield~~ 7b. The restriction of the analysis to the TBE forest does not show any clear correlation between ~~the existence of maxima or minima in NEE~~ NEE extremes and the phasing of wet and dry seasons, neither when considering the NEE from the prior nor when considering the NEE from both ~~inversions estimates, even though~~ inversion estimates. This is different from J2011 that indicates a maximum of the NEE a few months before the beginning of the dry season and a minimum of the NEE at the beginning of the wet season. ~~In particular, the~~ The prior and the inversions ~~indicated several local maxima or minima in the NEE . This could reflect the signature of~~ indicate several local extremes of NEE throughout the year that may reflect the overlapping of significantly different seasonal cycles for different sub-regions within TBE forests.

The strong spatial heterogeneity of the time variations of the NEE in TBE forests ~~, which~~ has been discussed in the introduction~~, is illustrated here along with the spatial heterogeneity of the time variations of the precipitation in~~ . Fig. ~~6c–f. Figure 6c–f are based on monthly averages of~~ S2 illustrates it this with results of local NEE mean seasonal cycle estimated from EC measurements across TSA. This figure also shows the mean seasonal cycle of the precipitation at these sites to illustrate the spatial heterogeneity of the drivers of NEE ~~measurements at four flux towers located in central eastern, and southern Amazonia (Fig. 7). The sites at Caxihuanã (BR-Cax, Fig. 6c) and Rebio Jarú (BR-Ji2, Fig. 6f) are covered by *terra firme* humid forest; the sites are described by Carswell et al. (2002) and von Randow et al. (2004) , respectively. Data cover the period 2000–2002 at both sites . At Santarém (BR-Sa3, Fig. 6e), data shown were collected at the Tapajós km 83 tower site, an area covered by tropical humid forest, over 2001–2002. A description of the site can be found in Goulden et al. (2004) and Miller et al. (2004) . The site at Bananal Island (BR-Ban, Fig. 6a), on the other hand, is located in a floodplain, in an area of transition between forest and savannah vegetation (Borma et al., 2009) . At BR-Ban data cover the period 2004–2005. At these four sites, mean NEE was removed. To examine if the inversion captured~~ within TSA.

To examine whether the inversion captures this spatial variability of the fluxes, we ~~analyzed~~ analyze the seasonal variations of the NEE estimates for the two zones depicted in Fig. ~~7.~~ 8. Zone 1 was located in northeastern Amazonia, close to the measurement stations SAN and GUY. Zone 2 was located in central eastern Amazonia. Both zones ~~were~~ are mainly covered by TBE forests, according to the vegetation classification of ORCHIDEE. According to Malhi et al. (2009), eastern Amazonia is drier, and shows a stronger seasonality than western Amazonia. However, we ~~did~~ do not identify a clear pattern of NEE seasonal variations that could be driven by the rainfall seasonality in any of the two sub-regions, except for J2011 in Zone 1 (Fig. ~~6g~~7c), since the other ~~model estimates exhibited, again ,~~ estimates again exhibited maxima and minima of NEE during both dry and wet seasons. Actually, in Zone 2 (Fig. ~~6h~~7d) the dry season ~~could~~ cannot not be clearly identified. In this zone, the prior flux and the inversions indicated several maxima and minima of NEE, but J2011 ~~exhibited~~exhibite, again, a clear seasonal cycle with a maximum in June and a minimum October as in Zone 1. While J2011 showed nearly the same amplitude and phasing of monthly mean NEE variations in both zones and over TBE forests (Fig. ~~6b~~7b), prior and inversions estimates of the seasonal variations differed both in phasing and amplitude between zone 1, 2 and the whole TBE forest area.

Divergent patterns ~~could be~~ are found in INVSAm with respect to MACCv10.1, which ~~remained~~ remains closer to the prior fluxes, even though the departure of MACCv10.1 from the prior NEE is significant in Zone 2 and for the whole TBE area (Fig. 7b and 7d). The comparison of these inversion results ~~showed~~ shows that significant flux corrections due to the assimilation of data in South America ~~were~~ are applied in Zone 1 (Fig. ~~6h~~7c), i.e., in northeastern Amazonia, where ~~the~~ stations SAN and GUY ~~were located.~~ are located. The influence of SAN over this zone is clearer when splitting the analysis period of the mean seasonal cycles between 2002–2005 and 2006–2010 (not shown). The differences between INVSAm and MACCv10.1 are more accentuated during the period 2002–2005, when SAN is active. However, there are still significant changes between these two estimates during 2006–2010. The changes between MACCv10.1 and INVSAm in Zone 2 (Fig. 7d) are also significant, even though Zone 2 seems hardly observed by the TSA observation network. As analysed in Sect. 3.2, the control of the long-range dipole (of its amplitude and latitudinal position) by the measurements in region TSA explains such an impact of these measurements on the results in Zone 2, as well as that of measurements outside South America, which explains the departure of MACCv10.1 from the prior NEE in zone 2. Zone 2 is actually located close to the frontier between the Northern and Southern patterns of the dipole in the TSA region. A latitudinal shift of the frontier through the assimilation of data in northeastern Amazonia can thus easily imply that positive (negative) increments from the inversion are reverted into negative (positive) increments.

In an attempt at getting clearer seasonal patterns in some of the other sub-regions of Amazonia, two additional zones ~~were~~ have been analyzed, located in southwestern and southeastern Amazonia, where the dry season is potentially earlier and more extreme (Fig. S2a,d). Both sub-regions ~~encompassed~~ encompass areas where the impact of the droughts of 2005 and 2010 was the highest according to Lewis et al. (2011). The results, however, ~~are not shown here since the results did not provide~~ do not provide any further information than ~~is given in zones 1 and 2.~~ Fig. 7c,d and are not shown. J2011 still ~~exhibited~~ exhibit the same amplitude of the seasonal cycle and the same location of maximum and minimum NEE as in zones 1 and 2 despite the extent of the dry season. Prior fluxes and inversions still showed maxima and minima during the dry season in some cases, and ~~inversions introduced~~ the inversions introduce only slight modifications to the amplitude and phasing of the NEE relative to the prior simulation.

~~Figure 8 shows the spatial distribution of the corrections applied by INVSAm and depicts large zones of contiguous negative and positive flux increments. When the mean corrections were positive (respectively negative), e.g., during July (respectively during February) in the area of the measurements sites (in the north of South America, which overlap the Zone 1 defined in Fig. 7), negative (respectively positive) corrections were applied south of this area (including the Zone 2 defined in Fig. 7), which seems to underlie the need for the inversion to balance the overall corrections in tropical South America in order to fit the measurements outside the continent. Such dipoles are a typical behaviour of inverse modelling systems in data-poor regions (Peylin et al., 2002) . This may be related to the setup of the uncertainties in the prior covariance matrix that would not perfectly fit with actual errors in the prior estimate, and that may extend the corrections too far from the measurement footprints. This questions the spatial variations of the corrections applied by the inversion to the seasonal cycle of the NEE~~This is an expected result due to insufficient data in the southern part of the TSA to constrain fluxes in that region.

3.3.2 Interannual variability

Figure 9a depicts the annual NEE anomalies of the prior simulation, MACCv10.1, INVSAm and an additional inversion called FLAT, compared to ~~the mean of~~ their mean NEE over 2002–2010, aggregated over the whole ~~study~~ TSA region (considering all PFTs). FLAT corresponds to ~~the inversion usingthe flat prior described in Sect. 2.2, and~~ a new inversion using, as a prior estimate, a "flat prior" whose annual anomalies are null over the ~~whole study region.~~ TSA region. Using the standard prior NEE as a basis, the flat prior is built by offsetting the annual budgets of NEE over the TSA region so that they equal the mean annual NEE over TSA and over the 2002–2010 period from the standard prior NEE. The spatial variability and the temporal variability at scales smaller than a year are conserved between the standard NEE and the flat prior, since the offsets are applied homogeneously in space and time within TSA and within one year. FLAT assimilates the data from the four surface sites in TSA in addition to those used by both MACCv10.1 and INVSAm. Of note is that even if increments on the NEE annual budget of a given year from an inversion are weak, the changes in the corresponding annual anomaly from the inversion can be high because the inversion modifies the 2002–2010 average against which the anomaly is computed. Prior fluxes, MACCv10.1 and INVSAm ~~predicted~~ display only small positive anomalies during the ~~years of drought~~ drought years (2005, 2010) compared to other years. FLAT ~~predicted~~ displays a negative anomaly (i.e., a strong uptake) in 2010, but it indicates a larger positive anomaly in 2005 than that of other estimates.

On the other hand, the strong NEE negative anomaly of 2009 in the prior fluxes, MACCv10.1 and INVSAm ~~was also predicted by~~ is also in FLAT, which suggests ~~a robust pattern~~ that this pattern is strongly driven by the atmospheric measurements, and which raises confidence in it.

As in Sect. ~~3.2~~3.3.1, we isolated the results for the TBE forests area (Fig. 9b). In this case, prior fluxes and both MACCv10.1 and INVSAm estimates ~~predicted~~ show diverging annual mean responses of forests to drought, with a positive anomaly in 2005 and a negative anomaly in 2010. ~~In~~ For 2009, when climatic conditions were abnormally humid across South America, the inversion estimates consistently ~~predicted~~ show a small positive anomaly, opposite to the response for the whole TSA region. The small anomalies in all inversions suggest a weak sensitivity of the NEE of TBE forests to interannual variations and that most of the IAV over the study area is not related to TBE forests.

Finally, we ~~analyzed~~ analyze the results in the two sub-regions shown in Fig. ~~7~~8, in an attempt to identify potential differences in the regional responses. NEE estimates from the prior, INVSAm and MACCv10.1 ~~showed~~ show various responses of forests to drought in these zones. In zone 1 (Fig. 10a) all these estimates ~~showed~~ present a positive anomaly in 2005 and a negative anomaly in 2010, while in zone 2 (Fig. 10b) they yielded negative anomalies during both years. J2011 ~~exhibited~~ exhibit abnormal anomalies much smaller than these NEE estimates (Fig. 10c and d)~~, which~~ . This prevents us from getting insights ~~on~~ into the IAV from the comparison of J2011 to the other estimates. However, the product of J2011 must be used cautiously, especially when evaluating IAV of NEE. J2011 relied on a limited number of EC stations across the Amazon basin, with short time series, to estimate MTE based on spatial gradients among the sites, and then extrapolated to temporal gradients. This is valid assuming that spatial and temporal NEE patterns have the same sensitivity to climate, which may be incorrect (Piao et al., 2013) . The example of the divergences of the results between MACCv10.1 and INVSAm in 2003 in Zone 2 illustrates, again, some weak ability to precisely constrain the fluxes in such a small area, which is quite distant from the measurement sites in TSA. Indeed, the analysis of the maps of increments from MACCv10.1 and INVSAm for the annual mean NEE in 2003 (not shown) demonstrates that the assimilation of data at SAN during this year shifts the northern border of the pattern of negative corrections in MACCv10.1 from North of Zone 2 to the south of Zone 2. Since, on average, over 2002–2010, both inversions apply positive increments in this Zone (see Fig. 6) this leads to a clear negative annual anomaly in Zone 2 and for the year 2003 for INVSAm.

4 Discussion and concluding remarks

Amazonian ~~forest plays~~ forests play a key role in the global carbon balance, but there are large uncertainties on the evolution of this terrestrial sink. Uncertainties stem from ~~the~~ incomplete knowledge of the processes behind land–atmosphere CO_2 exchange in this ~~type of forest~~region. Improving our understanding of the seasonal and interannual variations of Amazonian ~~forest~~ forests is thus a priority. In an attempt to gain insight into how these temporal variations of CO_2 fluxes vary across Amazonia, we analysed global inversions and incorporated new measurements of atmospheric CO_2 mole fractions in TSA into ~~a global atmospheric inversion~~ one of these inversions. The analysis of the global inversions at such spatial scales, which are generally ignored in global inversion studies, is justified by the use of a variational inversion system solving for the fluxes at $\sim 3°$and 8-day resolution. We showed that the two inversions applied large corrections to the estimates of NEE from a vegetation model that they used as prior information. The inverted NEE was strongly controlled by the assimilation of CO_2 measurements both outside and within the TSA region, and this control was characterized by zonal patterns of alternate positive and negative corrections, which we call "zonal dipole", in addition to more local patterns in the vicinity of the sites that were assimilated.

Despite an overall improvement by the inversion of the seasonal variations of the simulated ~~concentrations~~ CO_2 mole fractions when compared to the measurements in TSA, several issues arose when analyzing the seasonal cycles of NEE from the inversion. The seasonality of the mean NEE over the whole TSA region remained basically unchanged between the inversion estimates (Fig. 7a). The prior and inversion estimates of this mean seasonal cycle of NEE at ~~basin scale were~~ the TSA scale are not in line with J2011 and ~~disagreed~~ disagree with the intuitive assumption that the seasonal cycle should be correlated with rainfall and solar radiation, especially in the tropical forest area. Furthermore, they ~~did~~ do not exhibit a clear seasonal pattern over TBE forests at basin scale or within the analyzed sub-regions. J2011 ~~yielded~~ displays a clear, homogeneous seasonal cycle all ~~over the domain~~the TSA region, which does not give confidence in its ability to distinguish regional heterogeneity.

The proximity of Zone 1 to the stations in northeastern Amazonia (SAN and GUY) (Fig. ~~7) suggested a~~ 8) suggests better confidence in the flux corrections applied by INVSAm to the prior fluxes in that zone than elsewhere in ~~the study area, especially since the analysis of the spatial distribution of such corrections over the whole study area in Fig. 8 gave low confidence in the corrections applied south of the measurement site area, and~~ TSA region.

The reliability in the seasonal patterns of the inverted fluxes is thus not high, which seems to ~~artificially~~ confirm that the zonal dipoles of increments from the inversion are artificial patterns, which balance the overall correction in ~~tropical South America.~~

~~The dipoles likely identified in Fig. 8 are characteristic of domains that are poorly constrained by atmospheric data in inversion studies (Peylin et al., 2002) . The footprint in the flux space of the set of four stations in South America used in this study covered a very limited area of Amazonia. This suggests that the extrapolation of the information from this area to the whole of Amazonia relies on~~ the Southern Hemisphere, and which are not necessarily consistent with the actual NEE in the TSA region. This is directly connected to the lack of CO_2 measurements in the TSA region, both in space and time. The limited overlap among the TSA observations is a critical issue since measurements are often only available at a single site at once, and consequently, temporary model errors at this site can get far more weight in the inversion than if it had been balanced by information from other sites. Furthermore, the lack of confidence in the INVSAm results in Zone 1, which is relatively close to the GUY and SAN, suggests a low reliability in the statistics of the uncertainty in the prior ~~fluxes, for which the reliability is relatively low, and on the need to balance the overall correction over TSA to fit the measurements made outside this region. Furthermore, with limited overlap among the TSA observations, the inversion system may have applied corrections in response to events registered by only a single station at a time. The reliability in the seasonal patterns of~~ NEE (in the inversion configuration), on which the extrapolation of the information from the vicinity of these sites to the

~~inverted fluxes is thus not high~~whole North East of the TSA region relies. This further supports the choice of avoiding computing posterior uncertainties in the inverted NEE as discussed in Sect. 2.1.

Such considerations also weaken the analysis of the IAV based on the inversion while J2011 does not provide a reliable IAV of the NEE in TSA, which could have supported such an analysis. But some patterns of the IAV in the NEE ~~from the inversion seem robust and strongly driven by~~ seem consistent between the different inversion estimates when the atmospheric measurements ~~: across Amazonia~~ have a strong control on it: across the TSA region, the estimates from the prior fluxes, MACCv10.1, INVSAm and FLAT indicate small positive flux annual anomalies (CO_2 release) during the drought in 2005 and a strong negative (CO_2 sink) anomaly in 2009, presumably related to lower temperatures and more humid conditions in 2009. However, in 2010 there is a divergence of the results between the FLAT estimate and the others.

In the TBE ~~forest~~forests, the highest source anomaly in 2005 seen in the prior fluxes, MACCv10.1 and INVSAm may be related to reduced photosynthesis during the drought, as found by Gatti et al. (2014), and/or tree mortality caused by ~~a~~ the squall event of January 2005 ~~Negrón-Juárez et al. (2010)~~ (Negrón-Juárez et al., 2010) . However, in 2010 these results indicate a small sink anomaly. This anomaly seems inconsistent with the hypothesis of a higher negative impact of the drought in 2010, which was more intense in terms of water stress and more geographically extensive (Lewis et al., 2011). On the other hand, it seems consistent with the recent results of Gatti et al. (2014), who found that the Amazon basin was carbon neutral during that year.

Even though some seasonal or interannual patterns from the inversion ~~could~~ look realistic, our study mainly reveals some critical issues that hamper the ability to derive an accurate estimation of the temporal variability of NEE and of its spatial heterogeneity across Amazonian forests. A denser monitoring network across the basin ~~,~~with continuous time series, as ~~done~~ initiated by Gatti et al. (2014), is ~~essential to better~~ needed to well constrain the fluxes in the region. In addition, the simulation of atmospheric transport ~~in this region needs~~ may need to be handled ~~using~~ with models that are better adapted to the local meteorological conditions. Regional transport models with higher spatial and temporal resolution and improved parameterizations of key atmospheric processes for the region (e.g., deep convection, Parazoo et al., 2008) have been developed (Moreira et al., 2013). The combination of a denser observation network and state-of-the-art regional modelling tools would overcome some of the critical limitations encountered here for the study of the temporal variability of biosphere CO_2 fluxes in Amazonia. Such regional inversion will require reliable regional configurations of the input error statistics, which could rely on extensions of the flux eddy covariance measurement networks in Amazonia. Finally, adaptive strategies for the representation of the observations in the model simulations as a function of the sites and of the meteorological conditions (Law et al., 2010) could help loosen the selection of the data for the assimilation.

Acknowledgements. We would like to thank Martin Jung (Max Planck Institute for Biogeochemistry) for the access to the upscaled NEE data. ~~This study was part~~ Data recorded at the GUY site were obtained in the framework of the GUYAFLUX project funded by the French Ministry of Research, INRA, and the CNES, in the framework of the PO Feder Région Guyane. The GUYAFLUX project also received support from an Investissement d'Avenir grant of the French ANR (CEBA: ANR-10-LABX-0025). This study was co-funded by the European Commission under the EU Seventh Research Framework Programme (grant agreement No. 283080, Geocarbon project) and ARIA Technologies. G. Broquet acknowledges funding and support from the Chaire industrielle BridGES, a joint research program between Thales Alenia Space, Veolia, CEA, UVSQ and CNRS.

References

Araújo, A. C., Nobre, A. D., Kruijt, B., Elbers, J. A., Dallarosa, R., Stefani, P., von Randow, C., Manzi, A. O., Culf, A. D., Gash, J. H. C., Valentini, R., and Kabat, P.: Comparative measurements of carbon dioxide fluxes from two nearby towers in a central Amazonian rainforest: the Manaus LBA site, J. Geophys. Res., 107, 8090, doi:10.1029/2001JD000676, 2002.

Baker, I. T., Prihodko, L., Denning, A. S., Goulden, M., Miller, S., and da Rocha, H. R.: Seasonal drought stress in the Amazon: reconciling models and observations, J. Geophys. Res., 113, G00B01, doi:10.1029/2007JG000644, 2008.

~~Balch, J. K.: Atmospheric science: drought and fire change sink to source, Nature, 506, 41–42, doi:, 2014.~~

Berrisford, P., Dee, D., Fielding, K., Fuentes, M., Kallberg, P., Kobayashi, S., and Uppala, S.: The ERA-Interim archive, Tech. rep., European Centre for Medium Range Weather Forecasts, Reading, 2009.

Bonal, D., Bosc, A., Ponton, S., Goret, J.-Y., Burban, B., Gross, P., Bonnefond, J.-M., Elbers, J., Longdoz, B., Epron, D., Guehl, J.-M., and Granier, A.: Impact of severe dry season on net ecosystem exchange in the neotropical rainforest of French Guiana, Glob. Change Biol., 14, 1917–1933, doi:10.1111/j.1365-2486.2008.01610.x, 2008.

Borma, L. S., da Rocha, H. R., Cabral, O. M., von Randow, C., Collicchio, E., Kurzatkowski, D., Brugger, P. J., Freitas, H., Tannus, R., Oliveira, L., Rennó, C. D., and Artaxo, P.: Atmosphere and hydrological controls of the evapotranspiration over a floodplain forest in the Bananal Island region, Amazonia, J. Geophys. Res., 114, G01003, doi:10.1029/2007JG000641, 2009.

Butler, M. P., Davis, K. J., Denning, A. S., and Kawa, S. R.: Using continental observations in global atmospheric inversions of CO_2: North American carbon sources and sinks, Tellus B, 62, 550–572, doi:10.1111/j.1600-0889.2010.00501.x, 2010.

Carswell, F. E., Costa, A. L., Palheta, M., Malhi, Y., Meir, P., Costa, J. d. P. R., Ruivo, M. d. L., Leal, L. d. S. M., Costa, J. M. N., Clement, R. J., and Grace, J.: Seasonality in CO_2 and H_2O flux at an eastern Amazonian rain forest, J. Geophys. Res., 107, LBA 43-1–LBA 43-16, doi:10.1029/2000JD000284, 2002.

Chevallier, F. and O'Dell, C. W.: Error statistics of Bayesian CO_2 flux inversion schemes as seen from GOSAT, Geophys. Res. Lett., 40, 1252–1256, doi:10.1002/grl.50228, 2013.

Chevallier, F., Viovy, N., Reichstein, M., and Ciais, P.: On the assignment of prior errors in Bayesian inversions of CO_2 surface fluxes, Geophys. Res. Lett., 33, L13802, doi:10.1029/2006GL026496, 2006.

Chevallier, F., Bréon, F.-M., and Rayner, P. J.: Contribution of the Orbiting Carbon Observatory to the estimation of CO_2 sources and sinks: Theoretical study in a variational data assimilation framework, J. Geophys. Res., 112, n/a–n/a, doi:10.1029/2006JD007375, 2007.

Chevallier, F., Ciais, P., Conway, T. J., Aalto, T., Anderson, B. E., Bousquet, P., Brunke, E. G., Ciattaglia, L., Esaki, Y., Fröhlich, M., Gomez, A., Gomez-Pelaez, A. J., Haszpra, L., Krummel, P. B., Langenfelds, R. L., Leuenberger, M., Machida, T., Maignan, F., Matsueda, H., Morguí, J. A., Mukai, H., Nakazawa, T., Peylin, P., Ramonet, M., Rivier, L., Sawa, Y., Schmidt, M., Steele, L. P., Vay, S. A., Vermeulen, A. T., Wofsy, S., and Worthy, D.: CO_2 surface fluxes at grid point scale estimated from a global 21 year reanalysis of atmospheric measurements, J. Geophys. Res., 115, D21307, doi:10.1029/2010JD013887, 2010.

Chevallier, F., Wang, T., Ciais, P., Maignan, F., Bocquet, M., Altaf Arain, M., Cescatti, A., Chen, J., Dolman, A. J., Law, B. E., Margolis, H. A., Montagnani, L., and Moors, E. J.: What eddy-covariance measurements tell us about prior land flux errors in CO_2-flux inversion schemes, Global Biogeochem. Cycles, 26, n/a–n/a, doi:10.1029/2010GB003974, 2012.

Ciais, P., Rayner, P., Chevallier, F., Bousquet, P., Logan, M., Peylin, P., and Ramonet, M.: Atmospheric inversions for estimating CO_2 fluxes: methods and perspectives, Climatic Change, 103, 69–92, 2010.

Enting, I. G., Trudinger, C. M., and Francey, R. J.: A synthesis inversion of the concentration and $\delta^{13}C$ of atmospheric CO_2, Tellus B, 47, 35–52, 1995.

Gatti, L. V., Miller, J. B., D'Amelio, M. T. S., Martinewski, A., Basso, L. S., Gloor, M. E., Wofsy, S., and Tans, P.: Vertical profiles of CO_2 above eastern Amazonia suggest a net carbon flux to the atmosphere and balanced biosphere between 2000 and 2009, Tellus B, 62, 581–594, doi:10.1111/j.1600-0889.2010.00484.x, 2010.

Gatti, L. V., Gloor, M., Miller, J. B., Doughty, C. E., Malhi, Y., Domingues, L. G., Basso, L. S., Martinewski, A., Correia, C. S. C., Borges, V. F., Freitas, S., Braz, R., Anderson, L. O., Rocha, H., Grace, J., Phillips, O. L., and Lloyd, J.: Drought sensitivity of Amazonian carbon balance revealed by atmospheric measurements, Nature, 506, 76–80, doi:10.1038/nature12957, 2014.

Gloor, M., Gatti, L., Brienen, R., Feldpausch, T. R., Phillips, O. L., Miller, J., Ometto, J. P., Rocha, H., Baker, T., de Jong, B., Houghton, R. A., Malhi, Y., Aragão, L. E. O. C., Guyot, J.-L., Zhao, K., Jackson, R., Peylin, P., Sitch, S., Poulter, B., Lomas, M., Zaehle, S., Huntingford, C., Levy, P., and Lloyd, J.: The carbon balance of South America: a review of the status, decadal trends and main determinants, Biogeosciences, 9, 5407–5430, doi:10.5194/bg-9-5407-2012, 2012.

Goulden, M. L., Miller, S. D., da Rocha, H. R., Menton, M. C., de Freitas, H. C., e Silva Figueira, A. M., and de Sousa, C. A. D.: Diel and seasonal patterns of tropical forest CO_2 exchange, Ecol. Appl., 14, 42–54, doi:10.1890/02-6008, 2004.

Grace, J., Malhi, Y., Lloyd, J., McIntyre, J., Miranda, A. C., Meir, P., and Miranda, H. S.: The use of eddy covariance to infer the net carbon dioxide uptake of Brazilian rain forest, Glob. Change Biol., 2, 209–217, doi:10.1111/j.1365-2486.1996.tb00073.x, 1996.

Hourdin, F., Musat, I., Bony, S., Braconnot, P., Codron, F., Dufresne, J.-L., Fairhead, L., Filiberti, M.-A., Friedlingstein, P., Grandpeix, J.-Y., Krinner, G., LeVan, P., Li, Z.-X., and Lott, F.: The LMDZ4 general circulation model: climate performance and sensitivity to parametrized physics with emphasis on tropical convection, Clim. Dynam., 27, 787–813, doi:10.1007/s00382-006-0158-0, 2006.

Huete, A. R., Didan, K., Shimabukuro, Y. E., Ratana, P., Saleska, S. R., Hutyra, L. R., Yang, W., Nemani, R. R., and Myneni, R.: Amazon rainforests green-up with sunlight in dry season, Geophys. Res. Lett., 33, L06405, doi:10.1029/2005GL025583, 2006.

INPE: Projeto de Monitoramento do Desmatamento na Amazônia Legal por Satélite (PRODES), available at: http://www.obt.inpe.br/prodes/index.php (last access: 4 May 2014), 2011.

Jung, M., Reichstein, M., Margolis, H. A., Cescatti, A., Richardson, A. D., Arain, M. A., Arneth, A., Bernhofer, C., Bonal, D., Chen, J., Gianelle, D., Gobron, N., Kiely, G., Kutsch, W., Lasslop, G., Law, B. E., Lindroth, A., Merbold, L., Montagnani, L., Moors, E. J., Papale, D., Sottocornola, M., Vaccari, F., and Williams, C.: Global patterns of land–atmosphere fluxes of carbon dioxide, latent heat, and sensible heat derived from eddy covariance, satellite, and meteorological observations, J. Geophys. Res., 116, G00J07, doi:10.1029/2010JG001566, 2011.

Kirchhoff, V. W. J. H., Aires, C. B., and Alvala, P. C.: An experiment to determine atmospheric CO concentrations of tropical South Atlantic air samples, Quart. J. Roy. Meteor. Soc., 129, 1891–1902, doi:doi10.1256/qj.02.142, 2003.

Krinner, G., Viovy, N., de Noblet-Ducoudré, N., Ogée, J., Polcher, J., Friedlingstein, P., Ciais, P., Sitch, S., and Prentice, I. C.: A dynamic global vegetation model for studies of the coupled atmosphere–biosphere system, Global Biogeochem. Cy., 19, GB1015, doi:10.1029/2003GB002199, 2005.

Law, R. M., Steele, L. P., Krummel, P. B., and Zahorowski, W.: Synoptic variations in atmospheric CO_2 at Cape Grim: a model intercomparison, Tellus B, 62, 810–820, doi:10.1111/j.1600-0889.2010.00470.x, 2010.

Lewis, S. L., Brando, P. M., Phillips, O. L., van der Heijden, G. M. F., and Nepstad, D.: The 2010 Amazon drought, Science, 331, p. 554, doi:10.1126/science.1200807, 2011.

Lloyd, J., Kolle, O., Fritsch, H., de Freitas, S. R., Silva Dias, M. A. F., Artaxo, P., Nobre, A. D., de Araújo, A. C., Kruijt, B., Sogacheva, L., Fisch, G., Thielmann, A., Kuhn, U., and Andreae, M. O.: An airborne regional carbon balance for Central Amazonia, Biogeosciences, 4, 759–768, doi:10.5194/bg-4-759-2007, 2007.

Maignan, F., Bréon, F.-M., Chevallier, F., Viovy, N., Ciais, P., Garrec, C., Trules, J., and Mancip, M.: Evaluation of a Global Vegetation Model using time series of satellite vegetation indices, Geosci. Model Dev., 4, 1103–1114, doi:10.5194/gmd-4-1103-2011, 2011.

Malhi, Y., Roberts, J. T., Betts, R. A., Killeen, T. J., Li, W., and Nobre, C. A.: Climate change, deforestation, and the fate of the Amazon, Science, 319, 169–172, 2008.

Malhi, Y., Aragão, L. E. O. C., Galbraith, D., Huntingford, C., Fisher, R., Zelazowski, P., Sitch, S., McSweeney, C., and Meir, P.: Exploring the likelihood and mechanism of a climate-change-induced dieback of the Amazon rainforest, P. Natl. Acad. Sci. USA, 106, 20610–20615, doi:10.1073/pnas.0804619106, 2009.

Marengo, J. A., Ronchail, J., Baez, J., and Alves, L.: State of the climate in 2009, in: The Climate of Tropical South America East of the Andes, vol. 91, American Meteorological Society, Boston, MA, USA, S148–S150, 2010.

Miller, S. D., Goulden, M. L., Menton, M. C., da Rocha, H. R., de Freitas, H. C., Figueira, A. M. E. S., and Dias de Sousa, C. A.: Biometric and micrometeorological measurements of tropical forest carbon balance, Ecol. Appl., 14, 114–126, doi:10.1890/02-6005, 2004.

Moreira, D. S., Freitas, S. R., Bonatti, J. P., Mercado, L. M., Rosário, N. M. É., Longo, K. M., Miller, J. B., Gloor, M., and Gatti, L. V.: Coupling between the JULES land-surface scheme and the CCATT-BRAMS atmospheric chemistry model (JULES-CCATT-BRAMS1.0): applications to numerical weather forecasting and the CO_2 budget in South America, Geosci. Model Dev., 6, 1243–1259, doi:10.5194/gmd-6-1243-2013, 2013.

Morton, D. C., Nagol, J., Carabajal, C. C., Rosette, J., Palace, M., Cook, B. D., Vermote, E. F., Harding, D. J., and North, P. R. J.: Amazon forests maintain consistent canopy structure and greenness during the dry season, Nature, 506, 7487, doi:10.1038/nature13006, 2014.

Negrón-Juárez, R. I., Chambers, J. Q., Guimaraes, G., Zeng, H., Raupp, C. F. M., Marra, D. M., Ribeiro, G. H. P. M., Saatchi, S. S., Nelson, B. W., and Higuchi, N.: Widespread Amazon forest tree mortality from a single cross-basin squall line event, Geophys. Res. Lett., 37, L16701, doi:10.1029/2010GL043733, 2010.

Olivier, J. and Berdowski, J.: Global emissions sources and sinks, in: The Climate System, A. A. Balkema Publishers/Swets & Zeitlinger Publishers, Lisse, 33–78, 2001.

Ometto, J. P. H. B., Nobre, A. D., Rocha, H. R., Artaxo, P., and Martinelli, L. A.: Amazonia and the modern carbon cycle: lessons learned, Oecologia, 143, 483–500, 2005.

Parazoo, N. C., Denning, A. S., Kawa, S. R., Corbin, K. D., Lokupitiya, R. S., and Baker, I. T.: Mechanisms for synoptic variations of atmospheric CO_2 in North America, South America and Europe, Atmos. Chem. Phys., 8, 7239–7254, doi:10.5194/acp-8-7239-2008, 2008.

Parazoo, N. C., Bowman, K., Frankenberg, C., Lee, J.-E., Fisher, J. B., Worden, J., Jones, D. B. A., Berry, J., Collatz, G. J., Baker, I. T., Jung, M., Liu, J., Osterman, G., O'Dell, C., Sparks, A., Butz, A., Guerlet, S., Yoshida, Y., Chen, H., and Gerbig, C.: Interpreting seasonal changes in the carbon balance of southern Amazonia using measurements of XCO_2 and chlorophyll fluorescence from GOSAT, Geophys. Res. Lett., 40, 2829–2833, doi:10.1002/grl.50452, 2013.

Peylin, P., Baker, D., Sarmiento, J., Ciais, P., and Bousquet, P.: Influence of transport uncertainty on annual mean and seasonal inversions of atmospheric CO_2 data, J. Geophys. Res., 107, 4385, doi:10.1029/2001JD000857, 2002.

Peylin, P., Law, R. M., Gurney, K. R., Chevallier, F., Jacobson, A. R., Maki, T., Niwa, Y., Patra, P. K., Peters, W., Rayner, P. J., Rödenbeck, C., van der Laan-Luijkx, I. T., and Zhang, X.: Global atmospheric carbon budget: results from an ensemble of atmospheric CO_2 inversions, Biogeosciences, 10, 6699–6720, doi:10.5194/bg-10-6699-2013, 2013.

Phillips, O. L., Aragão, L. E. O. C., Lewis, S. L., Fisher, J. B., Lloyd, J., López-González, G., Malhi, Y., Monteagudo, A., Peacock, J., Quesada, C. A., van der Heijden, G., Almeida, S., Amaral, I., Arroyo, L., Aymard, G., Baker, T. R., Bánki, O., Blanc, L., Bonal, D., Brando, P., Chave, J., de Oliveira, A. C. A., Cardozo, N. D., Czimczik, C. I., Feldpausch, T. R., Freitas, M. A., Gloor, E., Higuchi, N., Jiménez, E., Lloyd, G., Meir, P., Mendoza, C., Morel, A., Neill, D. A., Nepstad, D., Patiño, S., Peñuela, M. C., Prieto, A., Ramírez, F., Schwarz, M., Silva, J., Silveira, M., Thomas, A. S., Steege, H. T., Stropp, J., Vásquez, R., Zelazowski, P., Dávila, E. A., Andelman, S., Andrade, A., Chao, K.-J., Erwin, T., Di Fiore, A. C. E. H., Keeling, H., Killeen, T. J., Laurance, W. F., Cruz, A. P., Pitman, N. C. A., Vargas, P. N., Ramírez-Angulo, H., Rudas, A., Salamão, R., Silva, N., Terborgh, J., and Torres-Lezama, A.: Drought sensitivity of the Amazon rainforest, Science, 323, 1344–1347, 2009.

Piao, S., Sitch, S., Ciais, P., Friedlingstein, P., Peylin, P., Wang, X., Ahlström, A., Anav, A., Canadell, J. G., Cong, N., Huntingford, C., Jung, M., Levis, S., Levy, P. E., Li, J., Lin, X., Lomas, M. R., Lu, M., Luo, Y., Ma, Y., Myneni, R. B., Poulter, B., Sun, Z., Wang, T., Viovy, N., Zaehle, S., and Zeng, N.: Evaluation of terrestrial carbon cycle models for their response to climate variability and to CO_2 trends, Glob. Chang. Biol., 19, 2117–2132, doi:10.1111/gcb.12187, 2013.

Poulter, B., Heyder, U., and Cramer, W.: Modeling the sensitivity of the seasonal cycle of GPP to dynamic LAI and soil depths in tropical rainforests, Ecosystems, 12, 517–533, doi:10.1007/s10021-009-9238-4, 2009.

Randerson, J. T., van der Werf, G. R., Giglio, L., Collatz, G. J., and Kasibhatla, P. S.: Global Fire Emissions Database, Version 2.1. Data set from Oak Ridge National Laboratory Distributed Active Archive Center, Oak Ridge, Tennessee, USA, doi:10.3334/ORNLDAAC/849, available at: http://daac.ornl.gov/ (last access: 9 September 2013), 2007.

Saatchi, S., Asefi-Najafabady, S., Malhi, Y., Aragão, L. E. O. C., Anderson, L. O., Myneni, R. B., and Nemani, R.: Persistent effects of a severe drought on Amazonian forest canopy, P. Natl. Acad. Sci. USA, 110, 565–570, 2012.

Saleska, S. R., Miller, S. D., Matross, D. M., Goulden, M. L., Wofsy, S. C., da Rocha, H. R., de Camargo, P. B., Crill, P., Daube, B. C., de Freitas, H. C., Hutyra, L., Keller, M., Kirchhoff, V., Menton, M., Munger, J. W., Pyle, E. H., Rice, A. H., and Silva, H.: Carbon in Amazon forests: unexpected seasonal fluxes and disturbance-induced losses, Science, 302, 1554–1557, 2003.

Saleska, S. R., Didan, K., Huete, A. R., and da Rocha, H. R.: Amazon forests green-up during 2005 drought, Science, 318, 612–612, 2007.

Samanta, A., Ganguly, S., Hashimoto, H., Devadiga, S., Vermote, E., Knyazikhin, Y., Nemani, R. R., and Myneni, R. B.: Amazon forests did not green-up during the 2005 drought, Geophys. Res. Lett., 37, L05401, doi:10.1029/2009GL042154, 2010.

Samanta, A., Ganguly, S., Vermote, E., Nemani, R. R., and Myneni, R. B.: Interpretation of variations in MODIS-measured greenness levels of Amazon forests during 2000 to, Environ. Res. Lett., 7, 024018, doi:10.1088/1748-9326/7/2/024018, 2012.

Takahashi, T., Sutherland, S. C., Wanninkhof, R., Sweeney, C., Feely, R. A., Chipman, D. W., Hales, B., Friederich, G., Chavez, F., Sabine, C., Watson, A., Bakker, D. C., Schuster, U., Metzl, N., Yoshikawa-Inoue, H., Ishii, M., Midorikawa, T., Nojiri, Y., Körtzinger, A., Steinhoff, T., Hoppema, M., Olafsson, J., Arnarson, T. S., Tilbrook, B., Johannessen, T., Olsen, A., Bellerby, R., Wong, C., Delille, B., Bates, N., and de Baar, H. J.: Climatological mean and decadal change in surface ocean $p\mathrm{CO_2}$, and net sea–air $\mathrm{CO_2}$ flux over the global oceans, Deep-Sea Res. Pt. II, 56, 554–577, 2009.

Tarantola, A.: Inverse Problem Theory and Methods for Model Parameter Estimation, Society for Industrial and Applied Mathematics, Philadelphia, 2005.

Verbeeck, H., Peylin, P., Bacour, C., Bonal, D., Steppe, K., and Ciais, P.: Seasonal patterns of $\mathrm{CO_2}$ fluxes in Amazon forests: fusion of eddy covariance data and the ORCHIDEE model, J. Geophys. Res., 116, G02018, doi:10.1029/2010JG001544, 2011.

von Randow, C., Manzi, A. O., Kruijt, B., de Oliveira, P. J., Zanchi, F. B., Silva, R. L., Hodnett, M. G., Gash, J. H. C., Elbers, J. A., Waterloo, M. J., Cardoso, F. L., and Kabat, P.: Comparative measurements and seasonal variations in energy and carbon exchange over forest and pasture in south west Amazonia, Theor. Appl. Climatol., 78, 5–26, doi:10.1007/s00704-004-0041-z, 2004.

Wang, W., Ciais, P., Nemani, R. R., Canadell, J. G., Piao, S., Sitch, S., White, M. A., Hashimoto, H., Milesi, C., and Myneni, R. B.: Variations in atmospheric $\mathrm{CO_2}$ growth rates coupled with tropical temperature, P. Natl. Acad. Sci. USA, 110, 13061–13066, doi:10.1073/pnas.1219683110, 2013.

Xu, L., Samanta, A., Costa, M. H., Ganguly, S., Nemani, R. R., and Myneni, R. B.: Widespread decline in greenness of Amazonian vegetation due to the 2010 drought, Geophys. Res. Lett., 38, L07402, doi:10.1029/2011GL046824, 2011.

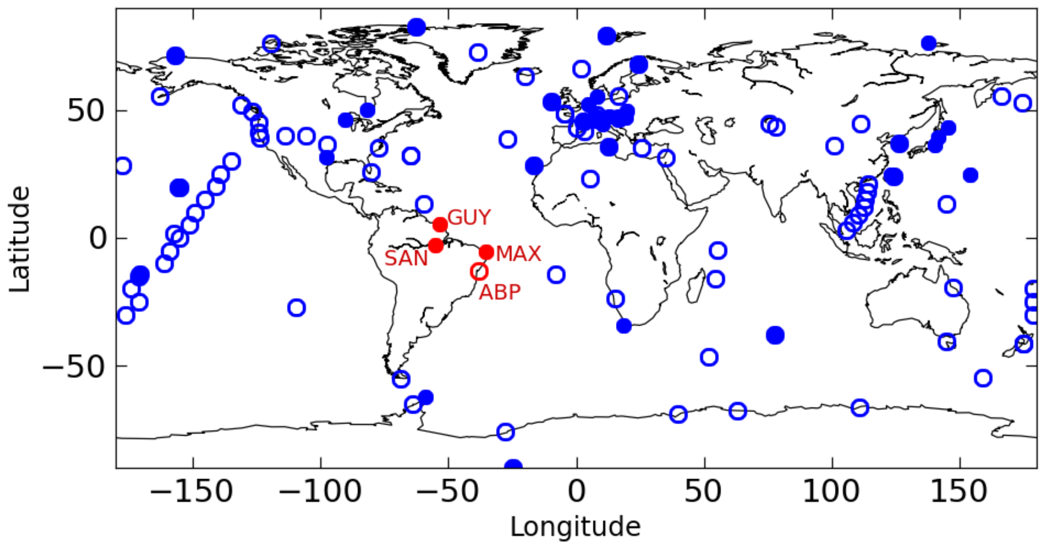

Figure 1. Location of the surface stations used in this study. Blue: surface stations used in ~~CH2010~~MACCv10.1, red: surface stations in South America added to the previous setup of ~~CH2010~~MACCv10.1. Filled circles: stations with continuous measurements, open circles: sites with discrete air sampling.

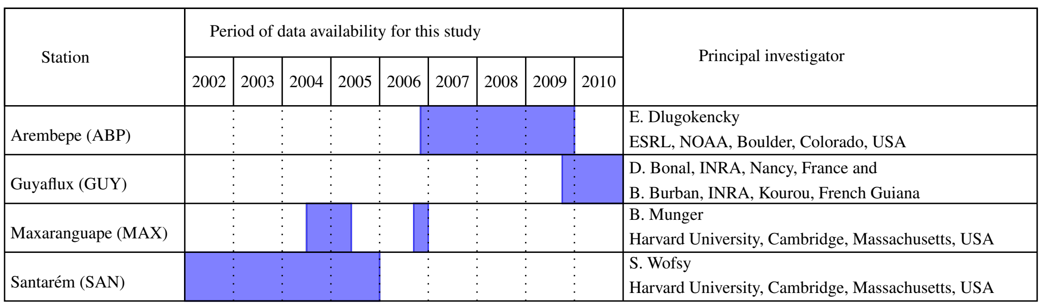

Figure 2. List of surface stations over South America added to the previous setup ~~of Chevallier et al. (2010)~~in MACCv10.1.

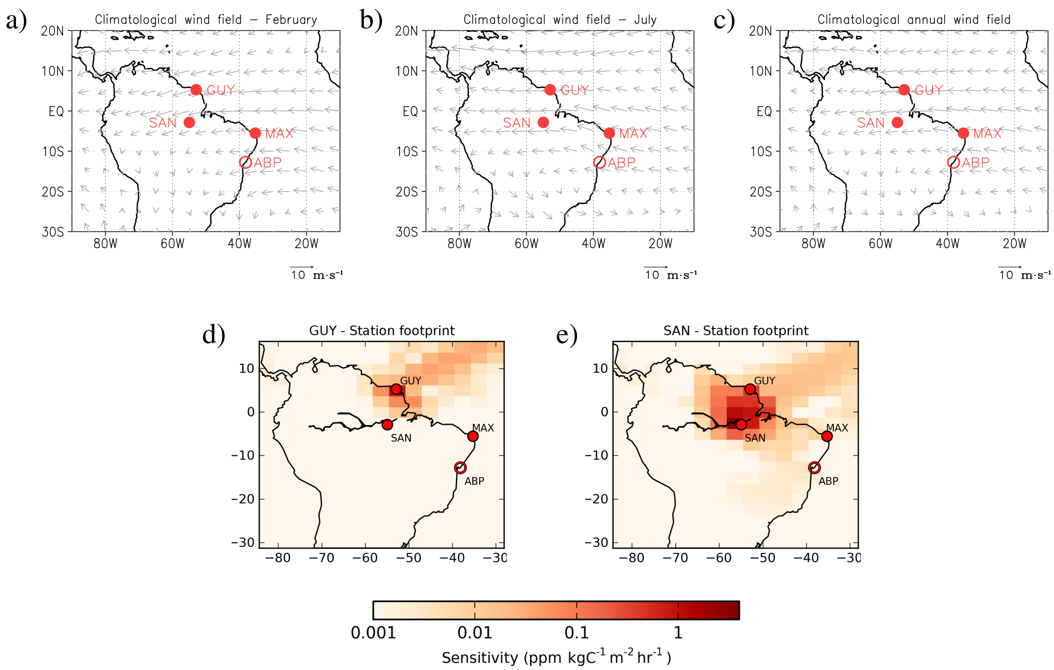

Figure 3. Top: Location of assimilated surface stations in South America and ~~mean~~ climatological wind speed/direction for February **(a)**, July **(b)**, and annual mean **(c)**, averaged over ~~2002–2010~~ 1981–2010 between the surface and a level of 600 hPa (Source: NCEP/NCAR Reanalysis). Sensitivity of surface atmospheric CO_2 mole fractions measured on 20 February 2009 at 10:00 UTC, at Guyaflux (~~left~~7:00 LT) (d) and Santarém (~~right~~6:00 LT) (e), to a constant increment of surface fluxes during the two days prior to the measurement. Sensitivity values are expressed in log-scale. Open circles: sites with discrete air samplings. Filled circles: measurements taken with continuous ~~analyzers~~analysers.

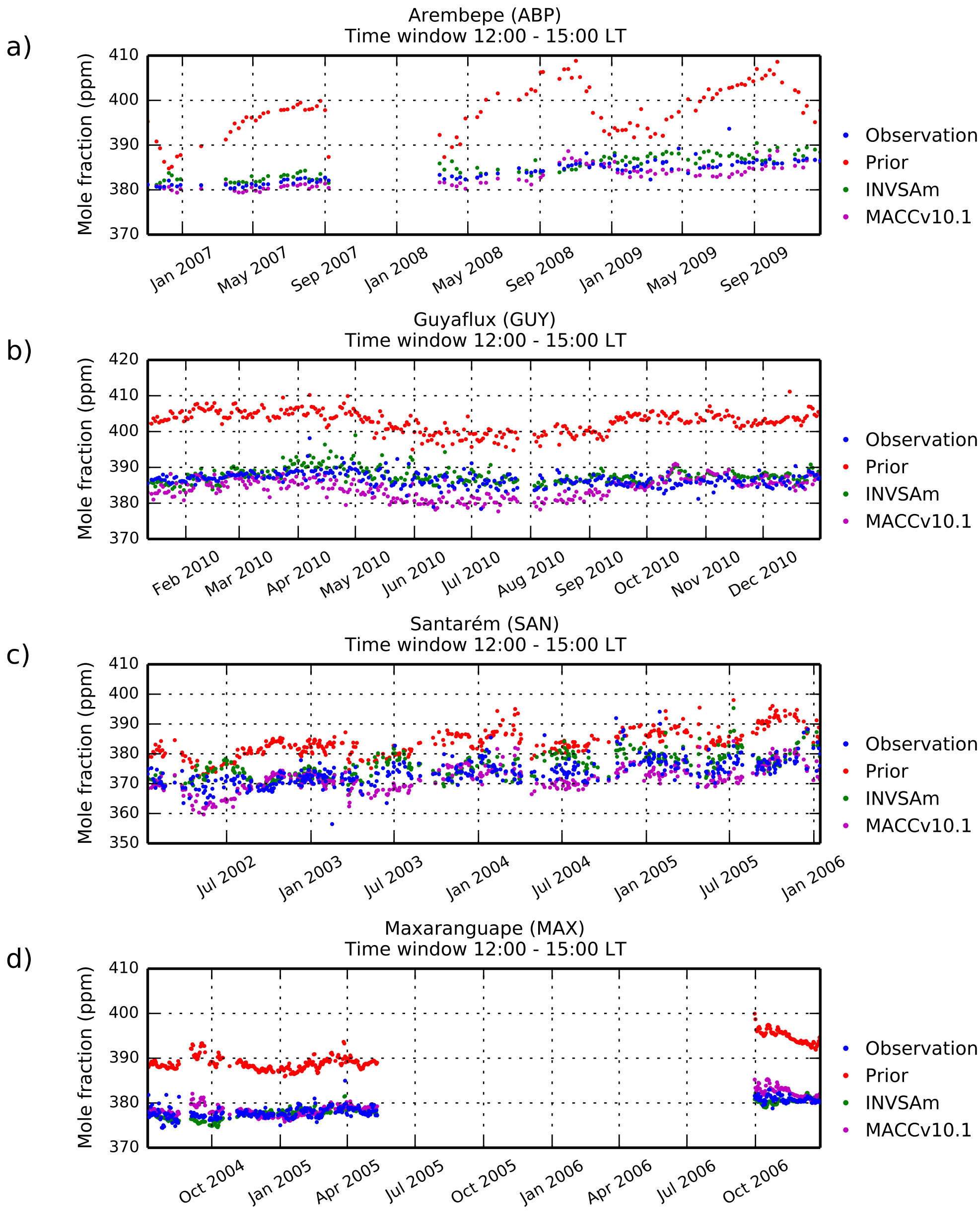

Figure 4. Comparison of assimilated CO_2 observations (blue) and corresponding simulated mole fractions using prior fluxes (red), INVSAm (green) and ~~CH2010~~ MACCv10.1 (purple). Measurements were collected at Arembepe **(a)**, Guyaflux **(b)**, Santarém **(c)** and Maxaranguape **(d)**. Data shown here correspond to daily average mole fractions between 12:00 and 15:00 local time (LT), when wind speed $> 2\,\mathrm{m\,s^{-1}}$. Note that the time scale differs between plots.

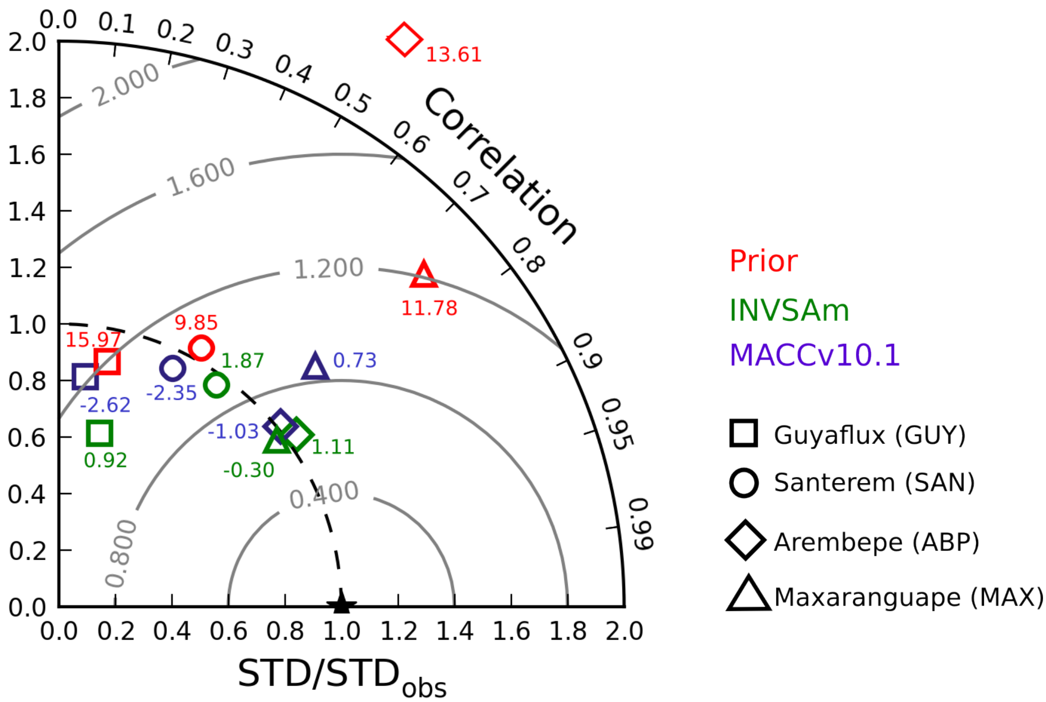

Figure 5. Taylor diagram of the statistics of misfits between observations and simulated CO_2 mole fractions between 12:00 and 15:00 LT at Guyaflux (square), Santarém (circle), Arembepe (diamond) and Maxaranguape (triangle), when wind speed $> 2\,\mathrm{m\,s^{-1}}$, using prior fluxes (red), INVSAm (green) and ~~CH2010~~ MACCv10.1 (purple). Radial distance from the origin: ratio of SD of simulated mole fractions and SD of the observations. Angle measured from the y axis: coefficient of correlation. Numbers next to the symbols: bias (in ppm). Gray circles: SD of the misfits (in ppm).

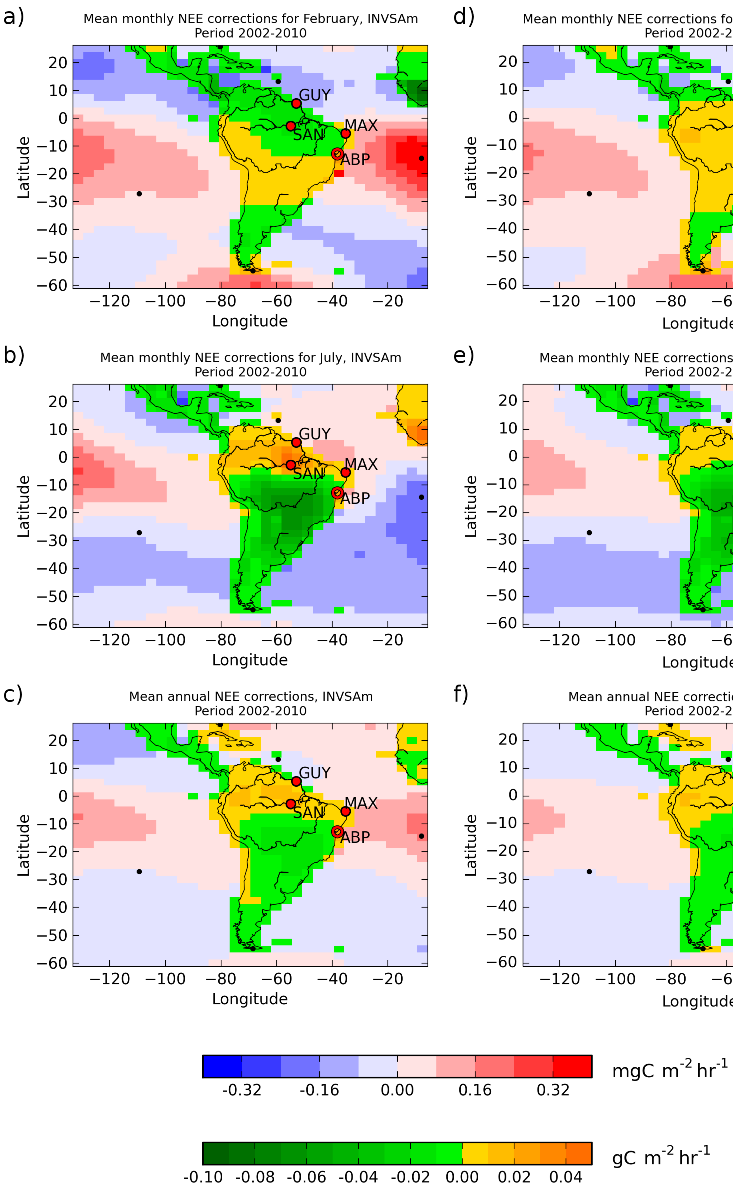

Figure 6. Spatial distribution of 2002–2010 mean flux corrections at the transport model resolution (3.75° × 2.50°) to ORCHIDEE from INVSAm (left) and MACCv10.1 (right) over an area larger than TSA region: mean for February **(a,d)**, July **(b,e)**, and mean over the full period 2002–2010 **(c,f)**. Flux increments over land and ocean are represented with two distinct colour scales and units: green–yellow for land, in $\mathrm{gC\,m^{-2}\,hr^{-1}}$; blue–red for ocean, in $\mathrm{mgC\,m^{-2}\,hr^{-1}}$. Red symbols: surface stations in South America added to the previous setup of MACCv10.1, where filled circles indicate locations of sites with continuous measurements; open circles indicate locations of sites with discrete air sampling. Black symbols: surface stations used in MACCv10.1.

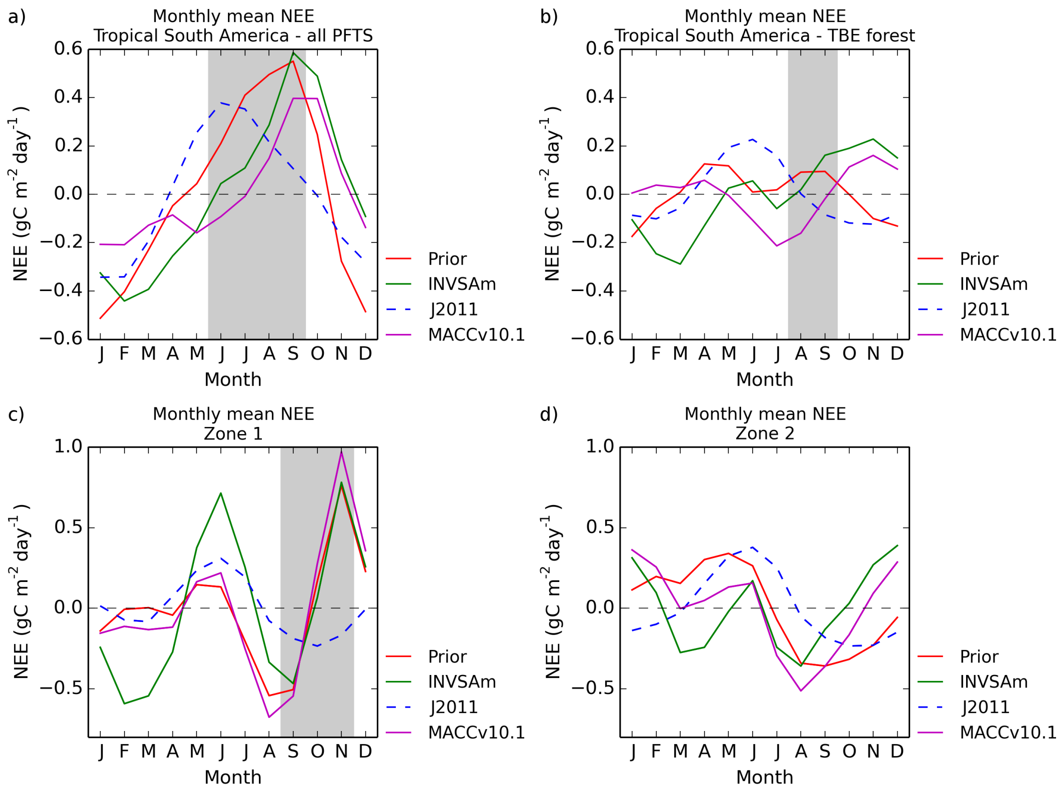

Figure 7. Monthly mean NEE anomaly integrated over **(a)** the ~~whole study~~ TSA region and **(b)** over pixels dominated by TBE forests in ORCHIDEE for 2002–2010. The shaded areas denote dry seasons, defined as months with precipitation $< 100\,\mathrm{mm}$, based on monthly totals from TRMM data over 2002–2010. Estimates from prior fluxes (red), INVSAm (green), ~~CH2010~~ MACCv10.1 (purple) and J2011 (dashed blue). ~~**(c–f)** Monthly mean NEE measurements from EC stations at **(c)** Bananal Island (2004–2005), **(d)** Caxihuanã (2000–2002), **(e)** Rebio Jarú (2000–2002), and Santarém (2001–2002). **(g–h)**~~ **(c–d)** Monthly mean NEE integrated over the zones 1 ~~**(g)**~~ **(c)** and 2 ~~**(h)**~~ **(d)** that are defined in Fig. ~~7.~~ 8.

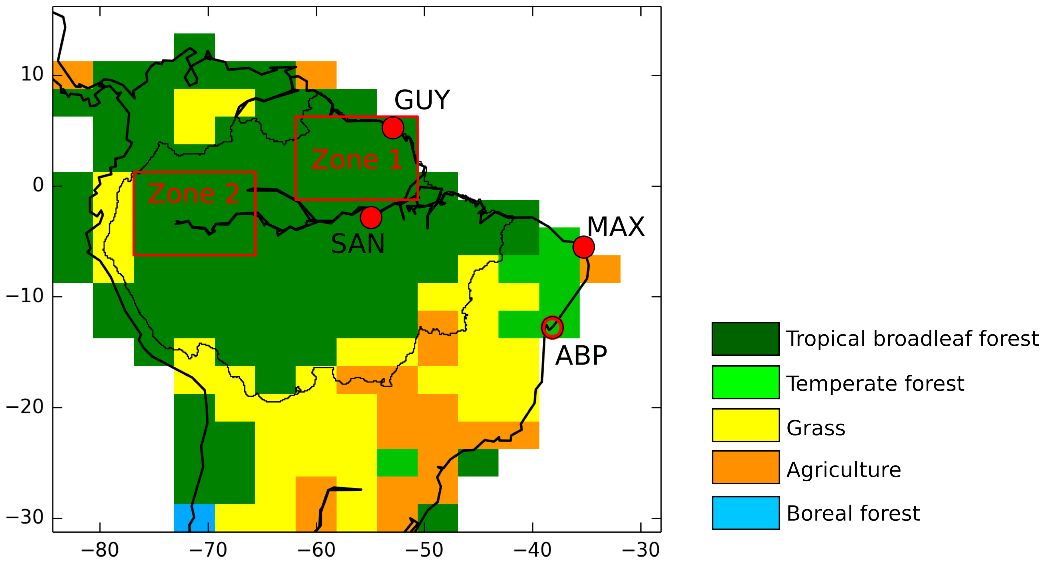

Figure 8. ~~Dominating~~ Dominant PFTs for each transport model grid cell (i.e. 3.75° × 2.50°) according to the ORCHIDEE vegetation map over the ~~study~~ TSA region. Open circles show location of sites with discrete air sampling; filled circles show location of sites with continuous measurements~~; and squares show locations of the EC measurement stations used in this study~~. Zones 1 and 2 indicate areas for which the NEE is presented in Figs. ~~6g~~ 7c and ~~h, 10.~~

~~Spatial distribution of 2002–2010 mean flux corrections at the transport model resolution (3.75×2.50) to ORCHIDEE from INVSAm over the study region: mean for **(a)** February, **(b)** July~~d, ~~and **(c)** mean over the full period 2002–2010. Filled circles indicate locations of sites with continuous measurements; and open circles indicate locations of sites with discrete air sampling~~respectively.

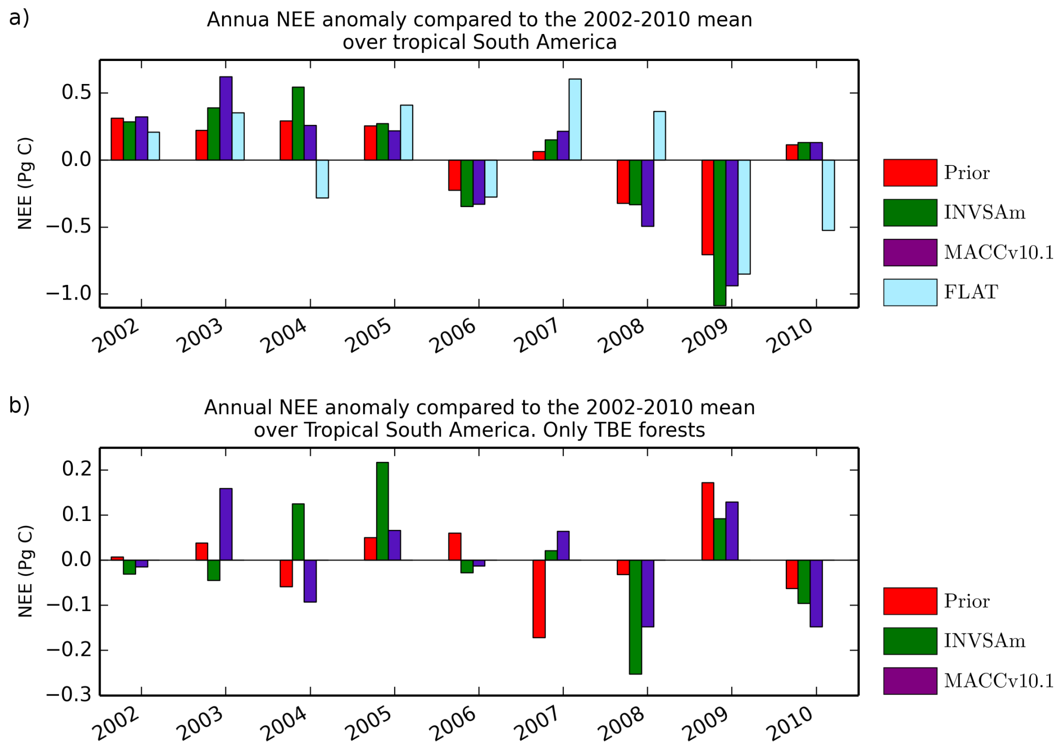

Figure 9. (a) Annual NEE anomaly compared to the mean of 2002–2010; estimates for the ~~whole study~~ TSA region. **(b)** Annual NEE anomaly compared to the mean of 2002–2010; estimates for the area dominated by TBE forests.

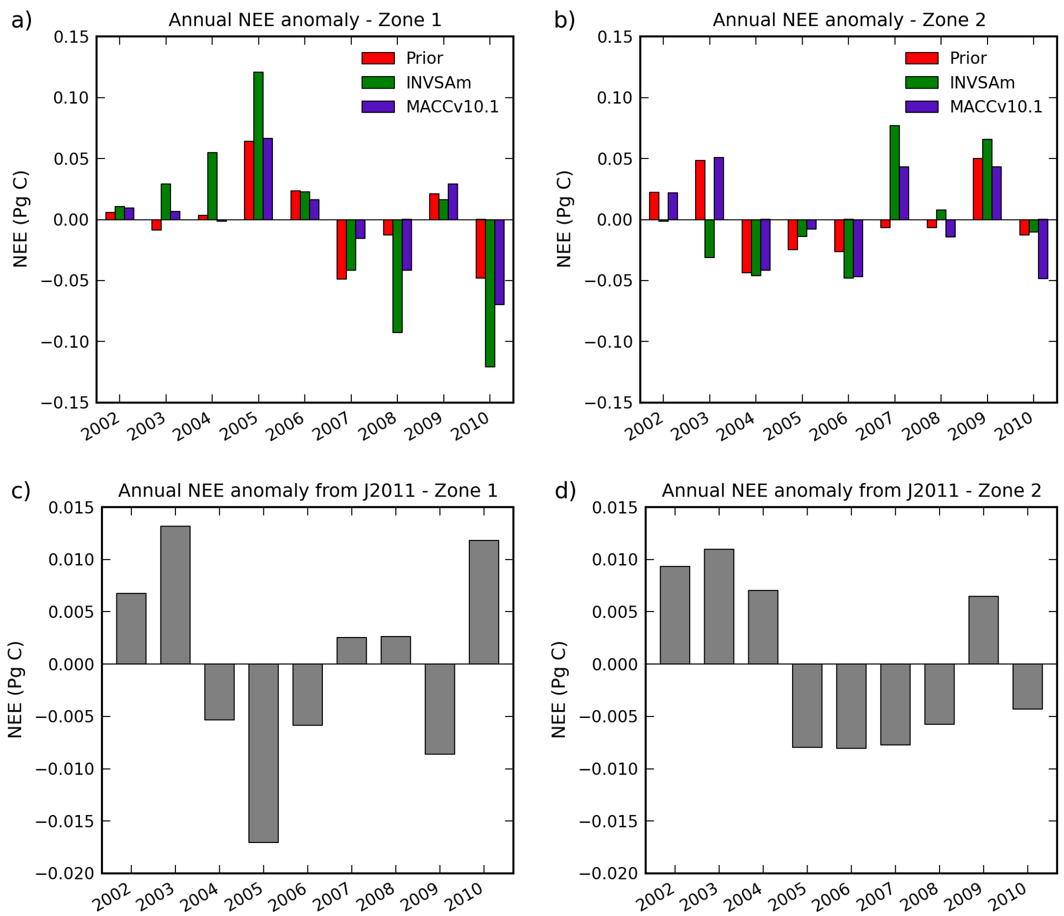

Figure 10. Annual NEE anomaly compared to the 2002–2010 mean for Zone 1 **(a, c)** and Zone 2 **(b, d)** as defined in Fig. ~~7.~~ 8. Estimates from prior fluxes (red), INVSAm (green), ~~CH2010~~ MACCv10.1 (purple), and J2011 (gray).